Juneau Airport Wind System (JAWS) Wind Sensor Severe Weather Performance Test Report

William Benner
Thomas Carty
Michael McKinney
Francis Law

August 2002

DOT/FAA/CT-TN02/18

Document is on file at the William J. Hughes Technical Center Library, Atlantic City International Airport, NJ 08405

U.S. Department of Transportation
Federal Aviation Administration

NOTICE

This report is available at the Federal Aviation Administration William J. Hughes Technical Center's Full-Text Technical Reports page: http://actlibrary.tc.faa.gov in Adobe Acrobat portable document format (PDF) form.

Technical Report Documentation Page

1. Report No.	2. Government Accession No.	3. Recipient's Catalog No.
DOT/FAA/CT-TN02/18		
4. Title and Subtitle JUNEAU AIRPORT WIND SYSTEM (JAWS) WIND SENSOR SEVERE WEATHER PERFORMANCE TEST REPORT		5. Report Date August 2002 6. Performing Organization Code ACB-630
7. Author(s) William Benner, Thomas Carty, and Michael McKinney, ACB-630; Francis Law, UAL Solutions Group		8. Performing Organization Report No. DOT/FAA/CT-TN02/18
9. Performing Organization Name and Address U.S. Department of Transportation Federal Aviation Administration William J. Hughes Technical Center Atlantic City International Airport, NJ 08405		10. Work Unit No. (TRAIS) 11. Contract or Grant No.
12. Sponsoring Agency Name and Address U. S. Department of Transportation Federal Aviation Administration William J. Hughes Technical Center Atlantic City International Airport, NJ 08405		13. Type of Report and Period Covered Technical Note 14. Sponsoring Agency Code
15. Supplementary Notes		

16. Abstract

The Weather Group of the Federal Aviation Administration (FAA) William J. Hughes Technical Center performed a wintertime assessment of wind sensors near Juneau International Airport (JNU), Alaska during the period November 2000–June 2001. The purpose of the field investigation was to assess the severe-weather performance capabilities of wind sensors currently used in the prototype JNU Wind Hazard Information System (JWHIS) developed by the National Center for Atmospheric Research (NCAR). In addition, alternate heated anemometers including ultrasonic, mechanical, and pressure-type sensors were assessed as possible candidates for use in the operational successor to JWHIS, the Juneau Airport Wind System (JAWS).

Pretest activities included wind sensor checkout and calibration in a wind tunnel at the Technical Center. A test bed was then set up on an existing equipment tower on a well-exposed mountain overlooking JNU. This ridge-top weather station has a suitable tower, equipment, and communications infrastructure to support installation and continuous operations of the test equipment. The site is subject to extreme meteorological and climatic conditions where snow and the buildup of rime ice on exposed surfaces can be substantial. Nine anemometers, all with heater capabilities, were installed along with other instrumentation including an ice detector, temperature/relative humidity probe, and Internet-capable video cameras. Data was acquired from the mountain via a high-speed wireless network in an unattended mode during the 6-month period. Continuous remote monitoring of sensor and video data was accomplished via a server with Web and FTP capabilities.

Approximately 3500 hours of test bed data were collected and analyzed over the 184-day period. Video motion clips were constructed and used to visually assess icing. In-depth data analysis was performed for the ~37 hours where winds exceeded the current limits for airport operations. With a few exceptions, the existing JWHIS mechanical anemometers exhibited minimal icing. Mechanical sensors from a second manufacturer experienced significant icing, and were found operationally unsuitable due to extended ice-related outages. Favorable performance was displayed by the ultrasonic anemometer. The sensor was determined to be degraded by icing 0.8% of the 6-month period. Further analysis of the periods of degraded performance (with respect to the JAWS 1-minute wind reporting requirement), revealed that in 84% of affected cases, there were at least 75% raw data samples available to derive a valid wind report. The pressure-type sensor exhibited encouraging performance; however, the amount of data collected was limited due to delayed sensor installation. This sensor is under further evaluation as part of a follow-on 2001–02 wintertime assessment being conducted in Juneau.

17. Key Words	18. Distribution Statement
Juneau Airport Wind System Anemometer, Ultrasonic Wind Sensor Wind Tunnel	This document is available to the public through the Technical Center Library, Atlantic City International Airport, NJ 08405

19. Security Classif. (of this report)	20. Security Classif. (of this page)	21. No. of Pages	22. Price
Unclassified	Unclassified	127	

Form DOT F 1700.7 (8-72) Reproduction of completed page authorized

ACKNOWLEDGMENTS

The authors would like to acknowledge the excellent work and support of Mr. Charles Houlroyd and Mr. Mark Vassalotti of Titan Systems, Mr. Daniel Coombs and Mr. Anthony Curcio of Basic Commerce Industries, and Mr. Harry Webster from the wind tunnel facility at the FAA William J. Hughes Technical Center. Mr. Francis Law of UAL Solutions Group is acknowledged for his excellent work in compiling and analyzing the data gathered at the test site and in the development of this report. In addition, the authors would like to express their appreciation for the support from Mr. Daniel Phillips of Haight & Associates, Inc., and to Mr. Robert Barron and Mr. Alan Yates from the National Center for Atmospheric Research. The installation and operation of the test site would not have been possible without their expertise, energy, and attention to detail.

TABLE OF CONTENTS

LIST OF ILLUSTRATIONS

LIST OF TABLES

EXECUTIVE SUMMARY

The Weather Group (ACB-630) of the Federal Aviation Administration (FAA) William J. Hughes Technical Center (hereafter referred to as Technical Center) performed a wintertime assessment of wind sensors near Juneau International Airport (JNU), Alaska during the period November 2000–June 2001. The purpose of the field investigation was to assess the severe-weather performance capabilities of wind sensors currently used in the prototype JNU Wind Hazard Information System (JWHIS) developed by the National Center for Atmospheric Research (NCAR). In addition, alternate heated anemometers including mechanical, ultrasonic, and pressure-type sensors were assessed as possible candidates for use in the operational successor to JWHIS, the Juneau Airport Wind System (JAWS). The ultrasonic anemometer was of particular interest because of its growing use in other national and aviation weather systems within the FAA.

Pretest activities included wind sensor checkout and calibration in a wind tunnel at the Technical Center. The test bed was established on an existing equipment tower on a well-exposed mountain overlooking JNU. This site is one of three existing ridge-top weather stations associated with JWHIS, and has a suitable tower, equipment, and communications infrastructure to support installation and continuous operations of the test equipment. The site is subjected to extreme meteorological and climatic conditions where snow and the buildup of rime ice on exposed surfaces can be substantial. With assistance from NCAR, nine anemometers, all with heater capabilities, were installed along with other instrumentation including an ice detector, temperature/relative humidity probe, and Internet-capable video cameras. Data was acquired from the mountain via a high-speed wireless network in an unattended mode during the 6-month period. Continuous remote monitoring of sensor and video data was accomplished via a server with Web and FTP capabilities.

Approximately 3500 hours of test bed data were collected and analyzed over the 184-day period. Video motion clips were constructed and used to visually assess icing. In-depth data analysis was performed for the ~37 hours where winds exceeded the current limits for airport operations. With a few exceptions, the existing JWHIS mechanical anemometers exhibited minimal icing. Mechanical sensors from a second manufacturer experienced significant icing, and were found operationally unsuitable due to extended ice-related outages. Favorable performance was displayed by the ultrasonic anemometer. The sensor was determined through internal status as well as video data to be degraded by icing 0.8% of the 6-month period. Further analysis of the periods of degraded performance (with respect to the JAWS 1-minute wind reporting requirement) revealed that in 84% of affected cases, there were at least 75% raw data samples available to derive a valid wind report. During the entire field experiment, only 81 sporadic 1-minute wind reports were derived from 25% or less raw sensor data. The pressure-type sensor that was evaluated exhibited encouraging performance; however, the amount of data collected was limited due to delayed sensor installation. This sensor is under further evaluation as part of a follow-on 2001–02 wintertime assessment currently being conducted in Juneau.

1. INTRODUCTION.

The Weather Group, ACB-630 (formally ACT-320) of the Federal Aviation Administration (FAA) William J. Hughes Technical Center installed and field tested several anemometers near Juneau International Airport (JNU) in Alaska during the 2000-01 winter season. The purpose of the effort was to perform an investigation of the severe weather performance capabilities of anemometers currently used in the prototype Juneau Wind Hazard Information System (JWHIS) at JNU. The severe weather performance of several other wind sensors was also assessed. All of the sensors tested are candidates for use in the Juneau Airport Wind System (JAWS) which will replace the JWHIS.

As background, mountains and rugged terrain around the Juneau airport restrict flight paths and can create complex and turbulent wind-flow patterns. To reduce the risk of aircraft encountering severe turbulence, the FAA currently requires that two major departure routes at JNU be closed to Part 121 commercial aircraft whenever the JWHIS centerfield and/or three wind sensors on nearby mountains exceed wind limitations outlined in FAA Operations Specifications for Part 121 air carrier operations in Juneau [1]. The wind data collection and dissemination system currently installed at JNU were deployed jointly by Alaska Airlines and the National Center for Atmospheric Research (NCAR). The sensor suite consists of a series of anemometers placed strategically around the airport area on mountain ridge-tops to gather wind information.

The test effort outlined in this document is part of a much broader effort, which will ultimately transition some or all of the current prototype JWHIS into a fully operational wind information system designated as JAWS. This end-state system will provide wind information customized to the airport's challenging terrain, and may incorporate provisions of particular Operations Specifications. It is anticipated that the information provided by JAWS will assist users in maximizing the utilization of Juneau's turning-departure routes, as well as supporting overall airport operational decisions. An essential element of this system will be accurate and reliable wind sensors capable of supporting airport operations under snow and icing conditions.

The planning and conduct of the Juneau testing is based on the successes and lessons learned from a previous ACB-630 test effort on Mount Washington, NH. Conducted in the winter of 1999, this field demonstration assessed a variety of wind sensors under severe weather conditions including snow and rime icing [2]. The test bed was located near the summit and the Mount Washington Observatory (MWO). This area is subject to extreme snow and icing conditions where the buildup of rime ice on exposed surfaces is prevalent and often substantial. Conditions on Mount Washington are similar to the alpine and arctic zones characteristic to Juneau.

1.1 PURPOSE OF REPORT.

This test was performed in accordance with its associated test plan [3]. This test report provides the test method description, results, conclusions, and recommendations of the test program. The test planning components of the document describe the various test activities, including pretest preparations, test setup, and test conduct. In addition to the test documentation and presentation of the test results, this document also provides sufficient detail and procedural information for carrying out the test setup, data collection, and data analysis for similar follow-on test efforts.

1.2 SCOPE OF REPORT.

This document has been written and formatted in accordance with the Content and Format of Operational Test (OT) Reports as outlined in the FAA Test and Evaluation Process Guidelines [4]. The test guidelines have been tailored to account for the demonstration and assessment nature of this activity. The body of this report contains a description of the test site, test bed, and test approach. It also provides supplemental procedural information including individual sensor and equipment specifications, installation of sensors and communications equipment, product sheets and drawings. The balance of the report provides a detailed discussion on the data analysis, results, conclusions, and recommendations resulting from the test. A briefer version of this report has been recently presented at an aviation weather conference [5].

2. REFERENCE DOCUMENTS.

This section contains a list of publications and papers referenced in this document as part of the implementation of the test program.

1. FAA Operations Specifications for Alaska Airlines Operations in Juneau, AK, C64, Effective 21 April 1998.

2. A Wintertime Assessment of Wind Sensors on Mt. Washington, New Hampshire, Weather Branch, ACT-320, FAA Report DOT/FAA/CT-TN00/05, March 2000.

3. Juneau Airport Wind System (JAWS) Wind Sensor Severe Weather Performance Test Plan, Weather Branch, ACT-320, FAA William J. Hughes Technical Center, 24 April 2001.

4. FAA Acquisition Management System (AMS) Test and Evaluation Process Guidelines, Content and Format of FAA Operational Test (OT) Reports, Appendix C-3, April 2002.

5. Carty, Thomas, McKinney, Michael, and Law, F., An Assessment of Ice-Free Wind Sensors for the Juneau Airport Wind System, 10th Conference on Aviation, Range, and Aerospace Meteorology, American Meteorological Society, Portland, Oregon, 13-16 May 2002.

6. Colman, Bradley R. and Dierking, Carl F., The Taku Wind of Southeast Alaska: Its Identification and Prediction, *Weather and Forecasting*, American Meteorological Society, Boston, MA, March 1992.

7. Operators Manual, Juneau Wind Hazard Information System Operators Manual, 30 September 1999, NCAR/RAP, Co-Op DTFA01-98-C-00031 Modification 0003.

8. Hydro-Tech Anemometers in the Juneau Airport Wind System (JAWS), National Center for Atmospheric Research/Research Applications Program (NCAR/RAP), 8 August 2000.

9. Low-Level Wind Shear Alert System–Relocation and Sustainment (LLWAS–RS) Ultrasonic Wind Sensor Acceptance Test Report, Weather Branch, ACT-320, FAA Report DOT/FAA/CT-TN00/07, March 2000.

10. Operations Requirements Document for Juneau Airport Wind System (JAWS), Juneau International Airport, AK (JNU), FAA AUA-430, 28 August 2000.

11. Juneau Turbulence Wind Sensor Severe Weather Performance Test, Briefing for the Aviation Weather Research Program (AWRP) Program Management Review, 5 December 2000.

12. Juneau Airport Wind System (JAWS) Wind Sensor Severe Weather Performance Test, Briefing to JAWS Implementation Team, Weather Branch, ACT-320, 13 March 2001.

13. Juneau Airport Wind System (JAWS) Wind Sensor Severe Weather Performance Test, Briefing to JAWS Implementation Team, Weather Branch, ACT-320, 11 July 2001.

3. SYSTEM DESCRIPTION.

3.1 MISSION REVIEW.

The JAWS mission is to provide wind information customized to the challenging terrain around JNU, and to reduce the risk of aircraft encountering severe turbulence in the area. The system warning thresholds will be oriented around the wind limitations outlined in FAA Operations Specifications for Part 121 air carrier operations in Juneau. The fully operational end-state wind information system provided by JAWS will assist users in maximizing the utilization of Juneau's turning-departure routes, as well as supporting overall airport operational decisions. Relevant to this test, and an essential element of this system, is accurate and reliable wind sensors capable of supporting airport operations under snow and icing conditions.

3.2 TEST SYSTEM CONFIGURATION.

This section provides a description of the test site, environment, and climatology. A description of the test bed setup including sensors, equipment, and data communications interfaces is also provided.

3.2.1 Test Site Description.

Juneau International Airport is located approximately 11.2 kilometer (km) (7 miles (mi)) northwest of downtown Juneau at an elevation of 5.8 meter (m) (19 foot (ft)) above mean sea level. The location of the sensor test bed is the JWHIS Automatic Weather Station (AWS) designated as Eagle Crest. It is located on a mountain ridge-top on Douglas Island approximately 11.6 km (7.2 mi) and at a bearing of about 159° (~south-southeast) overlooking Juneau airport. It is noteworthy for wind direction determination that the area has a large East magnetic declination of 29° so that magnetic North lies 29° east of true North. A schematic map of the region showing the test site, the airport, operational departures, and the JWHIS anemometer locations is provided in figure 1. An aerial photograph of the same region and test site is shown in figure 2.

Specifically, the Eagle Crest AWS and test bed equipment are located at the top of the Eaglecrest Ski Area. The test site is situated on a mountain ridge-top location about 803 m (2634 ft) above mean sea level, and approximately 90 m (295 ft) from the ski resort's Eagle's Nest warming hut at the terminus of the chairlift. A topographic map showing the test site and its proximity to JNU is supplied in figure 3. The test bed location has excellent exposure for winds from all directions. The site is accessible by ski lift during the winter and by helicopter during the summer. The mountain ridge top location is subject to severe winter weather conditions, which may be considered as representative of the range of environmental conditions in which other JAWS weather stations and anemometers are subjected. Although the Sheep Mountain JWHIS weather station generally experiences more icing, the Eagle Crest site is more accessible, and its tower and equipment shelter better support the set up and maintenance of a test bed. In addition, the current Part 121 Ops Spec requires Eagle Crest winds be available under all scenarios. Sheep Mountain winds are not required at all times if other specified stations are reporting.

FIGURE 1. SCHEMATIC MAP SHOWING LOCATIONS OF THE EAGLE CREST TEST SITE AND JWHIS COMPONENTS

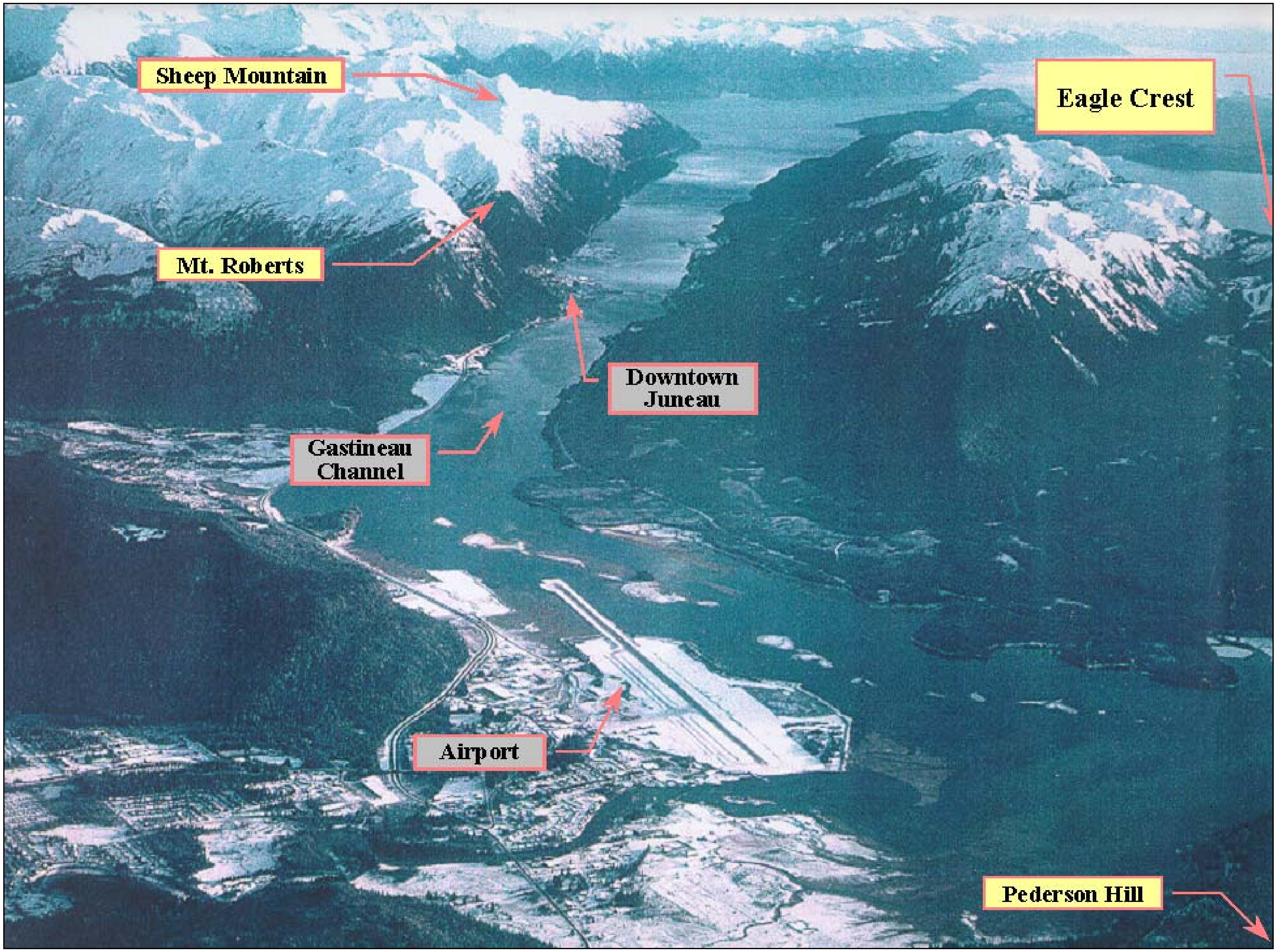

FIGURE 2. AERIAL VIEW OF TEST SITE, AIRPORT, AND JWHIS COMPONENTS LOOKING EAST-SOUTHEAST

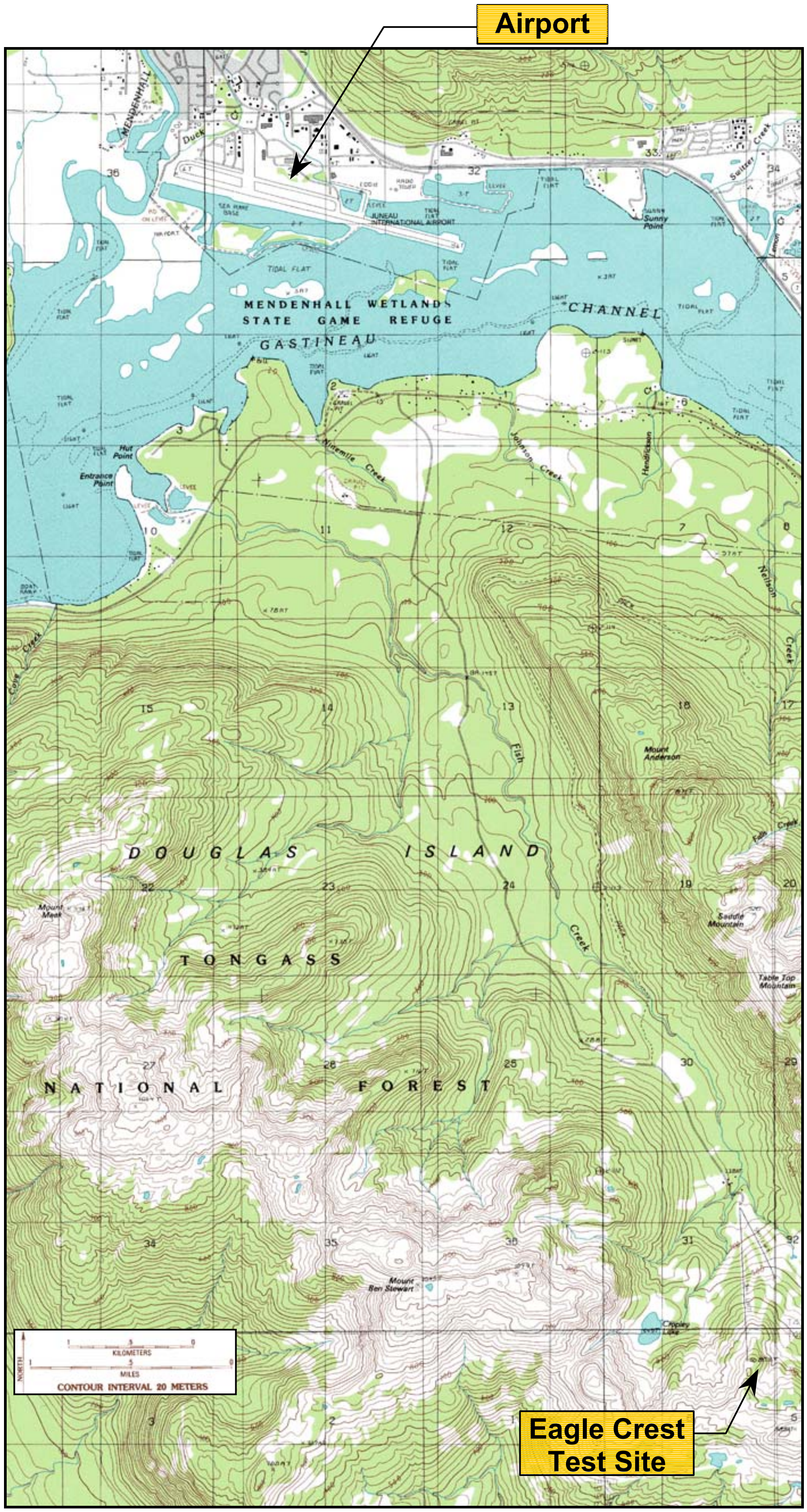

FIGURE 3. TOPOGRAPHIC MAP OF TEST SITE AND AIRPORT

An aerial photograph of the actual Eagle Crest AWS and test site is shown in figure 4. The photograph shows the new tower, and the lower part of the original triangular tower, which was partially destroyed by high winds in December 1999. Construction of the new tower was completed in October 2000, and its platform-type design is similar to the AWS tower on Sheep Mountain.

The region climatology is characterized by two predominate air flows as shown in the NCAR wind roses for Eagle Crest in figure 5. Cold continental air flows from the northeast are known locally in Juneau as Taku winds. Taku winds are strong down-slope winds that can exceed 50 meters per second (m/s) [6]. The contrasting moist maritime southeasterly flows from the Gulf of Alaska are largely responsible for the significant snow and icing conditions encountered along the mountain ridge-tops surrounding Juneau.

The average normal daily mean temperature for the Juneau airport area during the winter months is 28.0°Fahrenheit (°F), and the average annual snowfall is 99.0 inches (in). Snow and icing conditions, the latter being prevalent at higher elevations, are common in JNU from early fall through spring, and the buildup of rime ice on exposed surfaces can be substantial. The extent of icing is exemplified in the photographs shown in figure 6. This figure shows the buildup of rime ice on the JWHIS Automatic Weather Station at Sheep Mountain.

3.2.2 Test Bed Description.

The sensors and equipment were installed on the tower of the Eagle Crest AWS. The platform of the tower is 8 x 8 ft and is at a height of 30 ft above ground. As shown in figure 4, an equipment shelter is located directly beneath the tower. Electrical power is provided to the tower via underground cable from the ski resort's redundant diesel generator system at the Eagle Crest lodge and base area. Electrical service in the form of 18 amperes (A), 480 volts (V) triple-phase power is first supplied to the Eagle's Nest warming hut. The service is of sufficient capacity to run all equipment on top of the mountain, including the tower installation. A transformer housed in the hut is used to furnish 120/208 V triple-phase power directly to the tower. All loads at the tower are 120 V, with a balanced profile.

For the purposes of this test, the Eagle Crest sensors and equipment are logically categorized into two packages. The JWHIS sensor suite consists of the existing AWS sensors and equipment, which currently support JNU operations, while the Test Equipment is the additional package of sensors, instrumentation, and equipment that are under test control and will support the overall test activity. A complete list of the JWHIS and test equipment is provided in the Test Plan [3].

3.2.2.1 JWHIS Equipment.

The JWHIS equipment package is considered permanent since it supports FAR Part 121 operations for the Juneau airport. JWHIS equipment consists primarily of four wind sensors, a temperature and humidity probe, dataloggers, radio modems, and antennas for transmitting data to the airport. The equipment is maintained by NCAR and is described in the JWHIS Operators Manual [7].

(A)

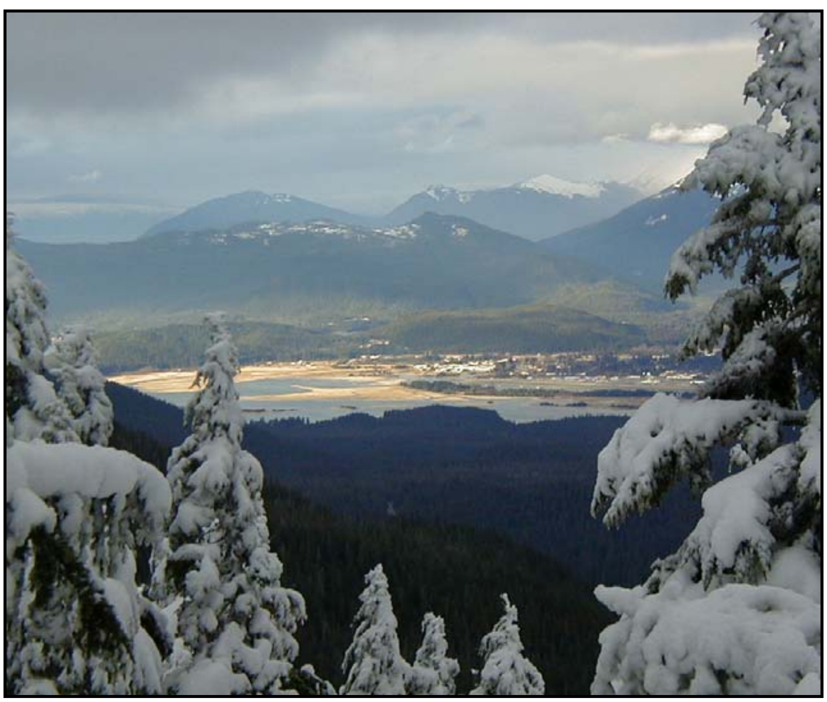

(B)

FIGURE 4. AERIAL PHOTOGRAPH OF THE EAGLE CREST TEST SITE LOOKING SOUTHEAST (A), AND THE AIRPORT AS VIEWED FROM THE SITE (B)

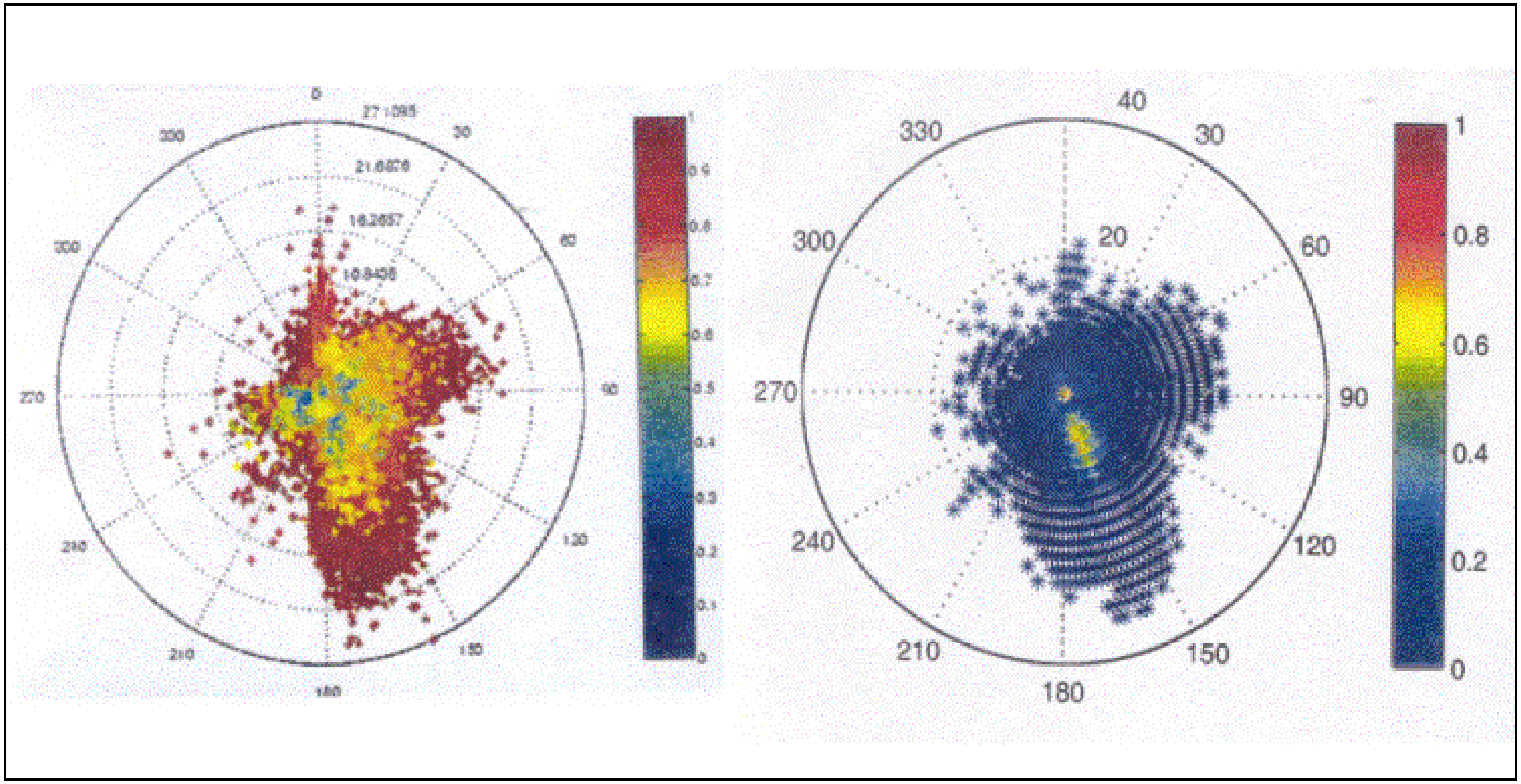

FIGURE 5. EAGLE CREST WIND ROSES SHOWING PREVAILING WINDS

(A) (B)

FIGURE 6. SHEEP MOUNTAIN AWS DURING FAIR WEATHER (A), AND WITH ICE BUILDUP (B)

The wind sensors consist of a primary pair (EC1) and backup pair (EC2) of Hydro-Tech mechanical anemometers manufactured by Taylor Scientific Engineering. Each pair consists of a Model WS-3 Heated Rotor Anemometer and a Model WD-3 Heated Direction Vane. Photographs of the anemometer and direction vane are shown in figure 7. The sensors are particularly designed for rugged applications and are electrically heated and temperature controlled. Each standard production model has a 1500-watt (W) heater. Heating is controlled by separate heater control units. The control units cycle power to the heaters based on a user-selectable percentage of the maximum allowed temperature. Rationale for the use of this wind sensor in the JAWS system has been explored in an NCAR white paper [8].

(A) (B)

FIGURE 7. HYDRO-TECH ROTOR ANEMOMETER (A), AND DIRECTION VANE (B)

Air temperature and relative humidity was measured by a Campbell Scientific HMP45C integrated temperature and relative humidity probe manufactured by Vaisala, Inc. The probe consists of a platinum resistance thermometer and capacitive-type relative humidity sensor housed directly in a 12-plate Gill solar radiation shield. No backup capability was considered necessary for temperature and humidity measurement.

Data acquisition and wireless data transmission to JNU were accomplished independently for each anemometer pair using a Vaisala QLI50 Datalogger and Freewave 900 megahertz (MHz) wireless modem and antenna.

3.2.2.2 Test Equipment.

3.2.2.2.1 Wind Sensors.

A total of nine wind sensors were part of the study. The mechanical sensors included the four operational Hydro-Tech anemometers currently used in the prototype JWHIS system, and one test Hydro-Tech rotor anemometer. In addition, two NRG mechanical sensors were installed and tested. An ultrasonic and pressure-type sensor were also installed and assessed. The ultrasonic anemometer was of particular interest because of its growing use in other national and aviation weather systems. Since the ultrasonic and pressure-type sensors are solid state, have no moving parts, and are resistant to environmental corrosion, it is expected that they generally have a lower maintainability requirement and a higher overall reliability than the mechanical sensors.

3.2.2.2.1.1 Hydro-Tech Anemometers.

The operational JWHIS sensors consist of two pairs of Hydro-Tech mechanical wind sensors manufactured by Taylor Scientific Engineering. As described in section 3.2.2.1, each pair consisted of a Model WS-3 Heated Rotor Anemometer and a separate Model WD-3 Heated Direction Vane. The sensors are particularly designed for rugged applications and are electrically heated and temperature controlled. Each has a 1500-watt (W) heater. In addition, one Model WS-3 Heated Rotor Anemometer with a 1500 W thermostatically controlled heater was installed. This test sensor is identical to its JWHIS counterpart. Based on the manufacturer's wind tunnel data, which indicates a significant overspeeding by the sensor, all raw values of Hydro-Tech wind speed data were uniformly reduced by a factor of 20%.

3.2.2.2.1.2 NRG Anemometers.

Electrically heated mechanical wind sensors from NRG Systems, Inc. were also installed and tested. The NRG electrically heated IceFree II Anemometer and Wind Direction Vane shown in figure 8 are made of cast aluminum with a black anodized finish. The NRG sensors utilize constant temperature, self-regulating 200 W heaters. The wind speed sensor is a 3-cup design, which employs a modified cup to reduce errors created by vertical wind components.

3.2.2.2.1.3 Vaisala Ultrasonic Anemometer.

A modified Vaisala Model Handar 425AH ultrasonic anemometer was also installed and tested. This sensor is considered Commercial Off-the-Shelf (COTS) equipment since production model 425AH sensors are being used in the FAA Stand Alone Weather Sensors (SAWS) system,

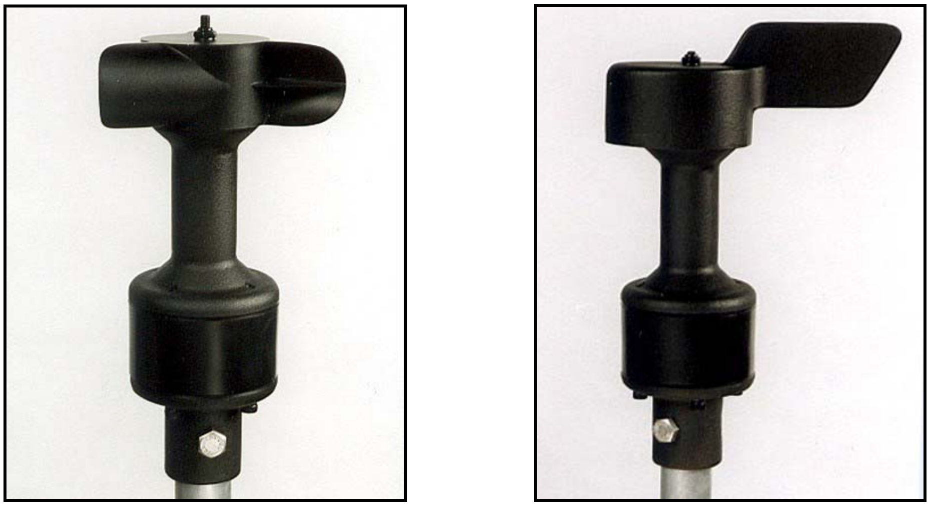

(A) (B)

FIGURE 8. NRG ANEMOMETER (A), AND DIRECTION VANE (B)

and production model 425T units are being used in the FAA LLWAS–RS program. The 425AH sensor is also used to provide airport centerfield winds for the JWHIS system. The modified 425AH was previously tested for severe weather performance at MWO, but results were inconclusive. The 425AH has an integrated microprocessor that acquires and processes wind data, and performs serial data communications. An array of three equally spaced ultrasonic transducers in a horizontal plane measures the transit time for sound to travel from one transducer to another. The transit time depends on the wind velocity along the sonic path. Unreliable readings, which may occur when large raindrops or ice pellets hit a transducer, are eliminated by an internal signal processing technique.

Production models of the 425AH have thermostatically controlled transducer heads with a total heat output of about 30 W. The modified "superheated" unit that was employed in this test has additional heating elements covering the sensor body and transducer arms, and consumes approximately 240 W. The test unit is the same physical sensor which was tested at MWO (as shown in figure 9); however, the firmware was upgraded from v2.03 to v6.02 to permit faster data acquisition, and the color of the heater elements was changed from red to black to deter the perching of birds. The sensor was mounted without the supplied bird spikes installed. It should be noted that this sensor is a prototype unit and no performance levels are implied or guaranteed by the manufacturer.

3.2.2.2.1.4 Rosemount Anemometer.

In addition to testing the three types of wind sensors identified above, a BFGoodrich Rosemount Aerospace Model 1774W Anemometer was acquired and installed. This wind sensor is solid state and heated, and uses pressure transducers to determine wind vectors. A photograph of the sensor is provided in figure 10. The anemometer detects wind by measuring the differential pressure across the wind probe. Two orthogonal pressure differential measurements are taken in order to determine the North-South and East-West wind vectors. The sensor uses RS-232 serial data communications.

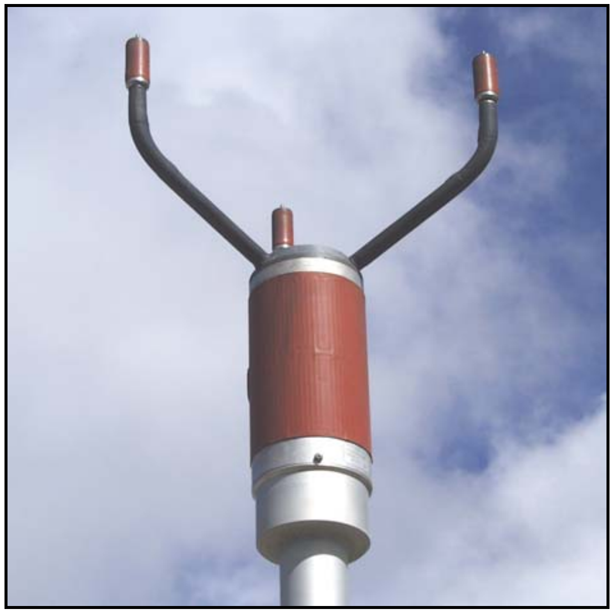

FIGURE 9. VAISALA HANDAR 425AH SUPERHEATED ULTRASONIC ANEMOMETER

FIGURE 10. BFGOODRICH ROSEMOUNT AEROSPACE MODEL 1774W ANEMOMETER

3.2.2.2.1.5 Metek Anemometer.

Original plans included installation of a Metek Model USA1 ultrasonic anemometer, which is shown in figure 11. This sensor measures vertical wind components in addition to the conventional horizontal wind. The primary purpose of this sensor is to measure and collect 3-dimensional wind data in order to determine the extent, magnitude, and effect of upslope winds on Eagle Crest. It is not under consideration for use in the final JAWS system. Because the survivability of the Metek sensor is questionable during the winter months in JNU, it was planned that the sensor would be installed and utilized in the spring of 2001. Unfortunately, the sensor was not installed during that time because of sensor procurement and installation problems. However, the sensor is included in the technical discussion in this report in order to support future installation and setup of the sensor.

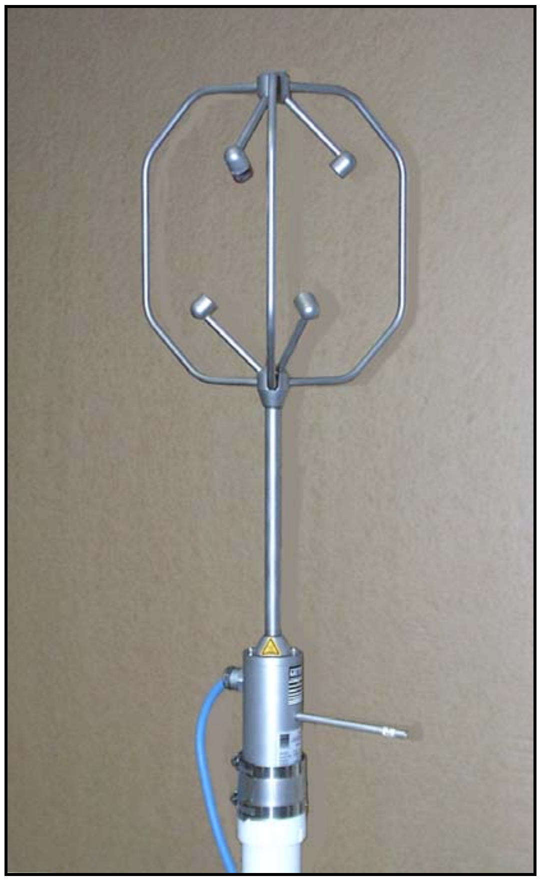

FIGURE 11. METEK USA1 ULTRASONIC ANEMOMETER

The characteristics and specifications for all the wind sensors are provided in table 1. These requirements have been compiled from manufacturers product brochures and specification sheets. Blank areas in the table indicate parameter values that were not specified by the manufacturer, or parameter values that were unable to be estimated as a by-product of the field test.

TABLE 1. WIND SENSOR SPECIFICATIONS

Sensor		Taylor Hydro-Tech Wx-3	NRG IceFree II HxE II	Vaisala Handar 425AH	Rosemount Aerospace 1774W	Metek USA-1
Sensor Type		Cup/ Vane	Cup/ Vane	Ultrasonic	Pressure Transducer	Ultrasonic
Speed	Range (m/s)	~1.8–90+	0–90	0–64	0-77	50
	Resolution (m/s)			0.1		0.1
	Accuracy (m/s)	2% and linear		±0.13 ≤49 ±5% >49	±0.38 ≤21 ±2% >21	±0.03 ≤20 ±2% >20
	Start Threshold (m/s)	1.3 (pulse)	1.1	~0		~0
	Distance Constant (m)	47 @ 9 m/s	7.6	~0		~0
Direction	Range (°)	0–360	0–360	0–360		0–360
	Resolution (°)	Continuous	Continuous	1		1
	Accuracy (°)	±1%		±2	±5° ≤15 ±3° >15	±3 for ≥4.1 m/s
	Start Threshold (m/s)	1.1	1.1	~0		~0
	Delay Distance (m)			~0		~0
	Time Constant (s)			~0		~0
Off-axis Response		Noted	Correction			100% (3-D)
Operating (°C)			-40 –+80	-50–+50	-55–+71	-30–+50
Max Power Consume (W)		1500	200	240†	200	55
Survivability (kt)		>90	90			50
De-icing		De-ice at 13–15 m/s, 3-4 g/cm/h				

† Superheated version

3.2.2.2.2 Ice Detection.

To provide an automated means of detecting icing conditions, a Rosemount Model 871FA Ice Detector was installed at the test site. The sensor measures the amount of ice mass accumulation on a cylindrical metal probe. The probe is vibrated at a natural resonance frequency of 40 kilohertz (kHz). As ice accretes, the frequency of the vibration decreases. Once a preset amount of ice mass has accumulated, the cylinder heater is activated to melt and remove the ice. The standard trip point is 0.5 millimeter (mm) (0.020 in) ice thickness with an accuracy of about ±25 percent. Because the sensor is designed for installation through the skin of an aircraft, a special metal housing was used to mount and protect the sensor body. A photograph of the sensor and the housing is shown in figure 12.

This ice sensor configuration is similar to that employed at MWO. For this study, extra modifications were applied to the sensor and installation since the behavior of the ice detector was erratic on occasions during the MWO effort. Sensor performance may have been affected by excessive ice buildup immediately around the probe, as the unheated housing may have allowed formation of ice around, rather than on, the probe. In order to prevent the buildup of ice and/or snow around the sensor, the sensor housing was wrapped in a conformal heating blanket, and the housing was tilted to promote the runoff of ice-melt water.

FIGURE 12. ROSEMOUNT ICE DETECTOR AND ENCLOSURE

Air temperature and relative humidity was measured by a Rotronic MP100H Temperature and Humidity Probe. The integrated probe consists of a platinum resistance thermometer and capacitive-type relative humidity sensor, and was housed directly in a 12-plate Gill solar radiation shield. To prevent the buildup of snow and ice directly on the sensor and shield, the unit was mounted in the specially fabricated cylindrical housing that was used in the MWO study. The enclosure is an aluminum canister with top and bottom openings to permit ventilation.

A total of four video cameras were set up to provide real-time visual monitoring and recording of icing on the sensors. Because of the shortcomings and numerous difficulties encountered with the video camera used during the MWO experiment, two different types of camera configurations (shown in figure 13) were employed in this effort to capture video images.

Arctic Hawk V60 video cameras by Silent Witness were used. Special conformal and temperature-controlled heater blankets were applied to the camera housings to prevent ice buildup. In addition, two Sony SPT-M324 black and white video cameras each mounted in a Videolarm AP21 camera enclosure were used. The enclosure is internally heated and pressurized to prevent icing and condensation buildup on the camera lens. External conformal heating blankets were also fabricated to further prevent ice buildup. One of these cameras was installed while the other was maintained at the site as backup. All cameras were connected via unshielded coaxial cable to a Sony video receiver/server located in the instrument shelter beneath the tower.

(A)

(B)

FIGURE 13. ARCTIC HAWK V60 VIDEO CAMERA (A), AND VIDEOLARM CAMERA ENCLOSURE (B)

The sensors were illuminated at night by two RAB Model QT250 Quartz flood lamps. Each is a 250 W quartz halogen lamp with 5,000 lumens. The relatively low wattage lamps minimized the possibility of heat transfer to the sensors.

3.2.2.3 Sensor Installation and Configuration.

Positioning and installation of the test sensors and the equipment on the tower were performed so that the permanent JWHIS sensors, which support JNU operations, were not affected by the additional test sensors and equipment. In addition, the sensors were situated and spaced so that they were optimally exposed to operationally significant winds, and that shadow effects caused by nearby equipment were minimized.

A schematic diagram of the tower equipment orientation with respect to the JNU airport and operationally significant winds is shown in figure 14. The figure shows the prevailing wind and the range of wind directions for which the Ops Spec wind restrictions are applicable. The prevailing wind shown in the figure is based on the southeast flow from the Eagle Crest wind rose shown in figure 5, and climate data for JNU. Although the Juneau area is also subject to a northeasterly flow known locally as Taku Winds, the test site is oriented with respect to southerly winds, which are typically associated with wet maritime events known for creating significant icing conditions.

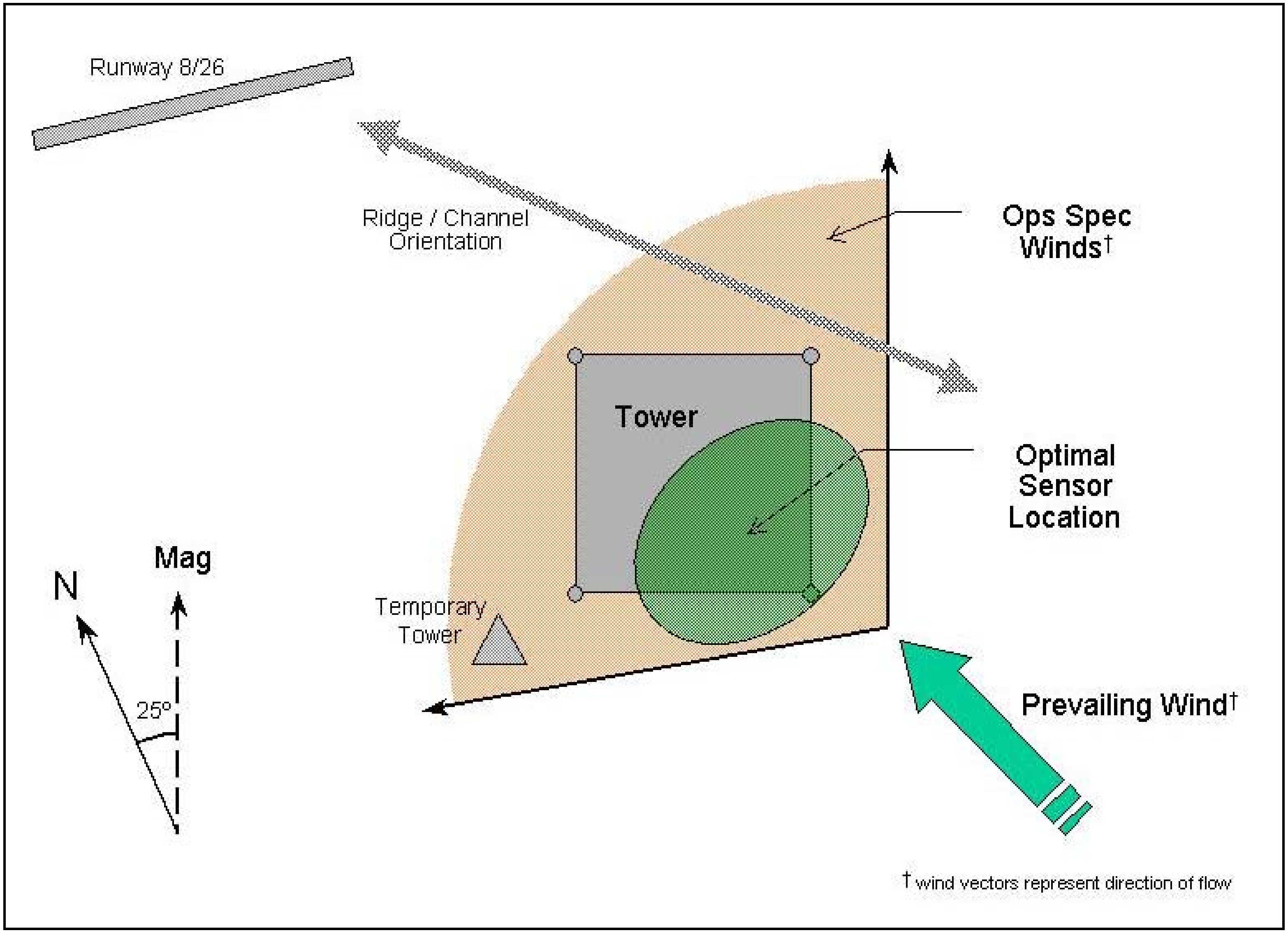

FIGURE 14. SCHEMATIC DIAGRAM OF PREVAILING WINDS AND TOWER ORIENTATION

The resulting area on the tower where wind sensors would be best exposed to the operationally significant winds is indicated in the figure.

Based on figure 14, the equipment layouts and installations shown in figures 15 and 16 were derived. The sensors were staggered vertically with the JWHIS wind sensors mounted 4 ft above the railing of the tower platform. The temperature/humidity sensor is located on the exterior wall of the instrument shelter. Figure 17 shows the various camera angles that were configured throughout the experiment.

3.3 INTERFACES AND DATA ACQUISITION.

The test bed data interfaces, acquisition, and recording setup were designed for complete unattended operation and maintenance during the test period. At the same time, the interface and data were collected from the JWHIS sensors in a manner that did not affect or degrade operations of those sensors.

3.3.1 JWHIS Data Acquisition.

A block diagram showing the data interfaces and data collection components of the JWHIS station at Eagle Crest is given in figure 18. The figure shows the redundancy and backup capabilities built into the JWHIS design. The EC1 package consists of the primary wind sensors and associated data processing, and communications equipment, while the EC2 package consists of the backup wind sensors, temperature data, data processing, and communications equipment.

The communications hub of the JWHIS anemometer network is located at the Alaska Airlines Operations Tower located on the airport. All Eagle Crest anemometer data, as well as JWHIS wind data from the other two ridge-top anemometer sites and the centerfield location, are routed to a patch panel and data ingest computer located in the crawlspace area under the Ops Center floor. The data communications is accomplished via 900 MHz spread-spectrum wireless modems manufactured by Freewave. The data that is transmitted from the sensor sites consists of 1-second wind and temperature data. As shown in figure 17, two separate modem and antennae pairs are used so the data stream of the backup EC2 data is completely independent from the primary EC1 data.

The RS-232 patch panel provides the means to split and route the EC1 and EC2 information as desired. The primary data path is EC1 and EC2 data to the NCAR anemometer ingest computer, located in the crawlspace. A second data path facilitates the display of EC1 wind data in the Alaska Airlines Operations Tower on display equipment owned by Alaska Airlines. The incoming 1-second anemometer data is averaged within the ingest computer to produce 1-minute data for display. These 1-minute averages are produced through a series of Data Quality Analysis (DQA) algorithms. Basically, a test is first performed to verify that: 1) the format of the incoming anemometer data conforms to the correct format, 2) data transmission errors are accounted for, and 3) values for wind speed and wind direction fall within realistic bounds. Next, the temporal continuity of the data is checked to ensure that the variance of the 1-second data is reasonable and consistent with what is expected in a continuous atmosphere.

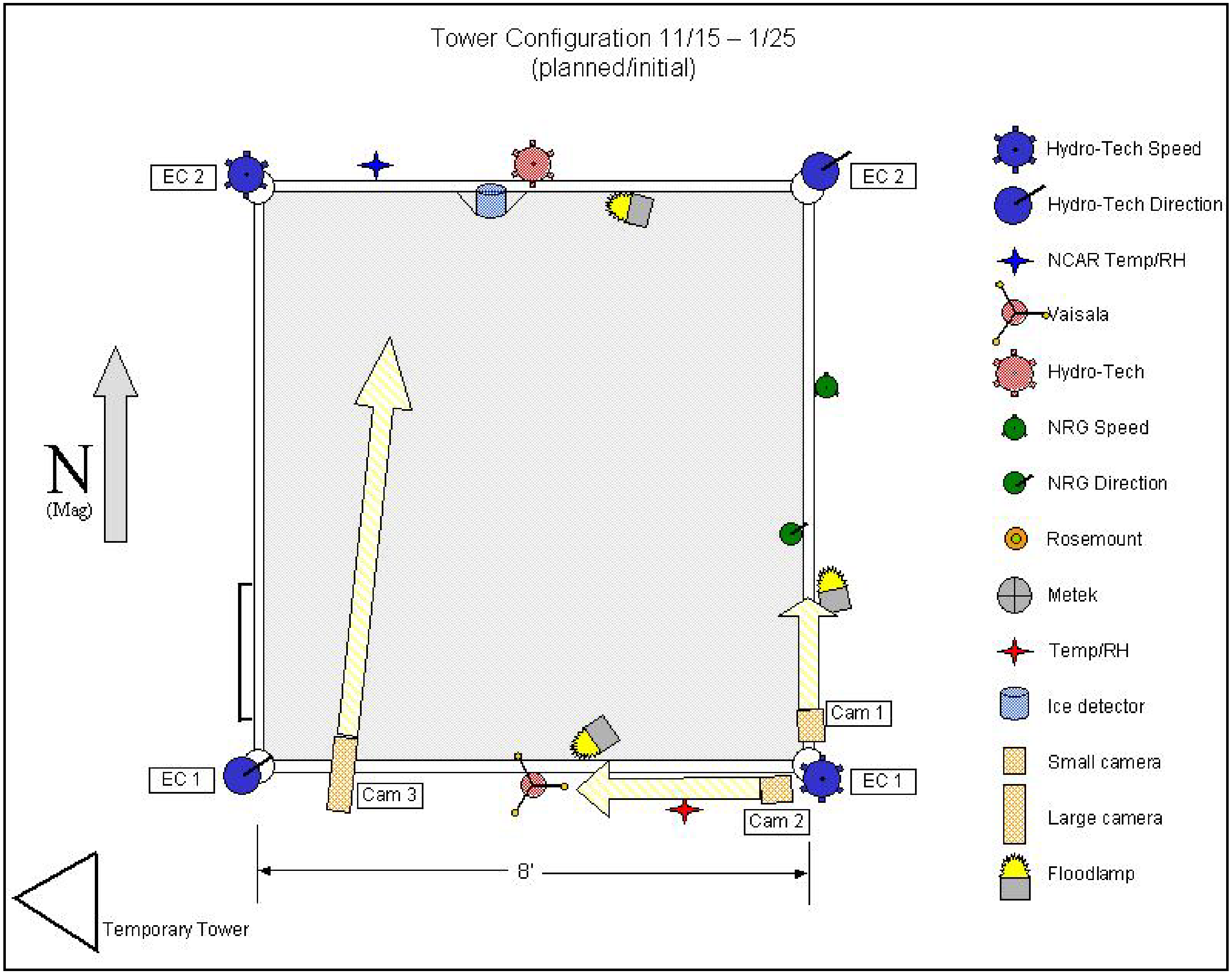

FIGURE 15. PLAN VIEW OF SENSOR AND EQUIPMENT LAYOUT

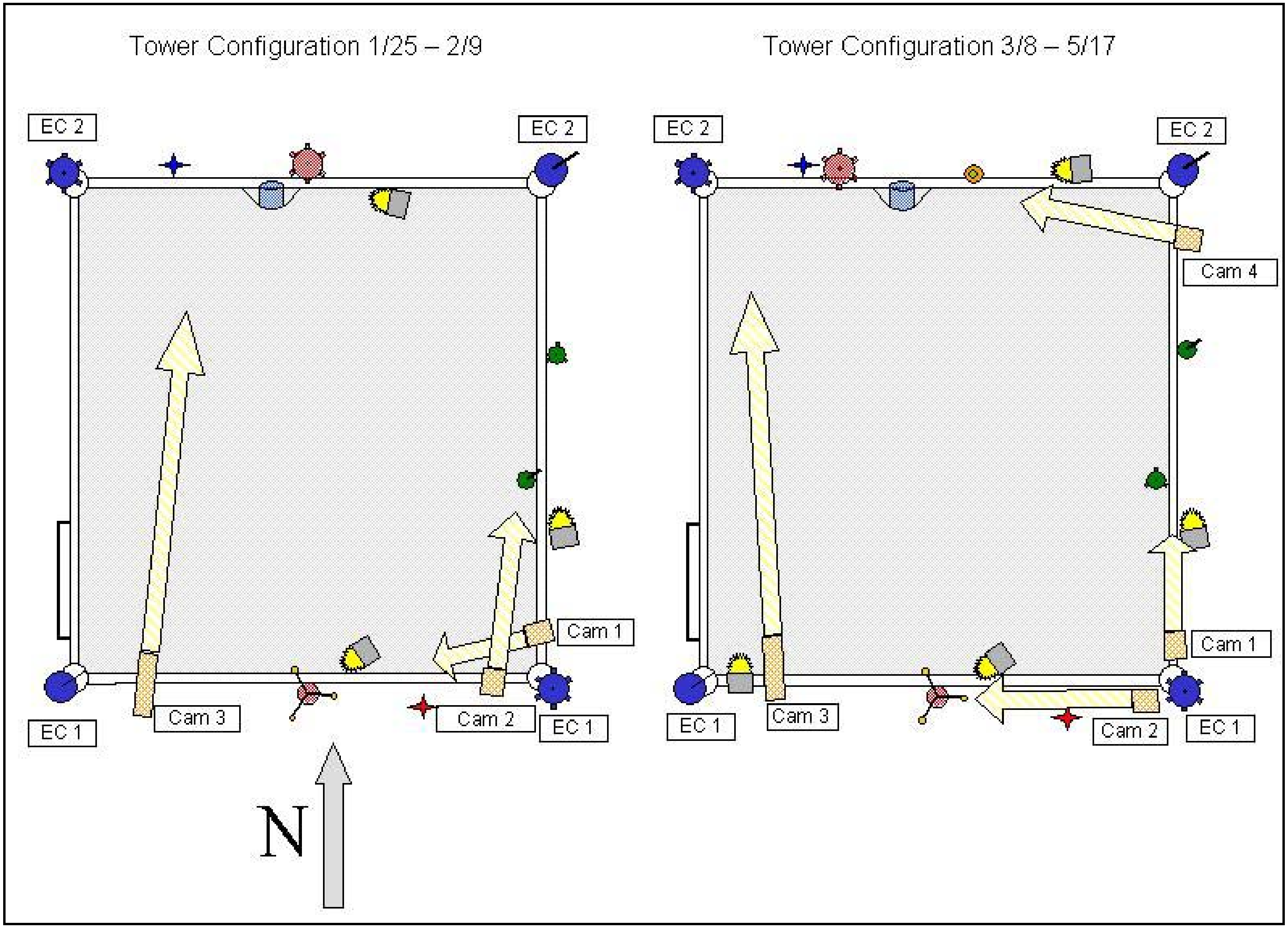

FIGURE 15. PLAN VIEWS OF TOWER CONFIGURATIONS (CONT'D)

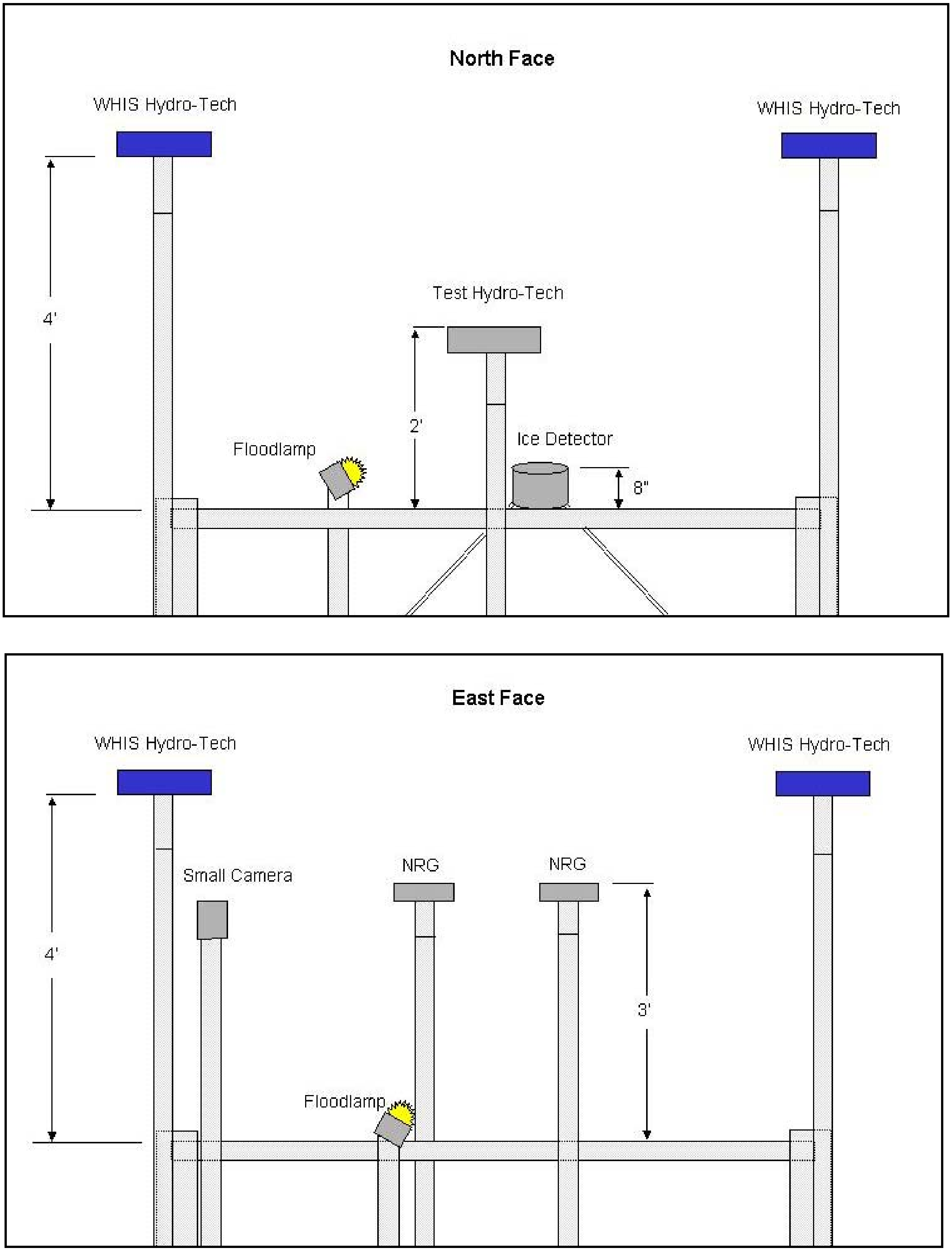

FIGURE 16. ELEVATION VIEWS OF TOWER AND EQUIPMENT

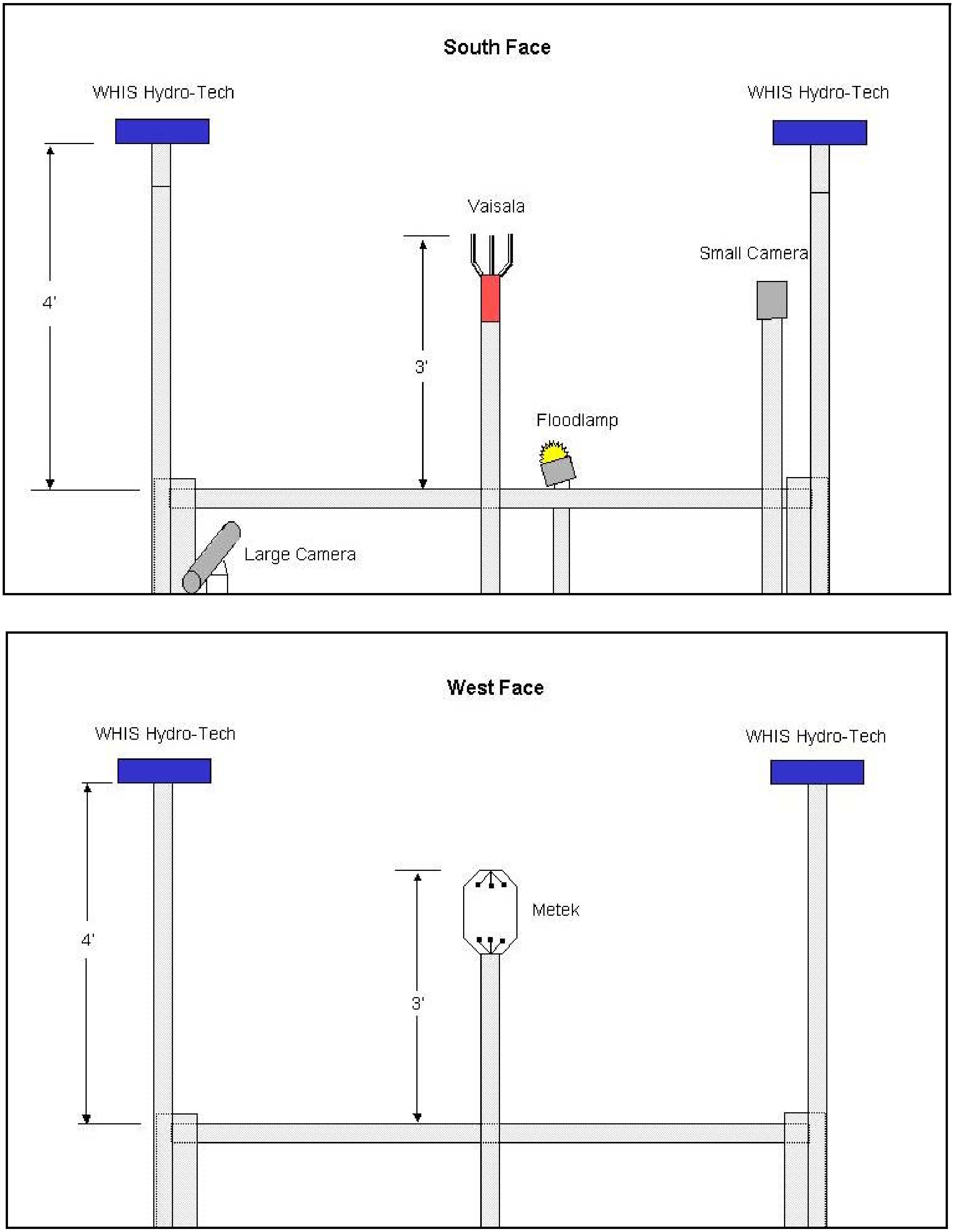

FIGURE 16. ELEVATION VIEWS OF TOWER AND EQUIPMENT (CONT'D)

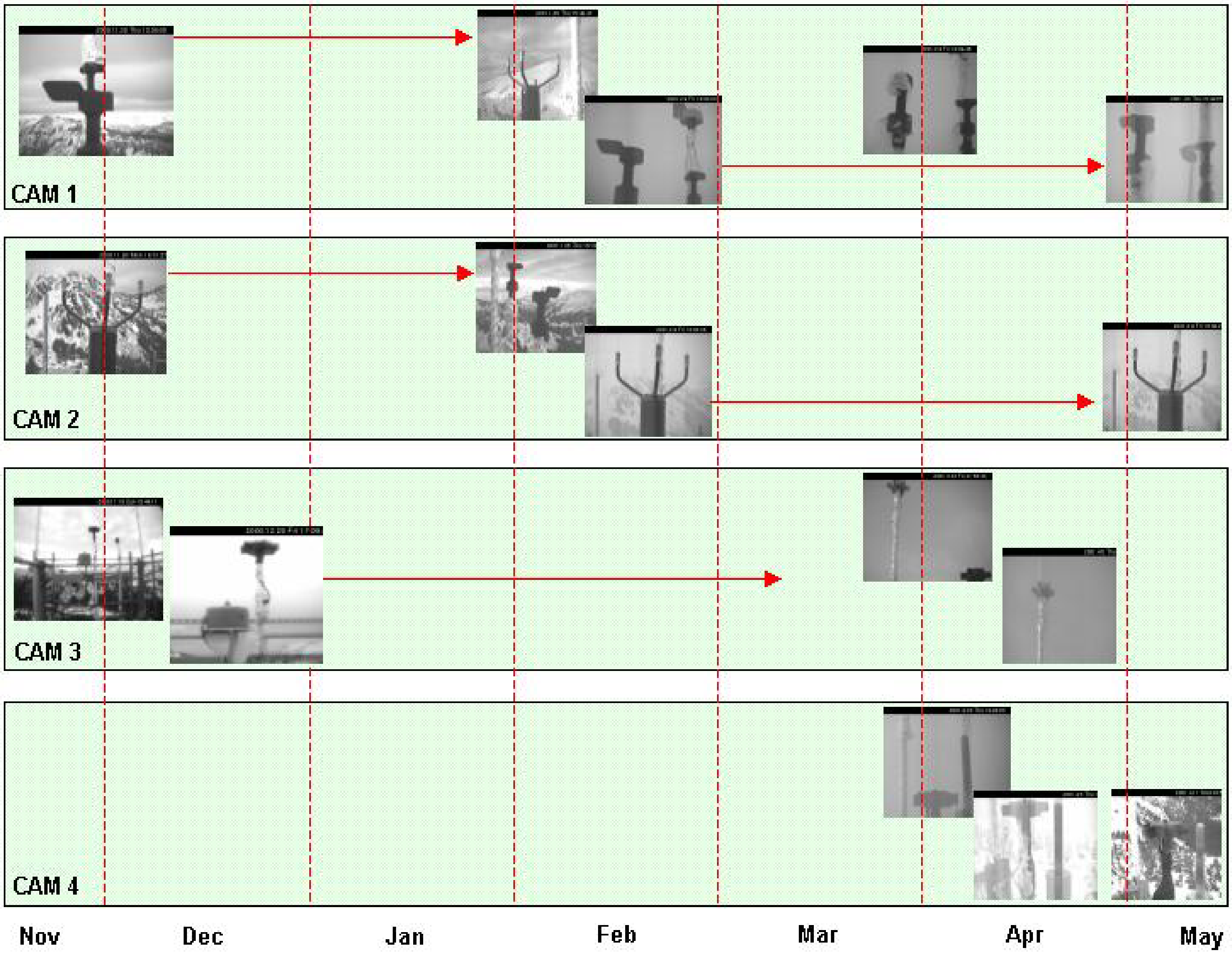

FIGURE 17. CHRONOLOGICAL SEQUENCE OF CAMERA CONFIGURATIONS AND VIEWS

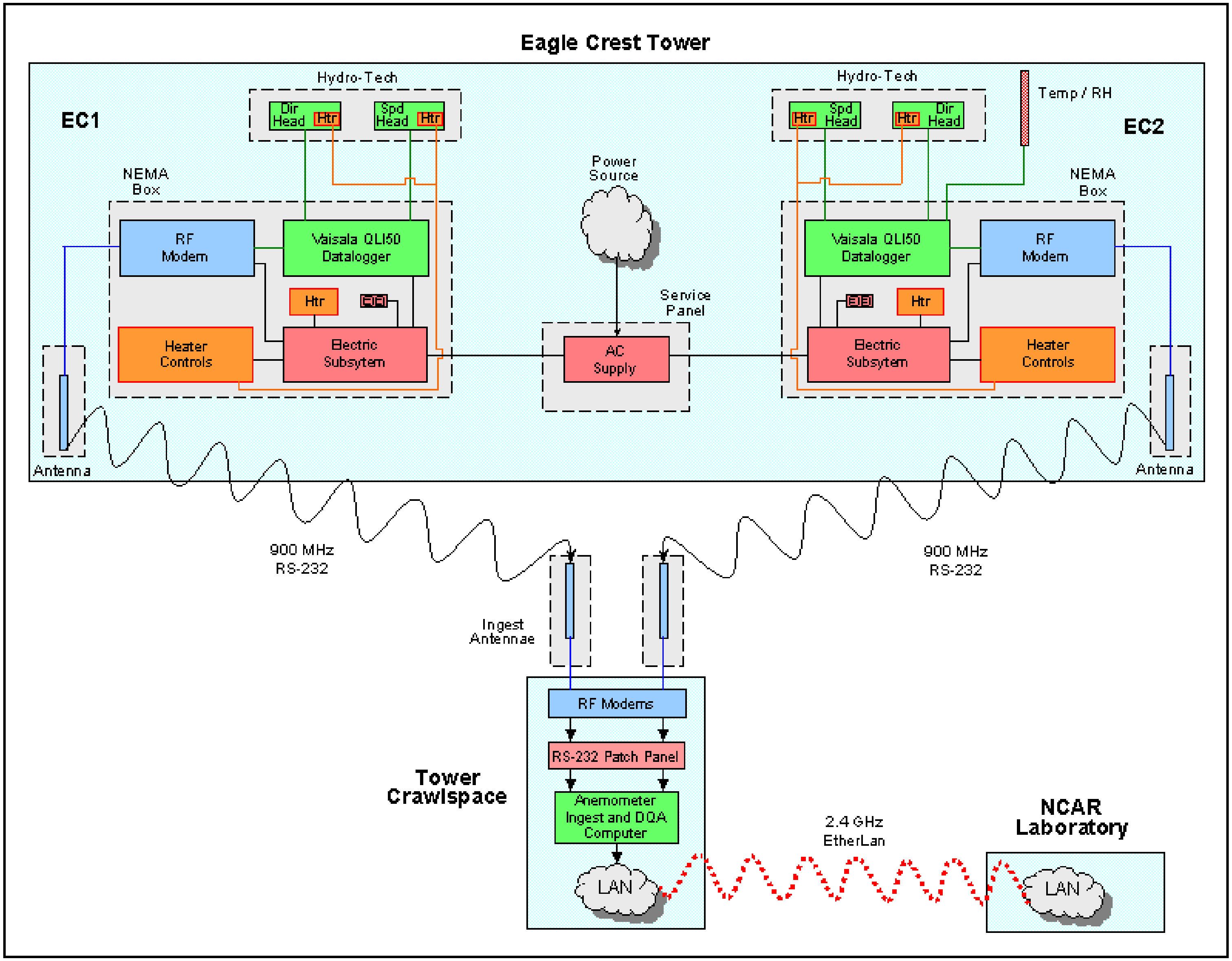

FIGURE 18. DATA INTERFACES AND COMMUNICATIONS FOR EAGLE CREST AUTOMATIC WEATHER STATION

The temporal test assigns a confidence to each data point, and a confidence weighted one-minute average is then calculated. A single wind value is finally derived from the 1-minute averages for the primary and backup sensors (i.e., EC1 and EC2) in order to mitigate iced-over anemometers and equipment failures.

The one-minute average wind data is transmitted to the NCAR laboratory via a 2.4 gigahertz (GHz) wireless Ethernet link. Additional processing is performed at the NCAR laboratory, and outputs are generated for displays located at various facilities in Juneau and Seattle. Processed data is also sent back to Alaska Airlines Ops via wireless Ethernet for display on NCAR equipment. This display equipment is collocated in the Ops center with Alaska Airlines' display equipment. The data is also transferred, via the Alaska Airlines Wide Area Network (WAN) to their dispatch office in Seattle, which also has NCAR equipment. The Juneau Automated Flight Service Station (AFSS) and National Weather Service (NWS) Office also each have a computer and display. Anemometer information is sent to these locations via dial up telephone lines with 56 kilobytes per second (kbps) modems. A subset of the information is available to the NCAR/Research Application Programs (RAP) personnel in Boulder via commercial Internet service

3.3.2 Test Data Acquisition.

Collection of the test data for this effort centered around a network of data acquisition and Ethernet communications devices using Internet Protocol (IP) between the mountain test site, the crawlspace, and laboratory on the airport. All data acquisition equipment for the weather sensors along with recorders and receiver/servers for the video cameras were installed in a separate enclosure in the instrument shelter located beneath the tower. The equipment was connected to an APC 1000XL Uninterruptible Power Supply (UPS) with a 670 W capacity. Communications and management software allowed for remote monitoring and auto-shutdown capabilities. It was estimated that the UPS unit would supply an estimated 1 hour of runtime power for the processing and communications equipment.

A data acquisition block diagram for the test equipment is provided in figure 19. Analog data from the Hydro-Tech, NRG, ice detector, and temperature/humidity sensors was captured and digitized by a Campbell Scientific CR23X Micrologger. Digital data from the datalogger, along with the RS-232 serial outputs from the ultrasonic sensors, were converted to 10BaseT Ethernet protocol by separate serial servers (or adapters). As a rule, all wind speed data was maintained in meters per second, and all wind direction data was referenced in degrees from magnetic north. Video images from the four cameras, in the form of Joint Photographic Experts Group (JPEG) files, were captured and transformed to Ethernet protocol using a Sony video multiplexer and server. The sampling rate and streaming output of the datalogger and ultrasonic anemometers was once per second. Because of the information type and file size, video image data was translated and made available on the network on a polling basis of adaptable frequency. The default polling frequency was 1 image per camera every 15 minutes.

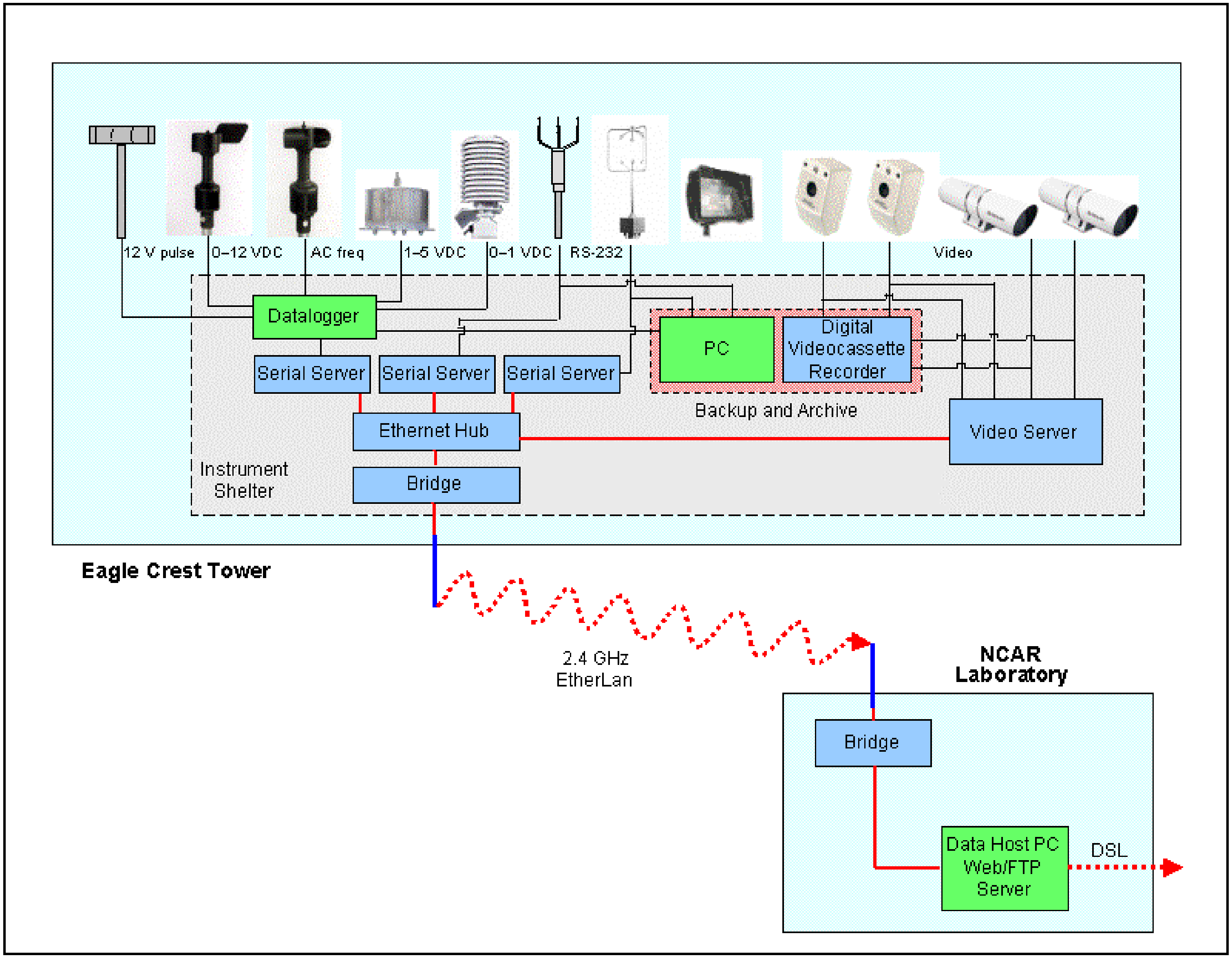

FIGURE 19. DATA ACQUISITION FOR TEST SENSORS AND EQUIPMENT

The serial servers and the video server were each assigned a separate IP address on the network, and brought together into an 8-port Ethernet hub. The sensor data and video images were then transmitted to the laboratory via a pair of high speed, long range wireless Local Area Network (LAN) bridges. This high-speed wireless network connection provided the bandwidth required for the combined sensor and video data.

Two backup devices in the instrument shelter were used to ensure full backup and archive of sensor and video data in the event of network or data transmission problems. A Gateway E-4400 800 MHz Pentium III computer with 256 Megabytes (MB) Random Access Memory (RAM) and 75 Gigabytes (GB) hard disk was used to directly collect the RS-232 serial output data from the datalogger and ultrasonic wind sensor. The Personal Computer (PC) operated under Windows Network (NT) Workstation 4.0 and utilized WinWedge data acquisition software to capture, parse, and record the raw serial data. One data file was created on the PC per day.

The second backup storage device was a Sony digital videocassette recorder, which recorded video images onto tape at a rate of 1 image per second. Both the serial server data and the video data was recorded every 1 second. Based on the data size estimates, it was determined the capacity of the 75 GB hard disk and a single video cassette tape would accommodate up to two months of continuous data recording.

A Yagi antenna on the laboratory roof and a wireless Ethernet bridge converted the mountain data to 10BaseT Ethernet protocol for ingest into the Technical Center's data processing PC in the NCAR laboratory. This PC was also protected with an APC 1000XL UPS and acted as the data host and server by performing the primary data collection, recording, and backup functions. The PC was a Gateway E-4200 800 MHz Pentium III computer with 256 MB RAM and an 18 GB hard disk. The Windows NT Server 4.0 operating system has integrated Internet Information Server (IIS) technology to furnish the Web and File Transfer Protocol (FTP) server capabilities that were exercised for remote on-line data monitoring and control, as well as data file downloads of daily sensor and video data. Internet access to the host was accomplished through a dedicated Digital Subscriber Line (DSL) modem and Alaska Communications Systems (ACS) Internet service operating at upload and download speeds of 256 and 320 kbps, respectively. The continuous DSL and Internet connection provided the greater speed and bandwidth required for the volumes of combined sensor and video image data.

The complete data set for this effort includes data from the JWHIS sensors, and data from the test sensors and cameras. A diagram of the integrated end-to-end data collection architecture showing the communications interfaces is shown in figure 20. JWHIS operational data from EC1 and EC2 was acquired directly from the RS-232 patch panel in the crawl space. This facilitated the independent acquisition of the required 1-second wind data, and ensured that the JWHIS operational data collection for JNU was not affected. The data was converted to Ethernet protocol via serial servers, and transmitted to the laboratory utilizing the existing NCAR network between the crawlspace and laboratory. The JWHIS data was captured from the network via the Internet, and assembled within the host PC. The 1-second EC1 and EC2 data was merged with the test data, and further processed and stored.

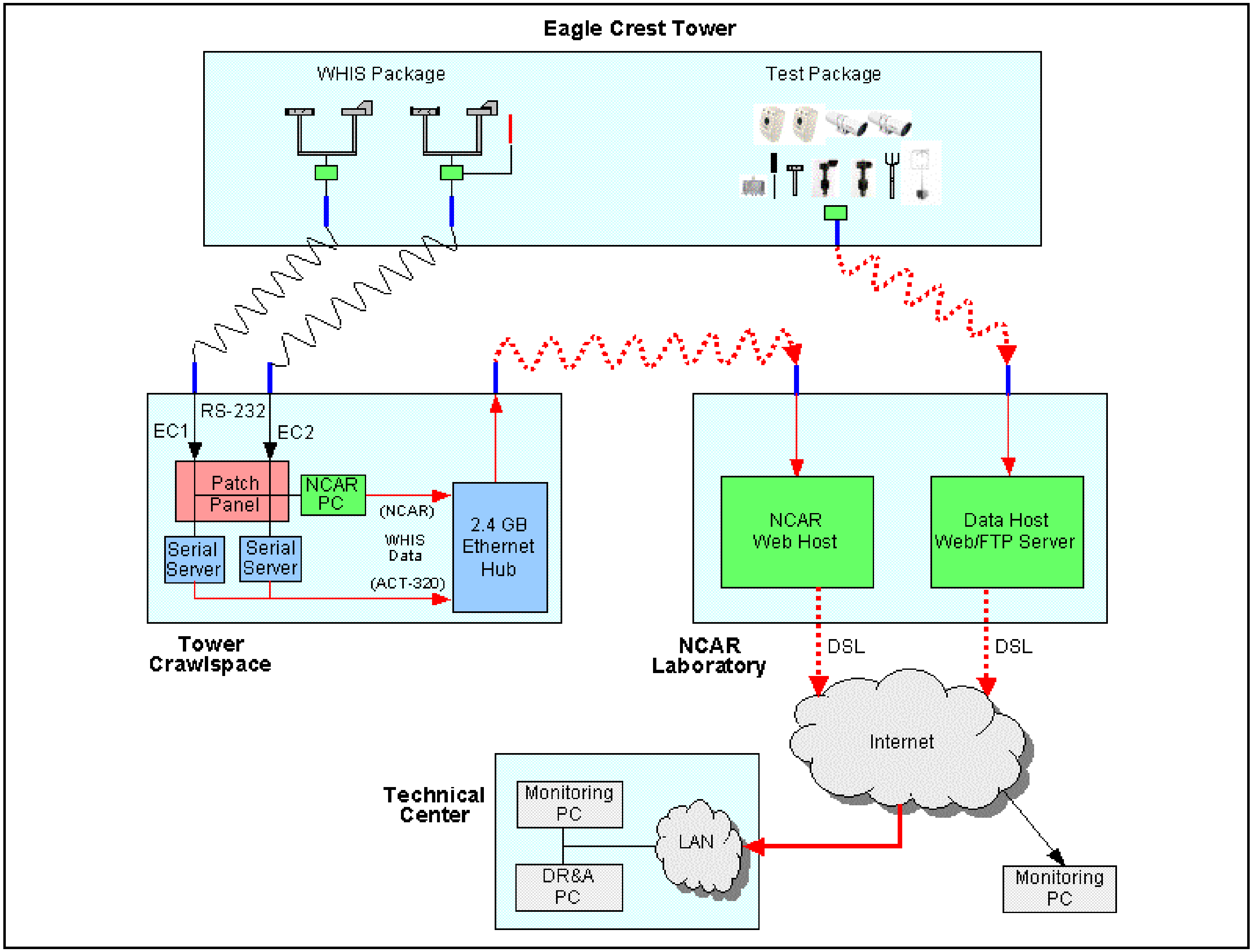

FIGURE 20. INTEGRATED DATA ACQUISITION AND COMMUNICATIONS ARCHITECTURE FOR COLLECTING JWHIS DATA AND TEST DATA

The test PC employed several software applications for the data processing and storage of the sensor and video data. Custom software was developed using Visual Basic to independently capture and parse the four channels of digital information, i.e., datalogger, ultrasonic anemometer, EC1, and EC2 data.

The software timestamps the 1-second data, parses the data into individual data fields, and stores the data to a file, which was available for download via the FTP server capability. Data and files were stamped in Coordinated Universal Time (UTC), and the time source and synchronization was based on a standard external clock source and utility used by the NCAR network. It should be noted that the time stamp on the legend of the camera video images is in local time.

A custom Visual Basic software application was developed and used to control the collection of the video images. As previously mentioned, the video images in the form of JPEG files were retrieved from the mountain on a request/reply basis by polling the video server. The default value of 1 image per camera every 15 minutes was used. As the JPEG images were retrieved, they were copied to a folder and made available for the Web On-Line Monitoring function, and stored in files for FTP download.

Custom Visual Basic software and Dynamic Data Exchange (DDE) capabilities were developed to process the 1-second sensor data and prepare the data for the Web server and remote On-Line Monitoring. The software generated for each weather variable, a 2-hour time series of running 1-minute averages updated every 1 minute. Charts in JPEG format were then generated for each time series. The time series, in the form of JPEG files, were displayed on the test site Web page. Microsoft FrontPage software and Web authoring tools were used to develop and maintain the Web site. The procedural development and content of the pages were similar to the Web site that was developed for the MWO effort. The Web page displayed and updated the sensor time series and camera images every 1 and 15 minutes, respectively.

The FTP capability was used for bulk file download and collection of sensor data and video images for later analyses. Sensor and video data that was collected was stored in files, each of which comprise 1 day of data.

4. TEST AND EVALUATION DESCRIPTION.

The testing activity was comprised of three separate phases: wind tunnel testing, laboratory mockup, and the actual field assessment of the sensors.

4.1 WIND TUNNEL TESTING.

4.1.1 Test Objectives and Criteria.

The objective of the wind tunnel testing was to verify the calibration of the wind sensors, and to verify the dynamic response of the sensors. Testing was also performed to determine the effects of off-axis winds.

4.1.2 Testing Description.

Before field installation at JNU, checkout and calibration of the anemometers were performed in a manner similar to the test description and procedure provided in the LLWAS–RS Ultrasonic Wind Sensor Acceptance Test Report [9]. The wind tunnel testing was carried out in the Aerolab Low Turbulence, Low Speed open-circuit type wind tunnel in the FAA Airport and Aircraft Safety Branch, AAR-420 wind tunnel facility at the Technical Center. The wind tunnel was designed to provide an environment to calibrate wind speed instruments employing a highly accurate airspeed measurement capability. Airspeeds ranging up to 71.5 m/s (160 miles per hour (mph)) can be achieved in the 51 x 71 x 122 centimeters (cm) (20 x 28 x 48 in) wind tunnel test section. The airspeed is measured via a static pressure tube and graduated inclined manometer.

For this effort, special mounting fixtures were designed and fabricated in order to provide three degrees of freedom for sensor positioning within the wind tunnel test section. The apparatus primarily permitted tilting of the sensor from the vertical so test runs could be performed to determine sensor response for varying wind angles of attack from the horizontal (i.e., off-axis winds). The sensors were mounted along the centerline of the test section on the fixture, which passed through the floor of the wind tunnel. For the Vaisala test runs, the sensor was tilted ~8º normal to the air flow (i.e., towards the test section side wall) in order to minimize cross-talk interference that may result from ultrasonic reflections off the wall surfaces. Tilts of -20, -10, 0, +10, and +20 degrees from the vertical were considered for all the sensors, where negative angles represent a sensor tilt away from the airflow, and positive angles represent sensor tilts towards the flow (e.g., representative of upslope and downslope winds, respectively). Photographs of the wind tunnel setup with wind sensors mounted in the test section are provided in figure 21. Close up photographs of the wind tunnel test section with wind sensors mounted at various tilts are provided in figure 22. Scale drawings of the sensors relative to the wind tunnel cross section are shown in figure 23. The ~8º tilt of the Vaisala sensor normal to the airflow is also depicted in figure 23.

Since the Vaisala sensor measures both wind speed and direction, the sensor was rotated in the azimuth direction for various tilt angles in order to determine any shadow effects that may be experienced by neighboring transducers. The four non-trivial 15° azimuth orientations shown in figure 24 were considered. For each Vaisala sensor test run, the orientation of the sensor was

FIGURE 21. PHOTOGRAPHS OF WIND TUNNEL TEST SECTION

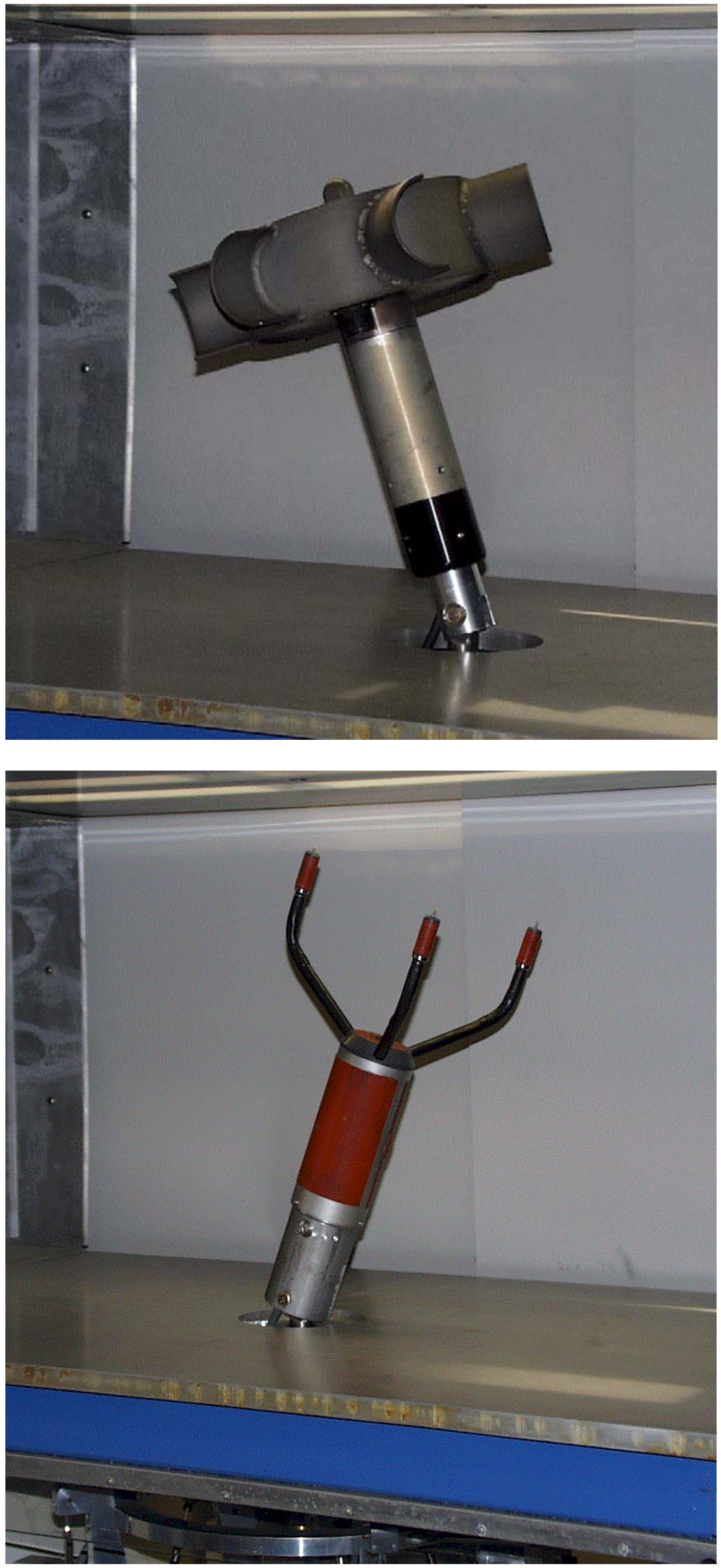

FIGURE 22. CLOSE UP VIEWS OF WIND SENSORS MOUNTED AND TILTED IN WIND TUNNEL TEST SECTION

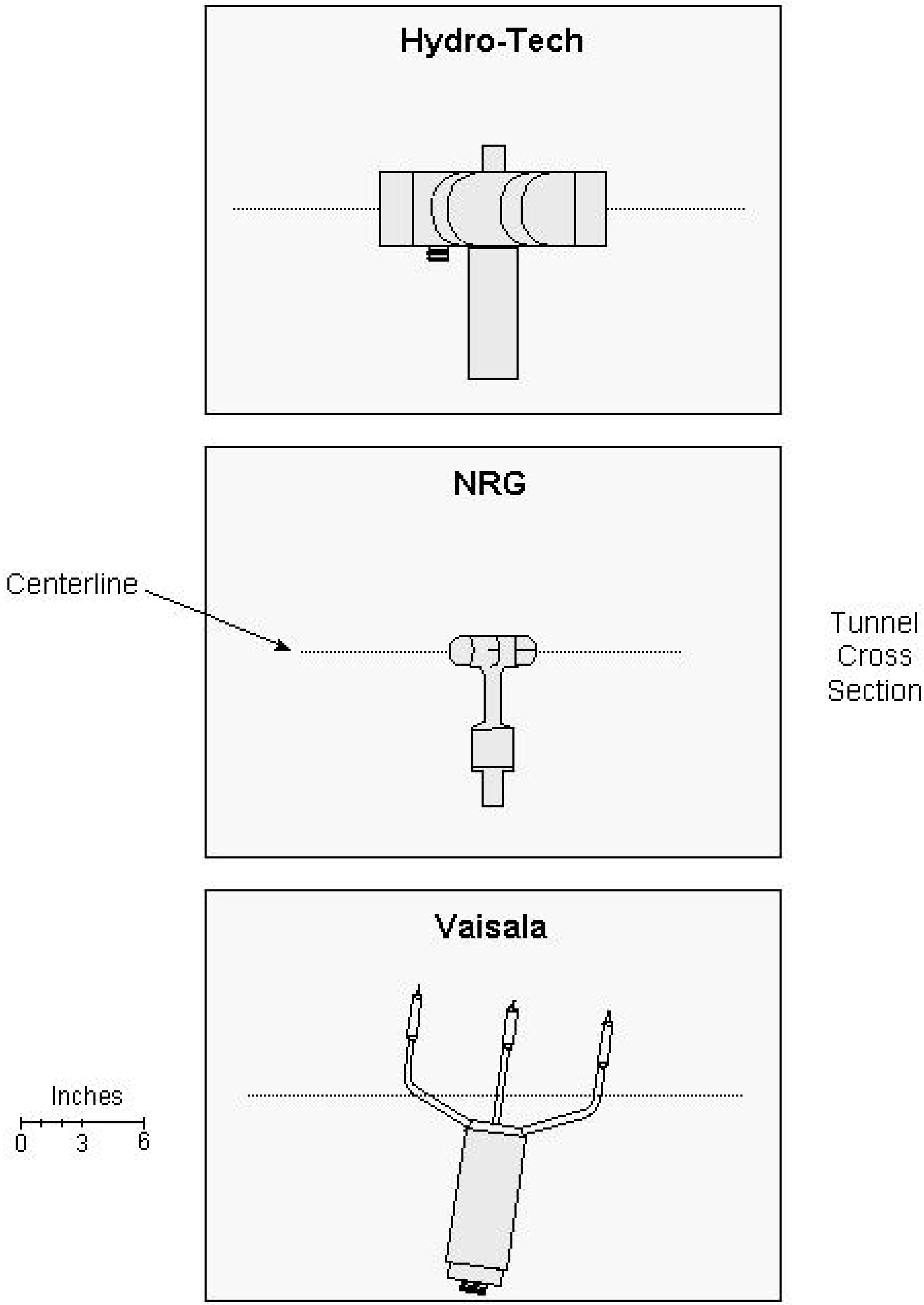

FIGURE 23. SCALE DRAWINGS OF WIND SENSORS POSITIONED IN THE WIND TUNNEL CROSS SECTION

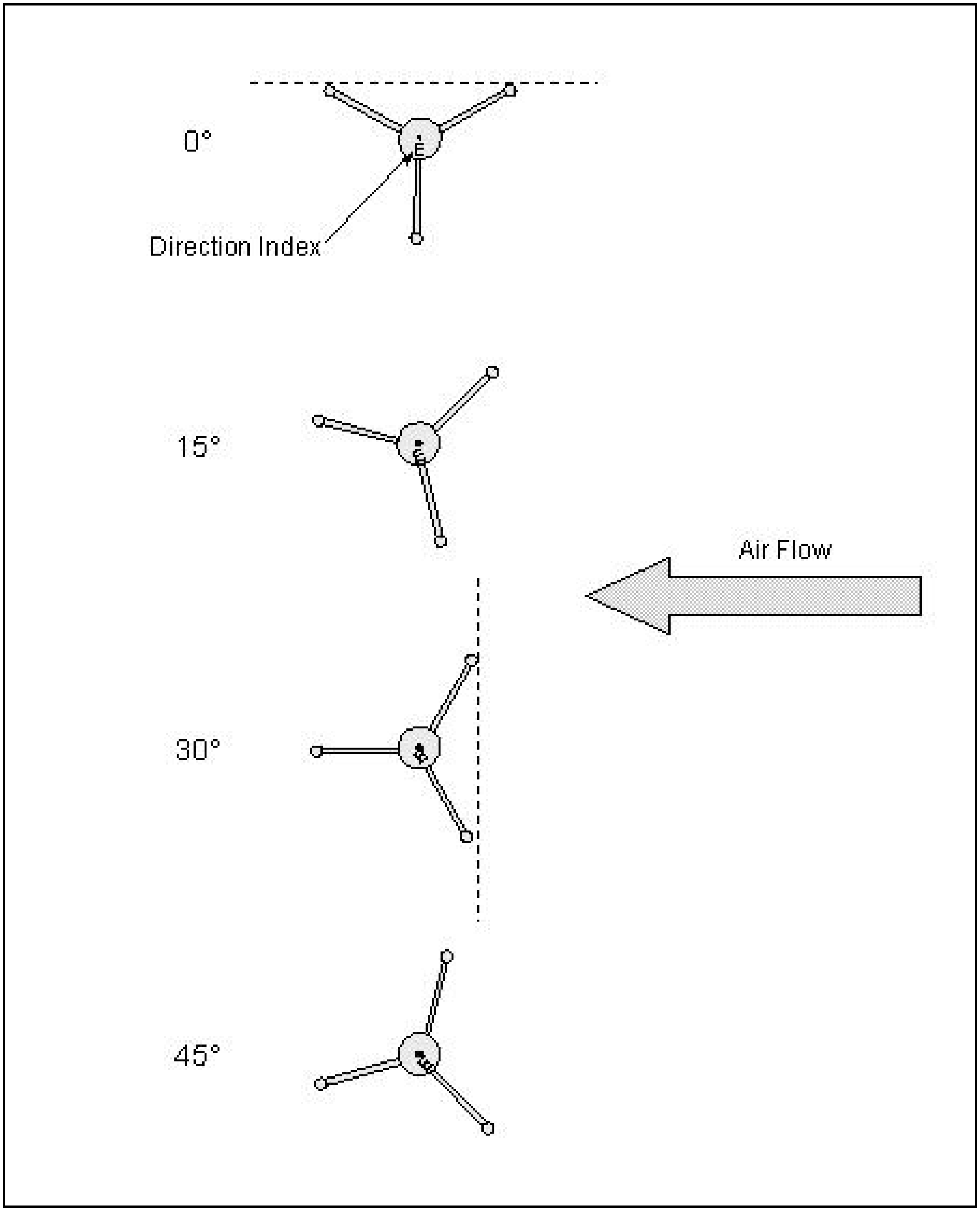

FIGURE 24. VAISALA WIND DIRECTION AZIMUTH ANGLES

established by rotating the sensor at one of the four varying azimuth angles. The angle was estimated visually, then by monitoring the wind direction output of the sensor in real time.

4.1.2.1 Wind Tunnel Test Types.

Sensors utilized in the test were tested as received from the manufacturers. Two separate types of tests were carried out on each sensor. The first type of test was conducted to verify the sensor wind speed accuracy, while the second type of test was carried out to verify the dynamic response characteristics of the mechanical sensors.

4.1.2.1.1 Accuracy Testing.

Accuracy testing was performed to checkout the calibration of the wind sensors, and for various tilts. Each test run was comprised of step increases in the wind tunnel speed for a fixed sensor tilt (and azimuth for the Vaisala sensor). In general, wind tunnel speeds were increased in 5-knot (kt) increments, then brought to and maintained at a steady state for the speed, tilt, and direction configuration while the wind tunnel air speed and sensor data were recorded over an approximate 30-s period.

4.1.2.1.2 Dynamic Response Testing.

The second type of wind tunnel test was performed to determine the dynamic response characteristics of the Hydro-Tech and NRG mechanical sensors, and for varying tilts. This testing was not performed on the Vaisala sensor since the dynamic response of the ultrasonic sensor to wind speed changes is nearly instantaneous based on the sensor's theory of operation and previous wind tunnel studies [9]. The response of the mechanical sensors was characterized by estimating their time constants assuming an exponential buildup of the sensor speed to an increase in wind tunnel speed. A time constant is the time required for an exponential quantity to change by an amount equal to 0.632 times (1-1/e) the total change that will occur. For example in a resistor-capacitor (RC) circuit, the time constant is the number of seconds required for the capacitor to reach 63.2% of its full charge after a voltage is applied. Then the observed exponential decay or buildup of the speed for the sensor should be 63% of the speed step size for the first time constant, then 63% of the remaining difference in each remaining time constant.

Estimating dynamic response is normally performed by introducing a discrete input step function and observing the output. Since an instantaneous increase in wind speed cannot be achieved by the wind tunnel fan, the step function was effectively accomplished by first bringing the tunnel airspeed to a constant speed of 40 kt, and maintaining that speed while physically retaining the sensor from spinning using a rod. The sensor rotor device was then released, and the sensor data is recording while the sensor responds and approaches the tunnel air speed.

4.1.3 Data Collection and Analysis Method.

A schematic diagram of the wind tunnel setup and data collection system is shown in figure 25. Test data sheets were used to manually record wind tunnel air speed and sensor data for each accuracy test run. The test sheet form is shown in figure 26. The reference wind tunnel air speed is determined by a manometer, and is recorded on test sheets during the tests. The electrical output of the wind sensors was also continuously recorded on a laptop PC. The sensor (or Unit Under Test) is connected to laptop PC via an RS-232 serial interface for the collection of 1-second anemometer data. A datalogger was used to convert the analog signal data from the mechanical sensors to RS-232 data for the PC. The PC is also used to handle the Vaisala sensor RS-232 serial interface and data protocol, and to send configuration commands to the sensor in order to set up the sensor in data collection mode. The PC hosted the special data acquisition software that was written using T.A.L. Enterprises Software Wedge, Version 3.00 software to collect wind data from the sensors.

The recorded data, along with the test sheet data, were translated into a Microsoft Excel 2000 workbook consisting of tabulated test data. Graphical plots of the data were created based on the data contained in the worksheets.

4.1.4 Results/Discussion.

Wind tunnel testing was conducted on 28 September 2000. A total of 35 test runs were performed. The test runs are summarized in table 2. The test runs in the table are ordered chronologically where the Test Run ID identifies the corresponding test sheet.

4.1.4.1 Accuracy Testing.

Results of the accuracy tests for the two mechanical sensors are shown in figure 27. The figures show the sensor data plotted against the wind tunnel airspeed for the various tilt angles. The solid diagonal line indicates perfect agreement. For reference, the 20% overspeed correction factor applied to the Hydro-Tech anemometer data (see section 3.2.2.2.1.1) is also indicated in the figure. As previously mentioned, negative tilt angles indicate a wind from beneath the sensor (i.e., sensor tilted from the vertical away from the wind flow). Since the raw wind data was plotted in units of m/s, a wind speed of 40 kt is indicated in the figures for reference.

The results show that both mechanical sensors overestimate wind speed, and the degree of overestimation increases with increasing tunnel wind speed. The Hydro-Tech anemometer errors are greater than the NRG errors. Off-axis winds affect both sensors, with the effects more pronounced for the Hydro-Tech sensor. This observation is consistent with prior wind tunnel test data provided by the manufacturer. The Hydro-Tech data indicates that the 20% overspeed correction factor currently used in the Juneau wind system may be an underestimate. Based on wind tunnel air speeds at 40 kt, the Hydro-Tech sensor overestimates the wind speed by as much as 45% for an upslope wind 20° from the horizontal.

Accuracy results for the Vaisala anemometer according to the various tilts and azimuth orientations are shown in figures 28 and 29.

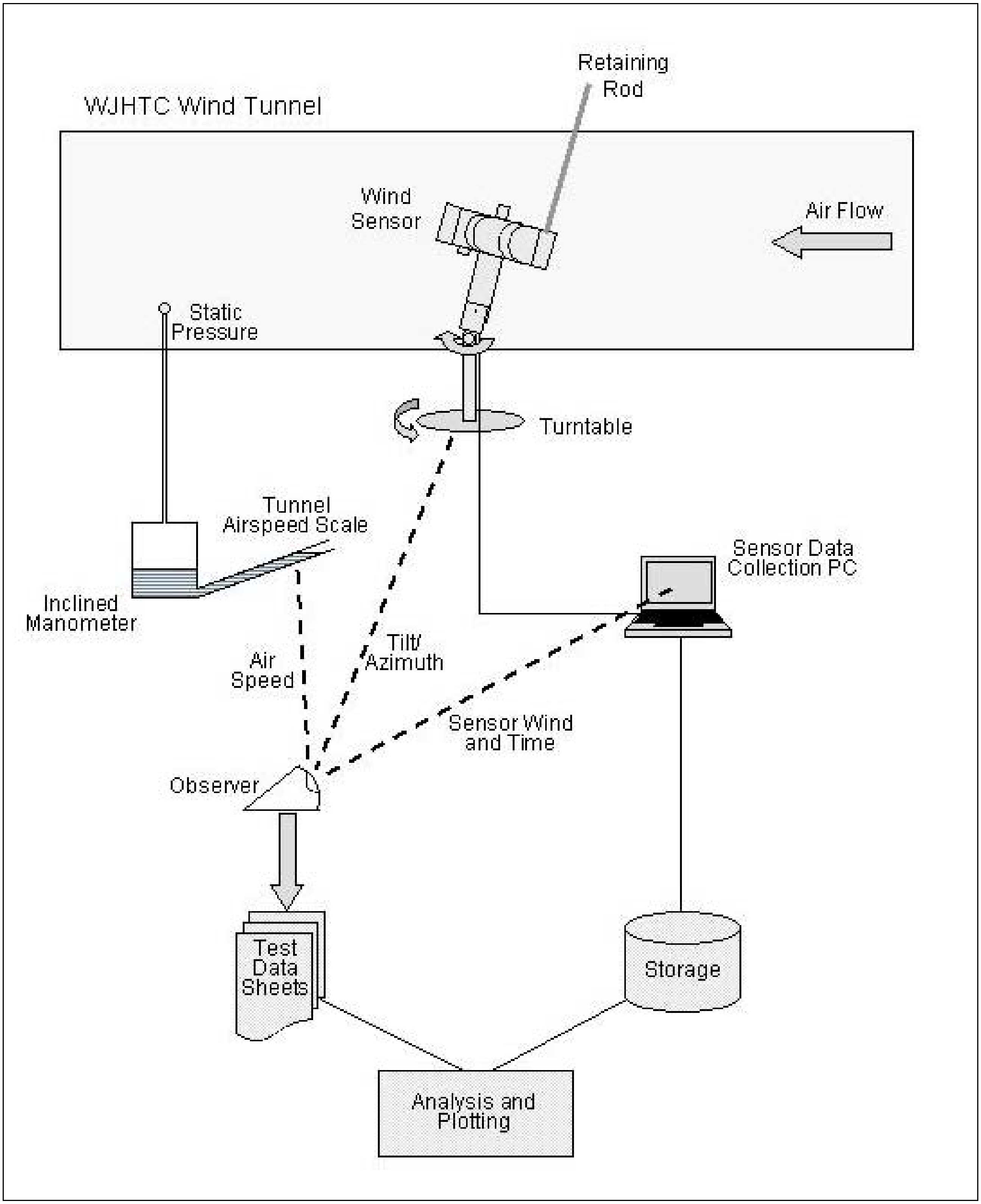

FIGURE 25. WIND TUNNEL SETUP AND DATA COLLECTION SYSTEM

JAWS Wind Sensor Tests
FAA William J. Hughes Technical Center
AAR-423 WIND TUNNEL
Weather Branch, ACT-320

Tester(s) ____________________
Outside T, P, WS, WD ____________________
Sensor, Model, SS No. ____________________
Test Date and Time: ____________________

WT Speed (nominal)		WT Air Speed (Actual)		UUT Wind Speed (m/s)	UUT Direction (deg)	Wind Speed Difference %Error	Comments
kn	fps	fps	m/s				
5	8.45						
10	16.9						
15	25.3						
20	33.8						
25	42.2						
30	50.7						
35	59.1						
40	67.6						
45	76.0						
50	84.5						
60	101.3						
70	118.2						
80	135.1						
100	168.9						
120	202.7						

FIGURE 26. WIND TUNNEL TEST DATA COLLECTION FORM

TABLE 2. SUMMARY OF WIND TUNNEL TEST RUNS

Sensor	Test Run ID	Test Type	Tilt (deg)	Azimuth (deg)
Hydro-Tech	1	Accuracy	0	N/A
	2	Accuracy	10	
	3	Accuracy	20	
	4	Accuracy	-10	
	5	Accuracy	-20	
	A	Response	-20	
	B	Response	-10	
	C	Response	0	
	D	Response	10	
	E	Response	20	
NRG	6	Accuracy	0	
	F	Response	0	
	7	Accuracy	10	
	G	Accuracy	10	
	H	Response	20	
	8	Accuracy	20	
	I	Response	-10	
	9	Accuracy	-10	
	J	Response	-20	
	10	Accuracy	-20	
Vaisala	11	Accuracy	0	0
	12	Accuracy	0	15
	13	Accuracy	0	30
	14	Accuracy	0	45
	15	Accuracy	10	0
	16	Accuracy	10	45
	17	Accuracy	20	45
	18	Accuracy	20	30
	19	Accuracy	20	15
	20	Accuracy	-10	0
	21	Accuracy	-10	45
	22	Accuracy	-20	45
	23	Accuracy	-20	30
	24	Accuracy	-20	15
	25	Accuracy	-20	0

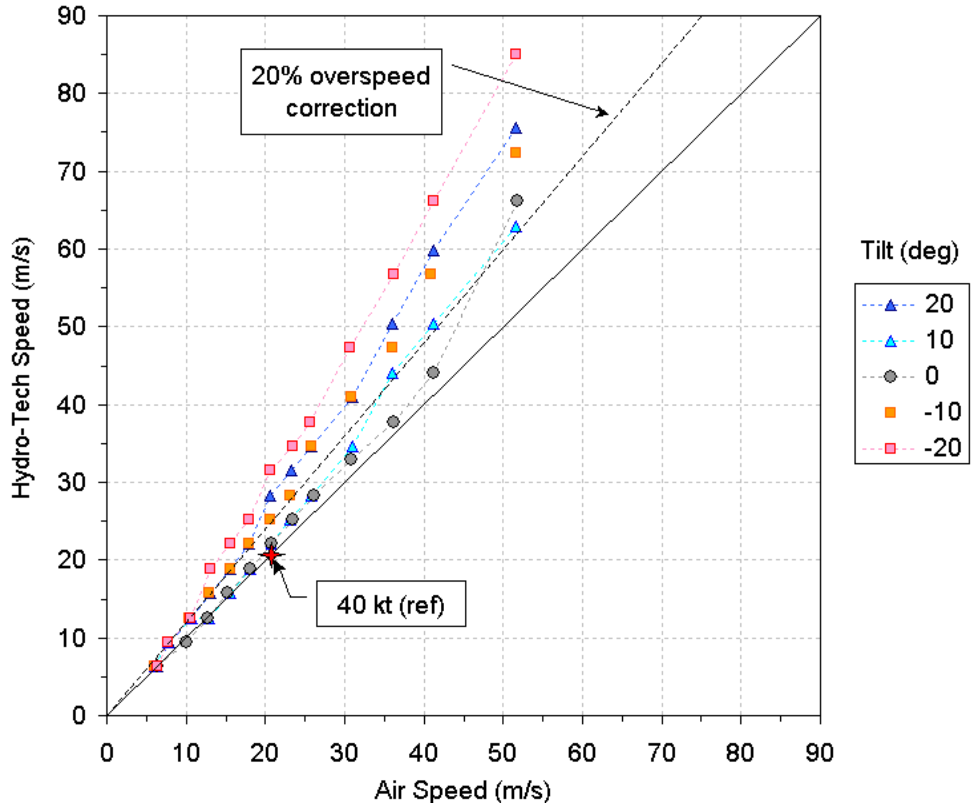

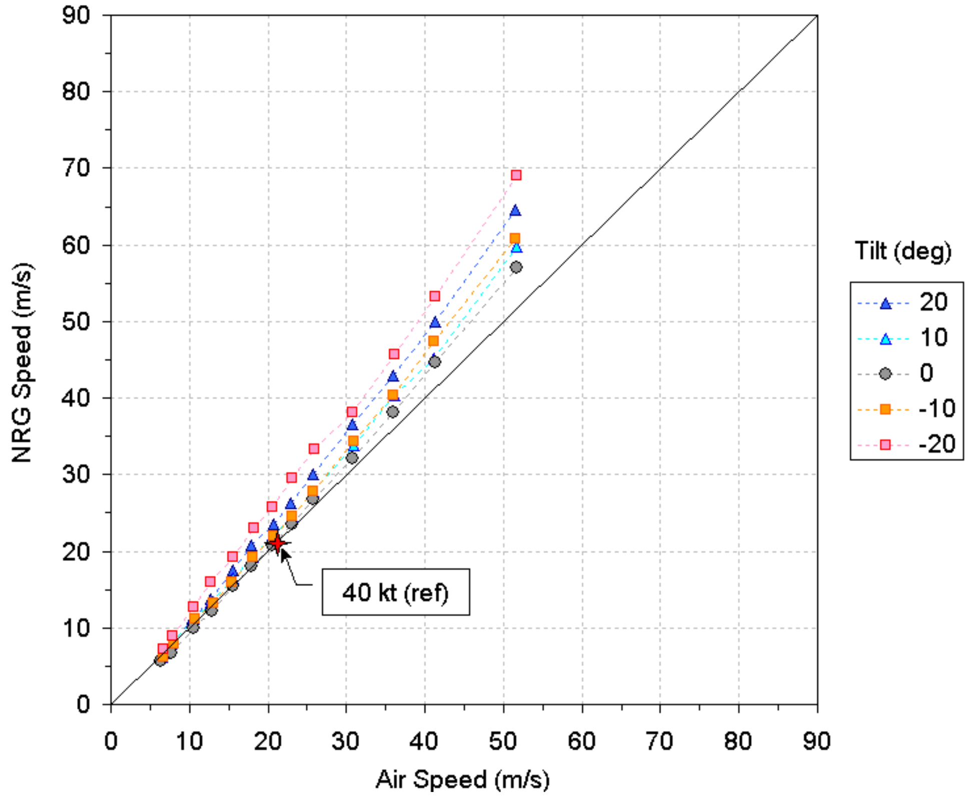

FIGURE 27. WIND TUNNEL ACCURACY RESULTS FOR HYDRO-TECH AND NRG WIND SENSORS

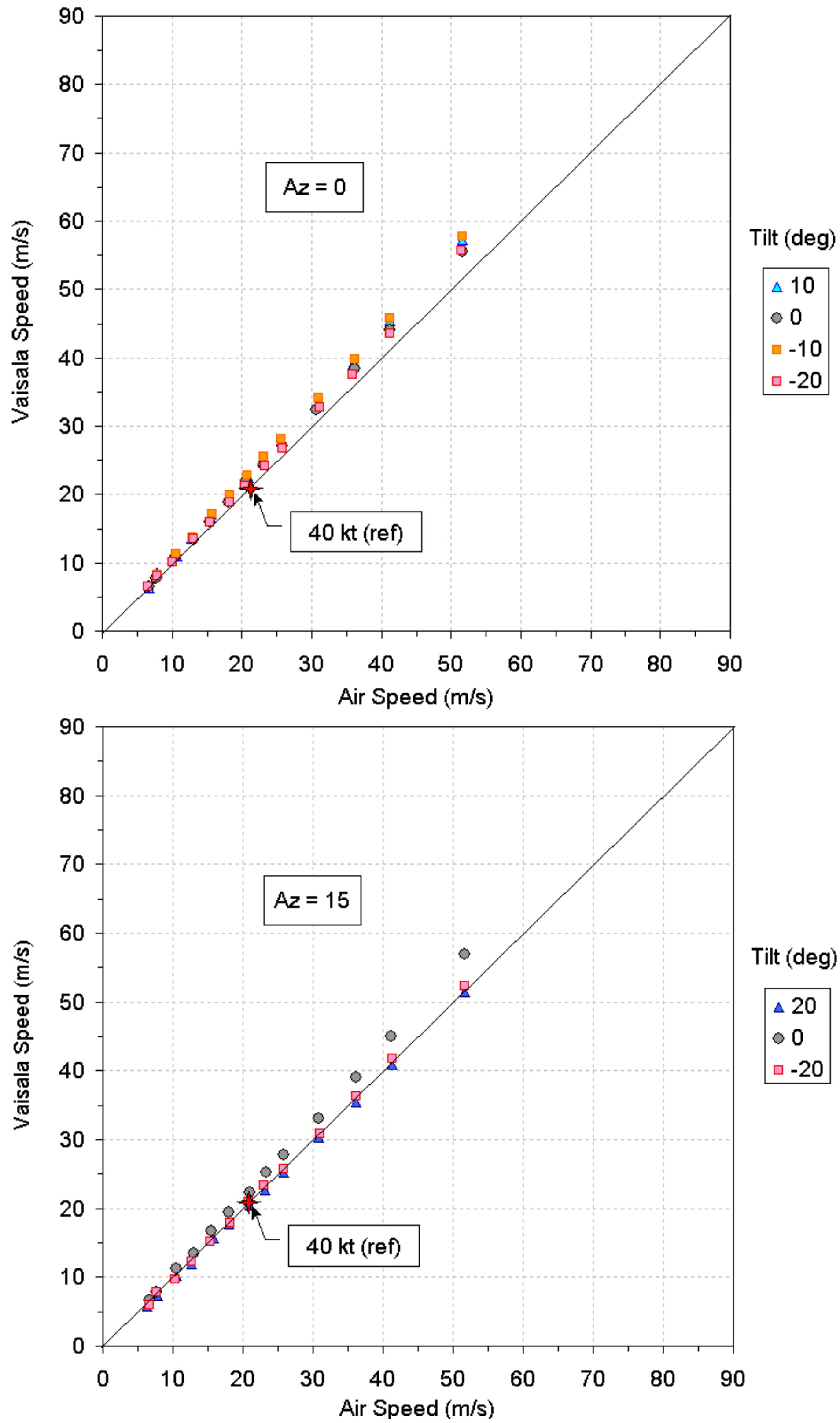

FIGURE 28. WIND TUNNEL ACCURACY RESULTS FOR VAISALA AT 0 AND 15 DEGREE AZIMUTH ORIENTATIONS

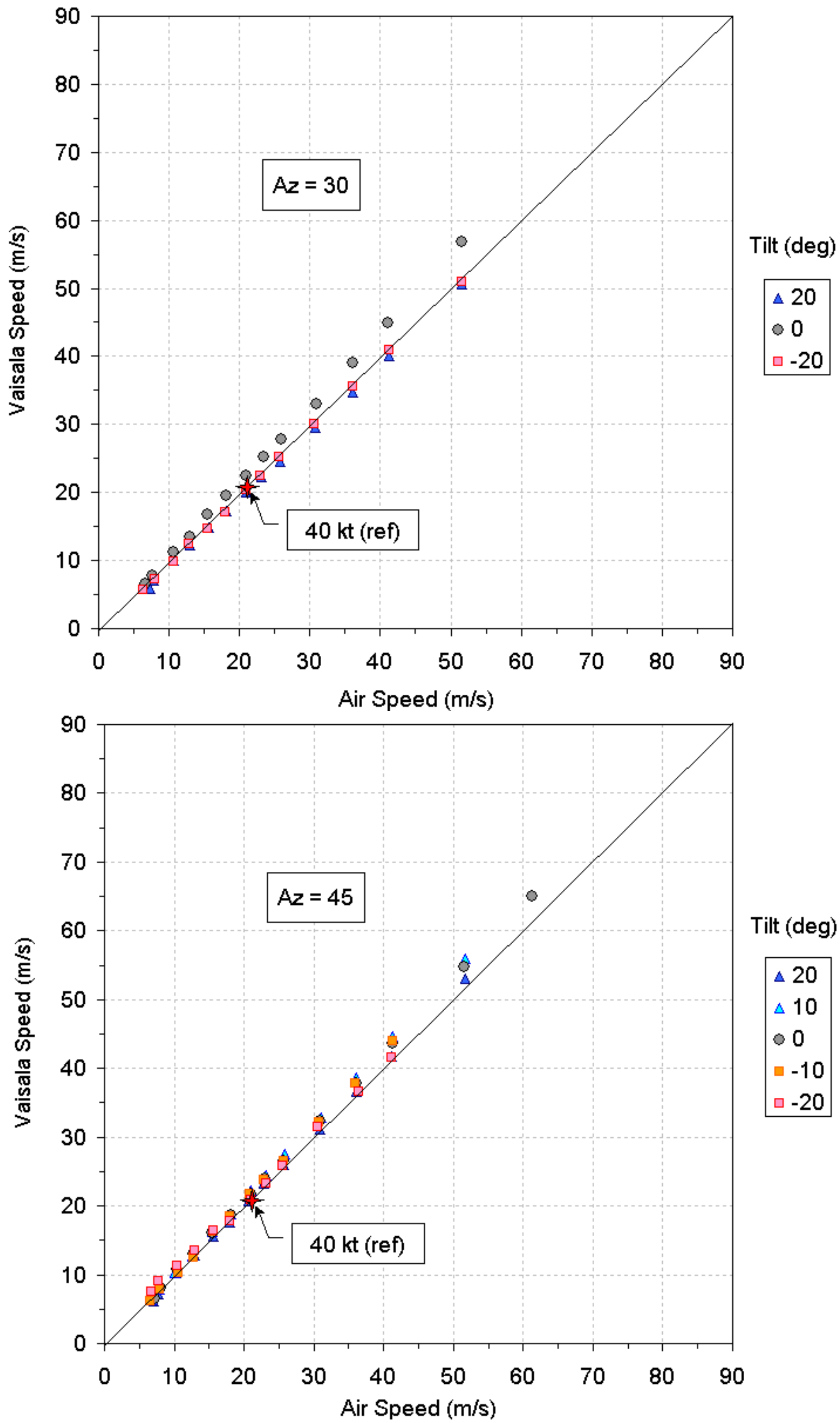

FIGURE 29. WIND TUNNEL ACCURACY RESULTS FOR VAISALA FOR 30 AND 45 DEGREE AZIMUTH ORIENTATIONS

These results indicate that the Vaisala sensor provides better overall agreement than the mechanical sensors.

The Vaisala sensor maintains and reports internal status, included indications of failed 1-second data. A failure qualifies as a bad data flag received from the sensor because of unreliable readings. The frequency of occurrence of sensor failures for the runs is summarized in table 3.

TABLE 3. VAISALA SENSOR FAILURES FOR WIND TUNNEL RUNS

Test Run ID	Tilt (deg)	Azimuth (deg)	Total Data (min)	1-sec Failures (sec)
11	0	0	9.30	14
12	0	15	8.47	0
13	0	30	9.47	0
14	0	45	8.53	38
15	10	0	10.35	30
16	10	45	8.57	16
17	20	45	7.87	0
18	20	30	9.33	2
19	20	15	12.23	1
20	-10	0	10.05	0
21	-10	45	9.60	89
22	-20	45	10.10	66
23	-20	30	9.57	79
24	-20	15	9.20	63
25	-20	0	7.90	0

4.1.4.2 Response Testing.

The dynamic response characteristics of the mechanical anemometers are shown in figure 30. The figures show, as expected, that the NRG sensor is more responsive than the more massive Hydro-Tech anemometer. The figures also show the overspeeding that was presented in the previous section.

Time constants were estimated from the response data in two ways. The true time constant was estimated with respect to the actual maximum steady state wind (overspeed wind) that the sensor finally achieved (see figure 30). In addition, time constants were also derived based on the 40 kt wind tunnel air speed as the maximum or final wind reference. The time constants derived from the response tests are displayed in figure 31.

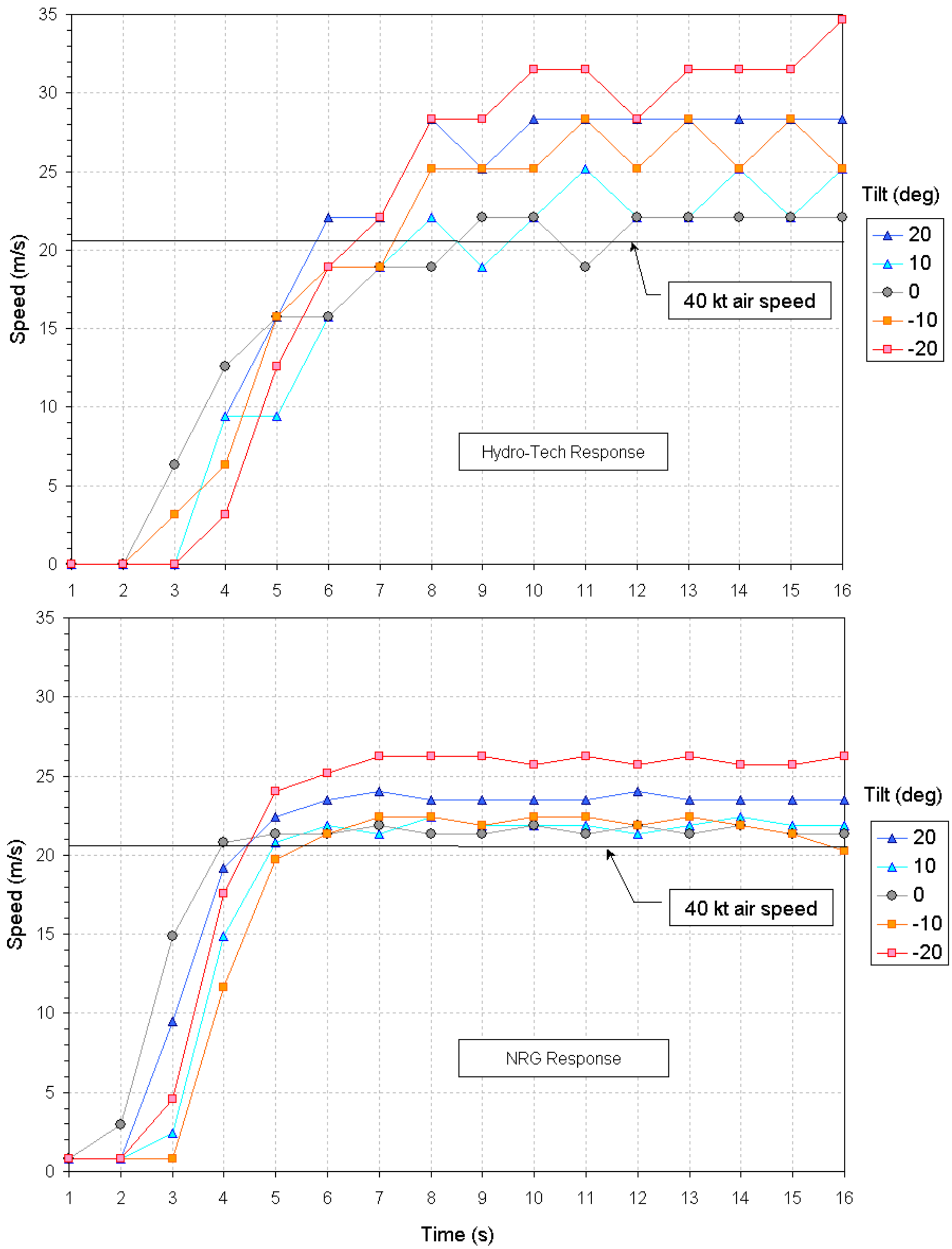

FIGURE 30. WIND TUNNEL RESULTS OF DYNAMIC RESPONSE FOR HYDRO-TECH AND NRG WIND SENSORS

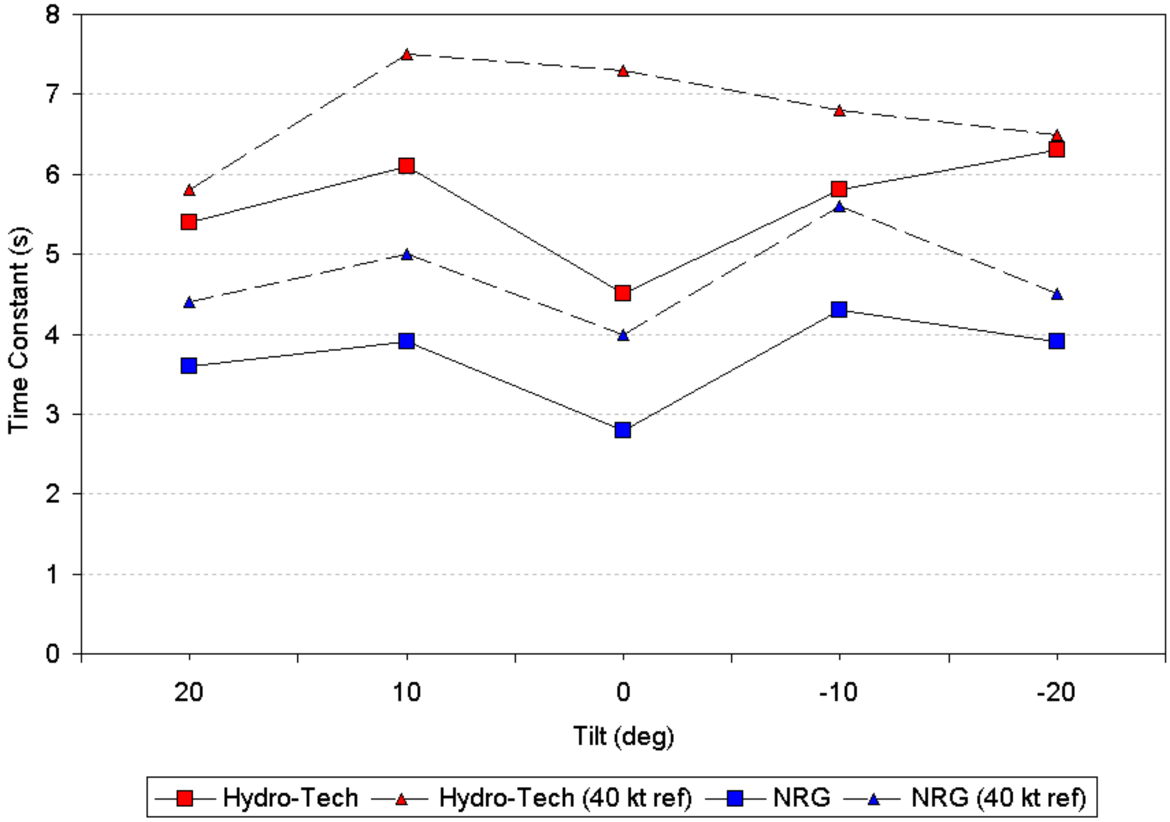

FIGURE 31. TIME CONSTANTS FOR HYDRO-TECH AND NRG WIND SENSORS AT VARIOUS TILTS

The time constants in the figure 31 show that the NRG sensor is more responsive than the Hydro-Tech sensor, and the relative response is slower for off-axis winds.

4.1.5 Conclusions.

In general the results were as expected. The mechanical sensors overestimate the wind speed at greater wind speeds. The ultrasonic sensor was more accurate over a wide range of wind speed ranges than the mechanical sensors.

4.2 LABORATORY MOCKUP.

4.2.1 Test Objectives and Criteria.

A mockup of the sensors and equipment was assembled in the Aviation Weather Research Program (AWRP) Laboratory at the Technical Center. The purpose of the mockup was to determine required mounting fixtures and optimal video camera lenses and exposures. In addition, the test bed mock up facilitated cabling and checkout of the test data acquisition and collection system before shipping and installation in Juneau.

4.2.2 Testing Description.

A simulated railing structure of the Juneau equipment tower was fabricated using Polyvinyl Chloride (PVC) piping. Photographs of the mock up are provided in figure 32. Special conformal heater blankets were applied to the cameras, and around the housing of the ice detector.

4.2.3 Data Collection and Analysis Method.

No special data collection activities were required in the test.

4.2.4 Results/Discussion.

Results of the mockup resulted in the wiring diagrams provided in appendix B.

4.2.5 Conclusions.

The conclusion of this test resulted in the packaging and shipping of the sensors and equipment to Juneau.

4.3 FIELD TEST.

4.3.1 Test Objectives and Criteria.

There were several objectives of this part of testing. The primary objective was to study the severe weather performance of wind sensors under rime icing conditions. Foremost, the severe weather performance of the Hydro-Tech sensor currently used in the JWHIS system was evaluated. In addition, the severe weather survivability and reporting performance of alternative wind measurement technologies and sensors were assessed. The overall approach to achieve this, and the test and evaluation aspects that were applied to this specific test program, centers around the installation of a weather sensors test bed at Eagle Crest.

An ancillary benefit in carrying out the research to achieve this objective was the better overall understanding that will be gained for quantitatively specifying wind sensor survivability and performance requirements in terms of varying icing conditions. Since there are no current specifications or standards on wind sensor performance in varying icing conditions, the research effort associated with this objective will have applicability to the development of the JAWS requirements specification, as well as other aviation weather efforts.

Another objective of testing was to assess the influence and effect of off-axis winds (i.e., winds with vertical wind components) on the sensors currently used in the mountainous terrain of Juneau, as well as the alternate wind sensors. Lower priority objectives were to explore optimal sensor mounting configurations, passive and active deicing technologies, and techniques to forestall or reduce the growth of rime icing on the sensors and masts.

The specific areas evaluated are the severe weather performance of the four types of wind sensors identified in section 3.2.2.2.1. In order to accomplish this, a weather sensors test bed was installed at Eagle Crest. Its environment and exposure is representative of extreme wind and

FIGURE 32. PHOTOGRAPHS OF LABORATORY MOCKUP

icing conditions that will be experienced by other anemometers at other locations in the JAWS system. The test bed facilitated the testing and comparison of several types of wind sensors against the current JWHIS sensor.

4.3.2 Testing Description.

After the laboratory mockup, the sensors and equipment were installed at Juneau in manner described in section 3.3 of this document. The roles and responsibilities of the various organizations and personnel that assisted and supported the testing are listed in table 4 below.

TABLE 4. TEST ORGANIZATION

Organization	Role
AUA-430	1. Provided overall direction and funding for the test program 2. Approved test plans and procedures
ACB-630	1. Developed the test plan 2. Carried out procurement of sensors and equipment 3. Conducted wind tunnel testing of wind sensors 4. Performed laboratory mockup of test bed 5. Assisted in sensor and equipment installation in JNU 6. Developed and maintained on-line and off-line data reduction and analysis programs 7. Developed test reports
NCAR	1. Assisted in coordinating equipment installations 2. Acquired DSL capability 3. Assisted in the design and fabrication of site-specific mounting hardware 4. Assisted in physically installing sensors and cameras 5. Established and maintained the service contract with the local engineering firm (Haight & McLaughlin) to provide routine and non-routine maintenance and installation services at the Eagle Crest test site
Haight & McLaughlin	1. Maintained tower infrastructure 2. Installed sensors and equipment on the tower 3. Maintained sensors and equipment

After the successful mockup of the test bed, the equipment was shipped to JNU for installation on the Eagle Crest tower. Installation was carried out by the local engineering and maintenance contractor and ACB-630, with the support of NCAR. Sensor calibration procedures were performed, and the azimuth alignment of the wind sensors was estimated by means of a compass and visual inspection. Cabling and final checkout of the installation were performed jointly by ACB-630 and the maintenance contractor. Additional test locations in Juneau were the crawlspace of the Alaska Airlines operations tower and the NCAR Laboratory.

Various photographs of the sensor and equipment installations on the Eagle Crest tower are provided in figures 33 through 36.

4.3.3 Data Collection and Analysis Method.

Data collection was performed as described in detail in Section 3.3 of this document. The data collection for this effort centered around a network of data acquisition and high-speed wireless Ethernet communications devices using Internet Protocol (IP) between the mountain site and the NCAR laboratory adjacent to the airport. Redundancy and backup capabilities built into the overall design facilitated continuous data acquisition and recording in an unattended mode during the 6-month period. Data was collected independently from the JWHIS sensors in a manner to ensure that operations of those sensors were not affected or degraded. Wind sensor and icing data, including video images of the sensors, were continuously collected in real time throughout the winter period of November 2000 through May 2001. Estimates of ice accumulation and rates from the ice detector were determined and correlated with the wind sensor data. The general method of test bed data collection was via an Internet capability. Real-time wind sensor data and video images were made available on-line. Data was also recorded and downloaded in order to further analyze and quantitatively determine sensor performance.

All data acquisition equipment for the weather sensors, along with recorders and receiver/servers for the video cameras, were installed in the instrument shelter located beneath the tower. An uninterruptible power supply with communications and management software allowed for remote power monitoring and auto-shutdown capabilities. Two backup devices in the shelter were used to ensure full archiving of sensor and video data in the event of network or data transmission problems. A PC in the shelter was used to directly collect data from the sensors. The second backup storage device was a digital videocassette recorder which recorded video images onto tape. Both the serial sensor and video data were recorded by the backup devices every 1 second.

Analog data from the Hydro-Tech, NRG, ice detector, and temperature/humidity sensors was captured and digitized by a datalogger. Digital data from the datalogger, along with the RS-232 serial output from the Vaisala sensor, were converted to 10BaseT Ethernet protocol by separate serial servers. Video images from the four cameras were captured and transformed to Ethernet using a video multiplexer and server. The sampling interval of the weather sensors and the camera images was 1 second and 15 minutes, respectively.

FIGURE 33. VIEWS OF THE TOWER PLATFORM AND SENSOR INSTALLATIONS

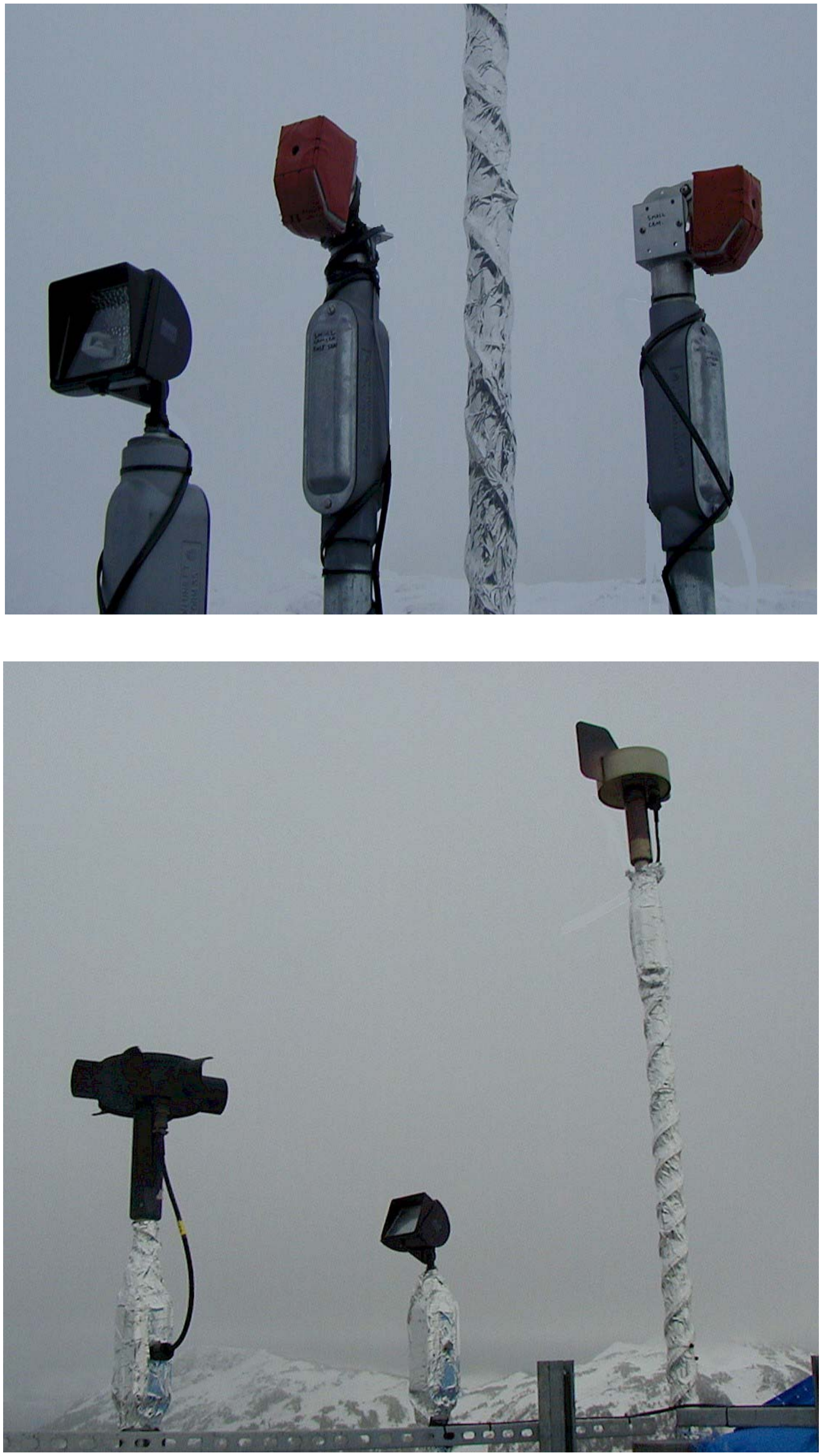

FIGURE 34. VIEWS OF SENSOR INSTALLATIONS

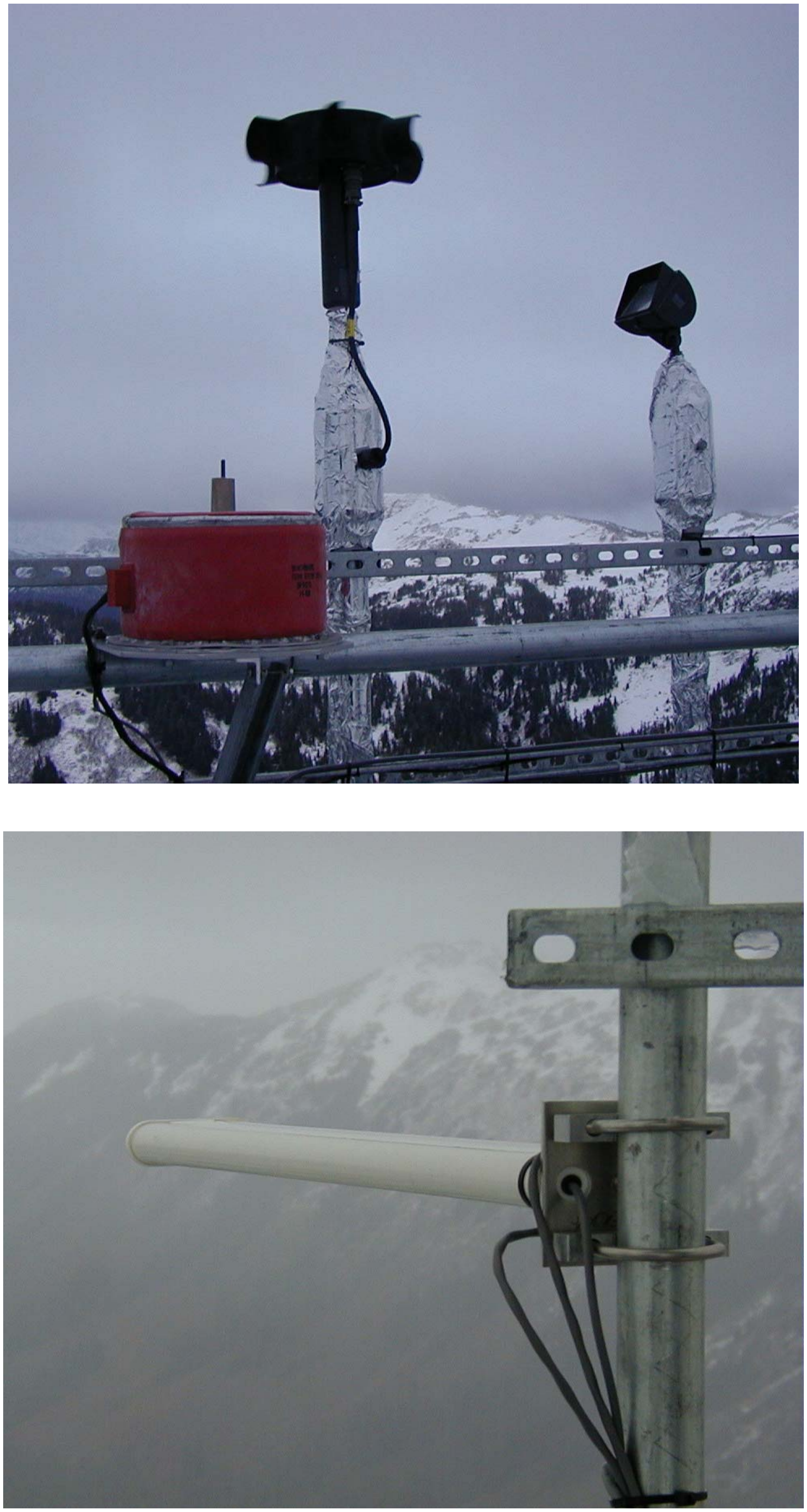

FIGURE 35. VIEWS OF SENSORS AND YAGI ANTENNA

FIGURE 36. PHOTOGRAPHS OF TEMPERATURE CANISTER AND LARGE CAMERA

Data transmission from the mountain-top test bed to the laboratory was accomplished via a hybrid network of 900 MHz long range spread-spectrum wireless modems and a 2.4 GHz wireless Ethernet link. The later component high-speed wireless network connection provided the bandwidth necessary to carry the combined sensor and video data.

Initial data processing was performed in a separate ACB-630 host PC in the laboratory. This computer employed several software applications for performing the primary data collection, recording, and backup of sensor and video data. In addition, the PC furnished Internet Web and FTP server capabilities for the dedicated test web site that was established and exercised for remote on-line data monitoring and control, as well as data file downloads of daily sensor and video data. Internet access was provided through a dedicated DSL modem. The continuous DSL and Internet connection provided the required speed and bandwidth to carry the volumes of combined sensor and video image data.

The web site facilitated continuous remote monitoring of sensor and video data. Software within the PC generated for each weather variable, 2-hour time series plots of running 1-minute averages updated every 1 minute. The web page displayed and updated the sensor time series and camera images every 1 and 15 minutes, respectively. The web site was accessible through an Internet client software package such as Netscape or Internet Explorer. Samples of the Juneau web pages are provided in figures 37 and 38.

FTP services were used for the bulk file download of sensor data and video images to the Technical Center. Detailed analyses and plotting of the data were performed at the Technical Center using Visual Fortran 95 and Excel. The bulk of the detailed data reduction and analysis was performed off-line by adapting custom sets of Digital Visual Fortran 95 and Microsoft Excel 2000 data analysis and plotting packages that were developed and employed for the MWO study. The programs perform full data decoding, and implement a variety of data quality analysis, normalization, and sensor data comparison routines. Final data visualization, analyses, and interpretation were accomplished using graphical and plotting routines provided in Excel.

Based on temperature, ice detector data, and video images, scenarios of icing events were identified. A summary of the data collected over the study was compiled and categorized into separate cases according to prevailing weather conditions, and various wind, temperature, relative humidity, and icing scenarios. A variety of digital time series and statistical analyses were performed on the individual histories of sensor data. Correlations were then performed among the sensors in order to identify degraded performance. In addition to the test bed data, hourly Aviation Routine Weather Reports (METARs) for JNU were also routinely collected through United States Weather Pages via the Internet.

Hourly mean winds were depicted in the form of Wind Roses using Lakes Environmental Software WRPLOT View 1.5 for Windows. A wind rose is polar graph depicting the distribution of wind directions by 16 points of compass. Around the rose are 16 histograms, which show the distributions of wind speeds at each point of compass according to 6 wind speed classes. The software also generates rose statistics (including %calm) and wind rose plots for user-specified date and time ranges. The software program is designed to accept several conventional meteorological data formats. In this case, the data was reformatted into NWS-MET144 (SCRAM) meteorological data format for input into the wind rose program.

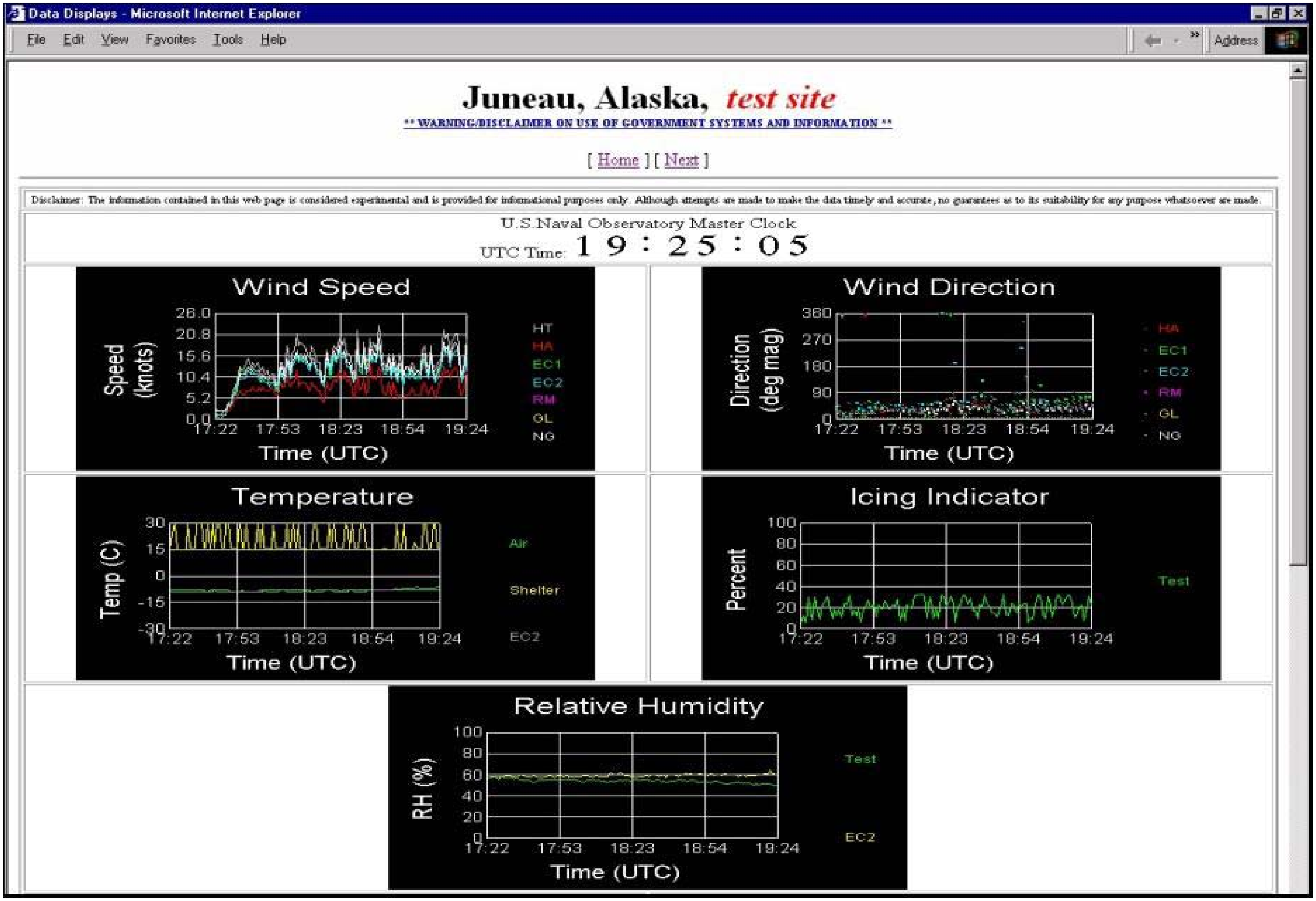

FIGURE 37. WEB HOME PAGE

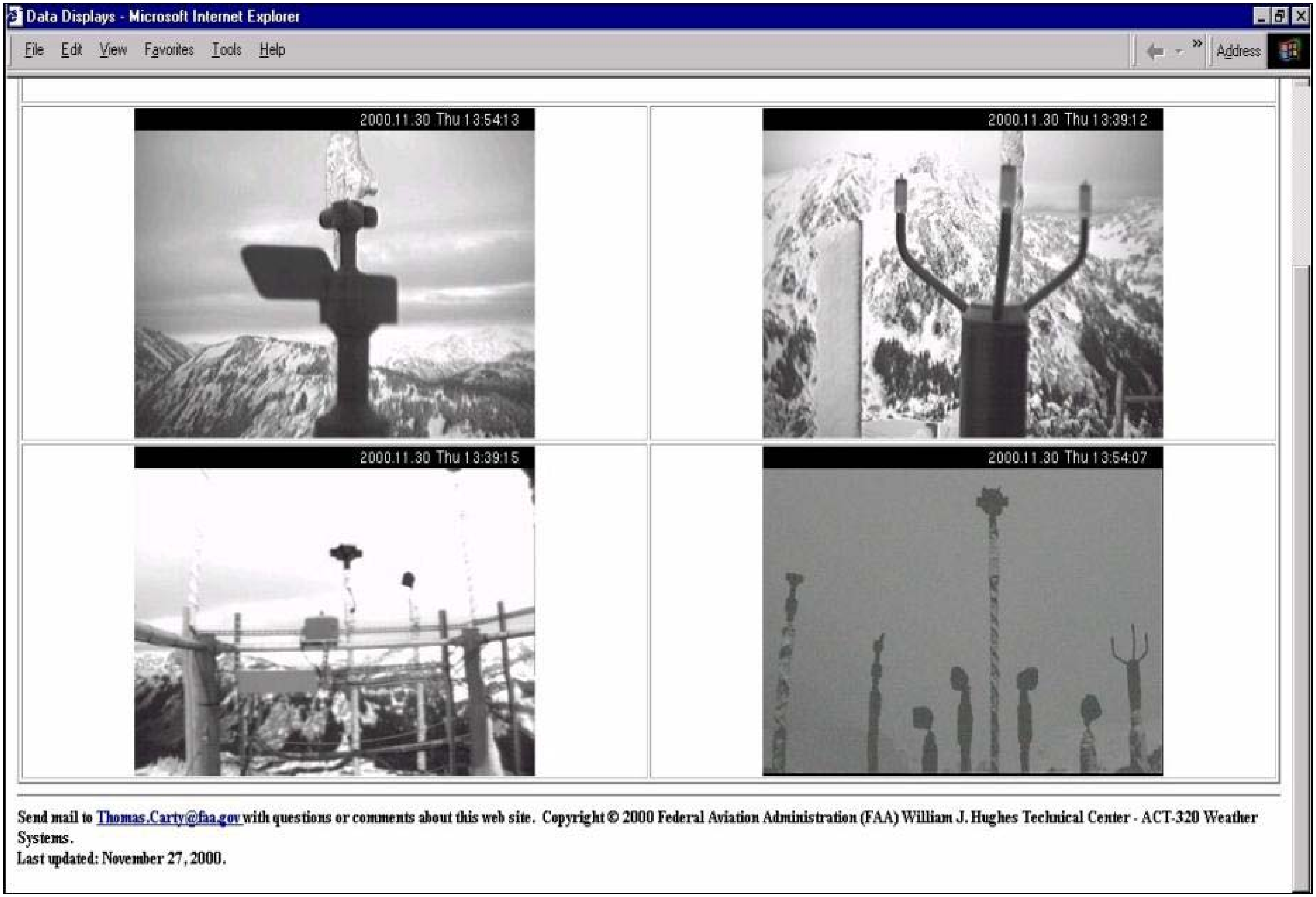

FIGURE 38. WEB CAMERA PAGE

Finally, the camera data was maintained by using PhotoImpact v6.0 imaging software by Ulead Systems, Incorporated. The software facilitated the construction and display of animated web slide shows of the camera images. These animated presentations show the wind sensors under varying icing conditions at a rate of 1 frame per second. These slide shows are represented as embedded objects in various figures in the remaining sections. In the electronic version of this report, the slide shows may be opened and activated through the context of the slide show icon label, then viewed using a web browser.

The evaluation techniques included comparisons of the performance of the sensors under various icing conditions and wind regimes. The relevant operational issues and test requirements for this testing are the aspects of sensor functionality and operations that are critical to the operational suitability and effectiveness of the JAWS system. The only current requirements are those based on the Ops Spec [1]. In addition, additional operational requirements may be derived from the JAWS Operations Requirements Document [10]. The derived test requirements and their related specific evaluation criteria are listed in table 5.

TABLE 5. LIST OF TEST REQUIREMENTS AND EVALUATION CRITERIA

Requirement	Description
1	Eagle Crest anemometers must be available and operational to support Fox, Lemon Creek, and RNP departure operations[1]
2	The sensors must remain operational and in an undegraded state to support the wind and weather minima in the Ops Spec
3	The sensors must return from degraded to an operational state within TBD minutes

It should be noted that there are no current specifications or standards on wind sensor performance for JAWS wind sensors, particularly in varying icing conditions.

Performance Thresholds are particular parameters and associated values required to provide a capability that will satisfy the JAWS mission. For JAWS, this operational capability is defined in terms the weather minima and wind restrictions in the Ops Spec. The applicable performance thresholds, and associated parameters and values for these performance thresholds, are listed in table 6. The threshold wind restrictions include gusts, i.e., steady state or average wind plus gust factor.

4.3.4 Results/Discussion.

Data collection effectively began on 15 November 2000. This report summarizes results from the Data Reduction and Analysis (DR&A) for the data collected over the period 15 November 2000 through 17 May 2001. Preliminary results, or Quick Look Test Reports, have been presented by ACB-630 in three separate briefings throughout the test period [12, 13, and 14].

[1] Ops Spec requires Eagle Crest operational, and Mt. Roberts or Sheep Mt. Operational for takeoff.

TABLE 6. JAWS PERFORMANCE THRESHOLDS

Operation	Parameters and Thresholds					
	Weather Minima			Wind Restrictions		
		Ceiling (ft)	Visibility (SM)			Wind Speed (kt)
Lemon Creek Departure, RWY 08	Day	1000	2	Airport	For airport winds 080 – 180°	25
				Eagle Crest		35
	Night	2000	5	Sheep Mt.		35
				Mt. Roberts		35
Fox IFR Departure, RWY 08	Day	800	2	Airport	For airport winds 080 – 180°	25
				Eagle Crest		35
	Night	2000	5	Sheep Mt.		35
				Mt. Roberts		35
RNP Departure, RWY 08	TBS		0.25	Airport		35
				Eagle Crest		45
				Sheep Mt.	300 – 030°	25
					031 – 299°	45
				Mt. Roberts	300 – 030°	35
					031 – 299°	45

Figures 39 through 43 summarize the amount of data collected over the 184-day (~6-month) period. The total amount of data for the wind and weather sensors, and for the video cameras is presented in figures 39 and 40, respectively. The daily totals for the datalogger data, which includes data from the Hydro-Tech and NRG wind sensors, as well as ice, temperature, and relative humidity data, are presented in figure 41. Similar daily totals for the Vaisala wind sensor and the operational JWHIS sensor EC1 are provided in figures 42 and 43.

The distribution of hourly mean winds that were experienced over the 184-day period are indicated in figures 44 through 48, and in tables 7 and 8. The wind rose given in figure 44 shows that the prevalent winds were from the Southeast sector, and is consistent with similar wind rose data presented in the Test Plan. The data is based primarily on the Vaisala data that was collected, and depicts the distribution of wind directions by 16 points of compass. Around the rose are 16 histograms which are the distributions of wind speeds at each point of the compass.

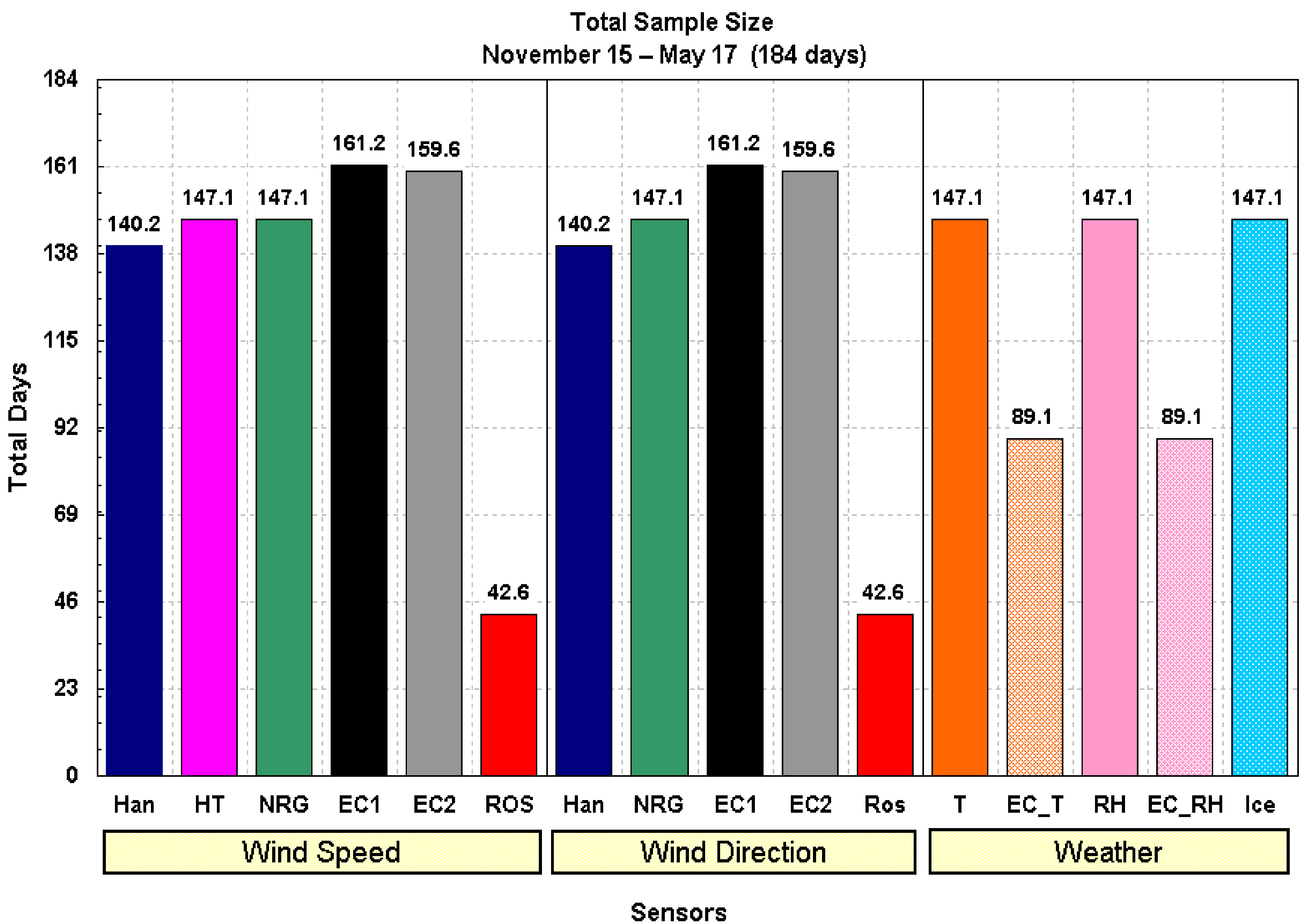

FIGURE 39. TOTAL SENSOR DATA COLLECTION

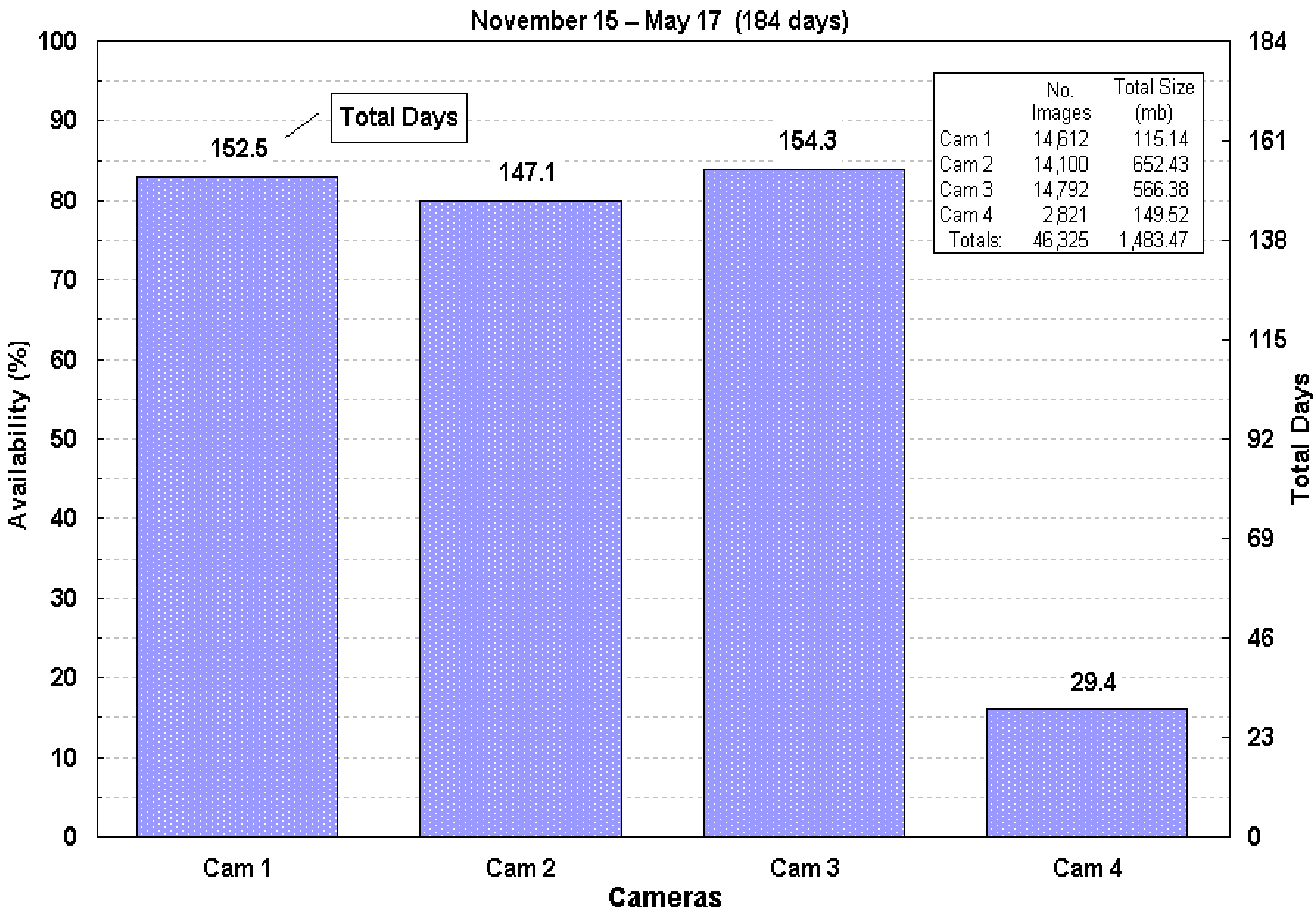

FIGURE 40. TOTAL DATA COLLECTION FOR VIDEO CAMERAS

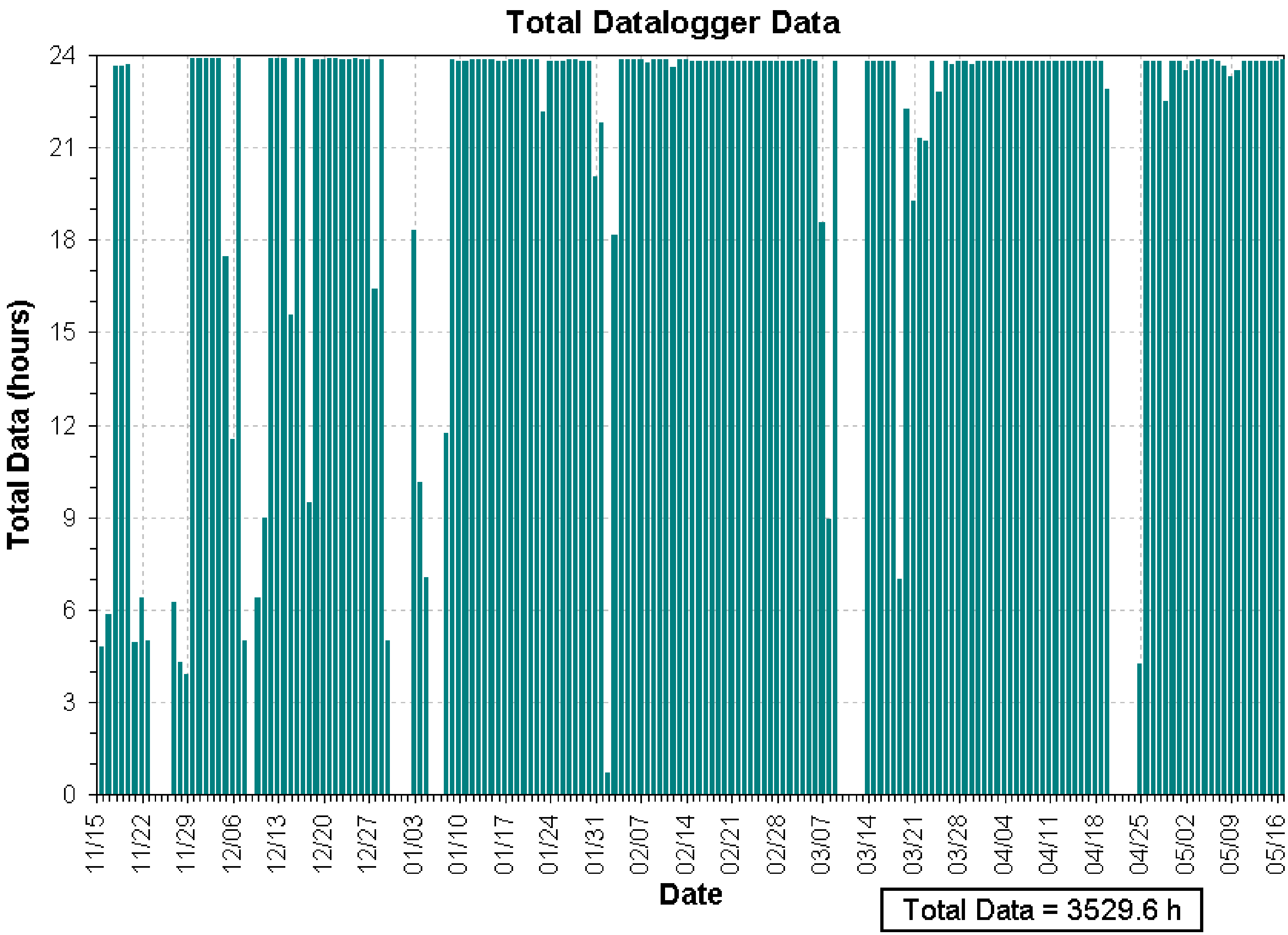

FIGURE 41. TOTAL DATALOGGER DATA COLLECTION

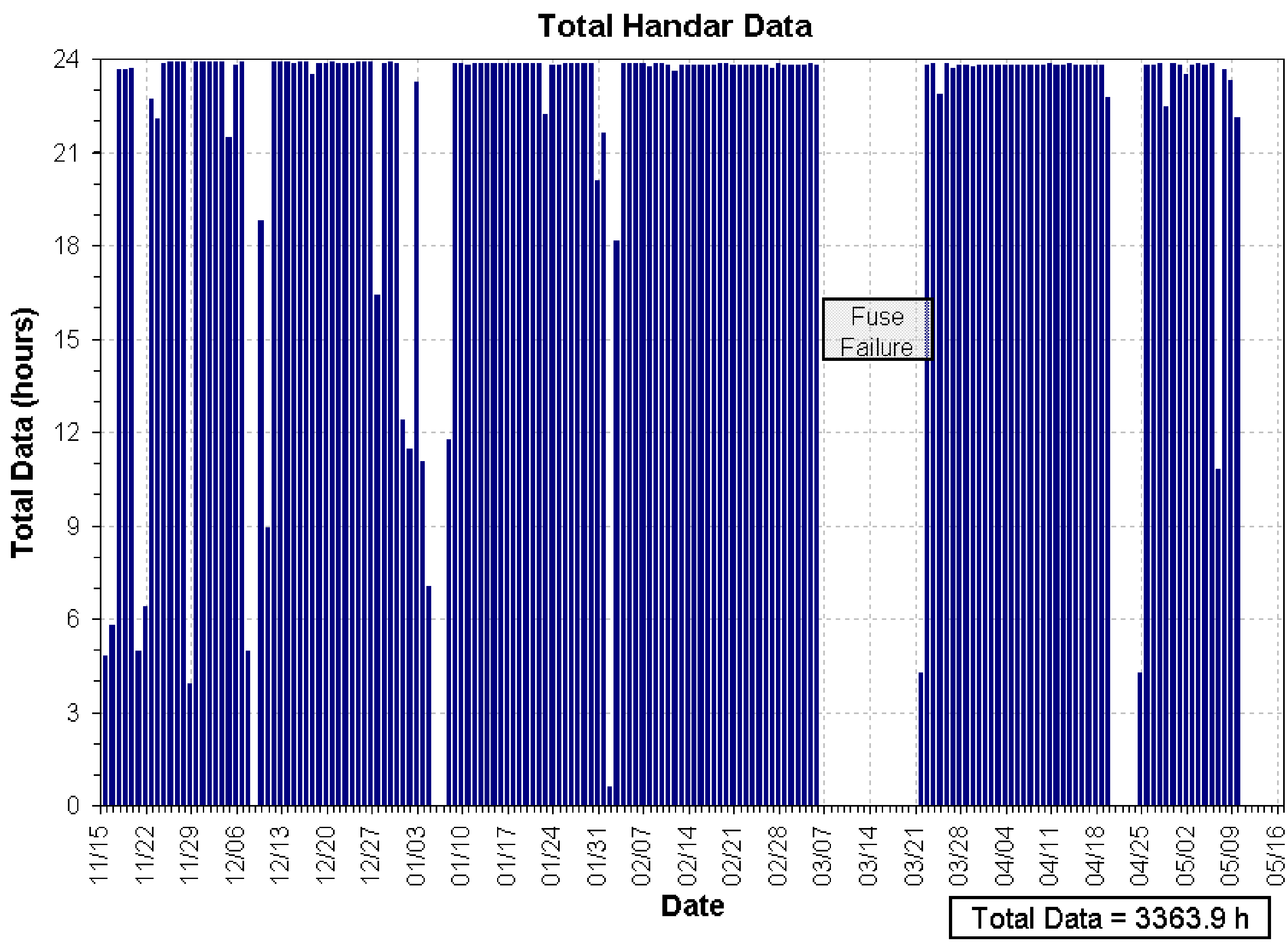

FIGURE 42. TOTAL VAISALA ULTRASONIC WIND SENSOR DATA COLLECTION

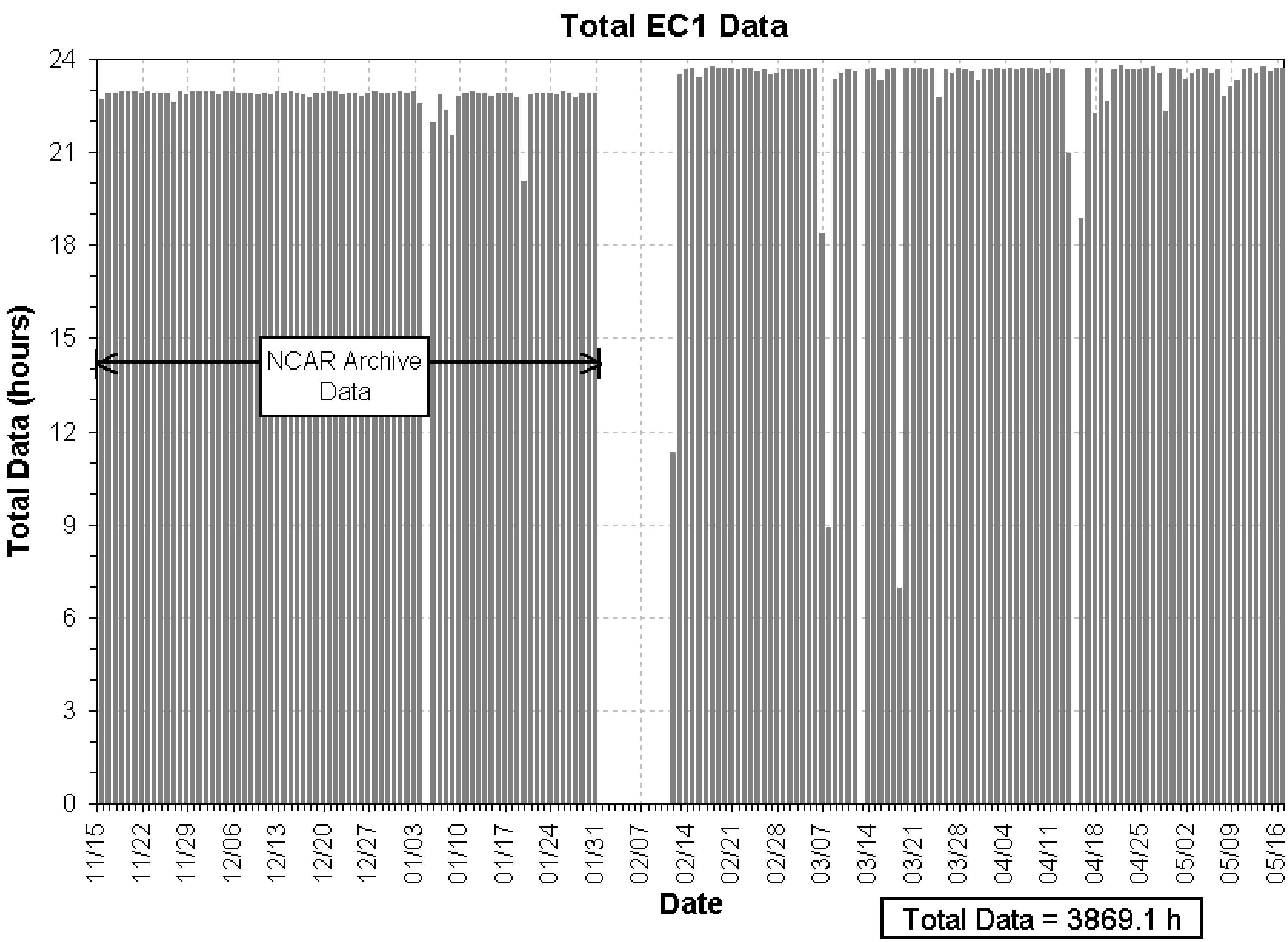

FIGURE 43. TOTAL EC1 DATA COLLECTION

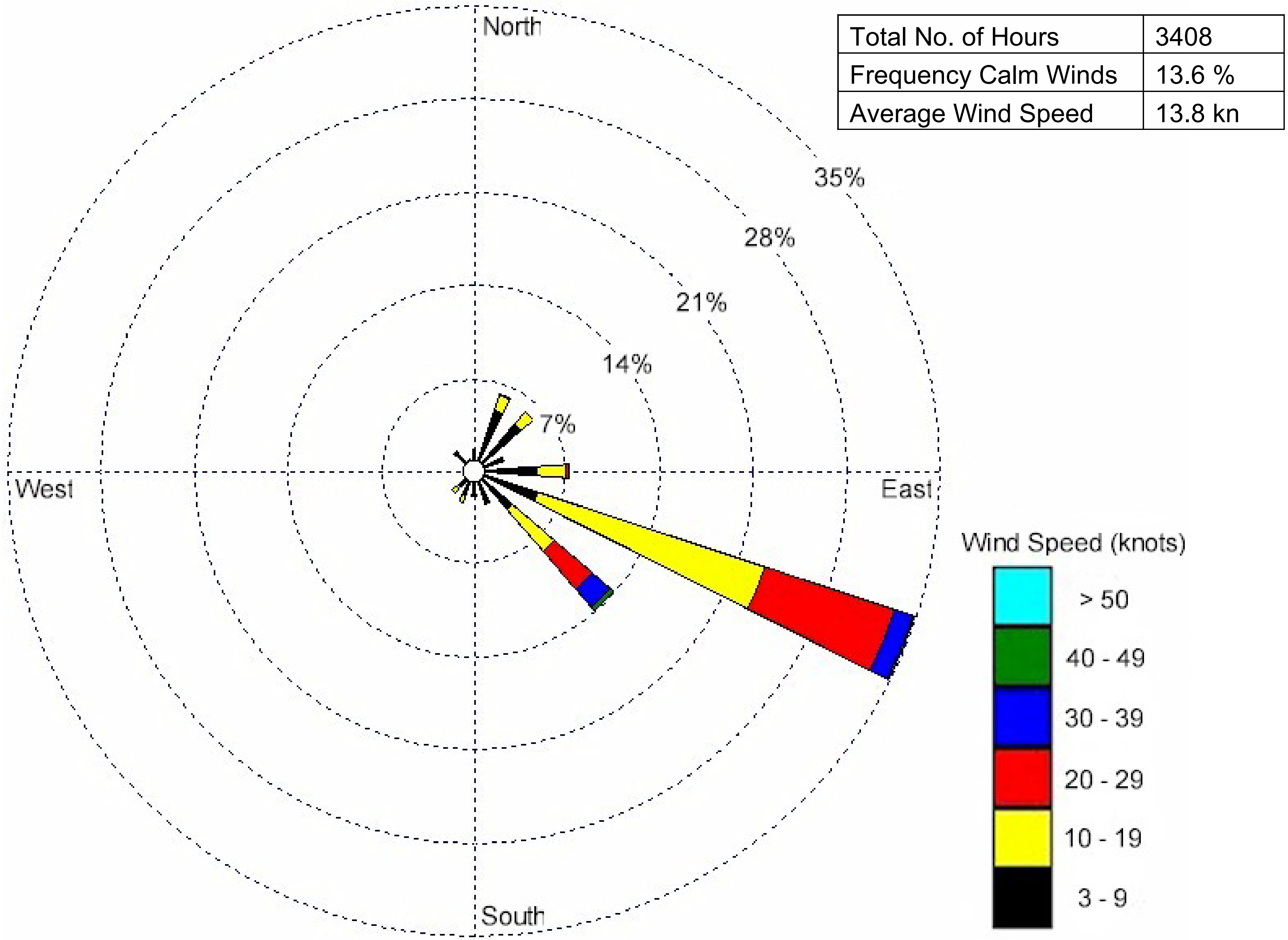

FIGURE 44. HOURLY WIND ROSE FOR NOVEMBER 15, 2000 – MAY 17, 2001

TABLE 7. FREQUENCY DISTRIBUTION IN HOURS

Wind Direction	Wind Speed Class (kt)						
	3 - 9	10 - 19	20 - 29	30 - 39	40 - 49	> 50	Total
N	54	4	1	0	0	0	59
NNE	166	43	4	0	0	0	213
NE	161	43	0	0	0	0	204
ENE	78	4	0	**0**	**0**	0	82
E	163	75	9	**0**	**0**	0	247
ESE	175	610	349	**51**	**4**	0	1189
SE	133	142	123	**62**	**14**	0	474
SSE	90	1	0	**0**	**0**	0	91
S	63	3	0	**0**	**0**	0	66
SSW	66	21	0	0	0	0	87
SW	52	23	1	0	0	0	76
WSW	11	3	0	0	0	0	14
W	14	0	0	0	0	0	14
WNW	27	0	0	0	0	0	27
NW	70	0	0	0	0	0	70
NNW	24	8	0	0	0	0	32
Total	1347	980	487	113	18	0	2945

TABLE 8. NORMALIZED FREQUENCY DISTRIBUTION IN PERCENT

Wind Direction	Wind Speed Class (kt)						
	3 - 9	10 - 19	20 - 29	30 - 39	40 - 49	> 50	Total
N	1.6	0.1	0	0	0	0	1.7
NNE	4.9	1.3	0.1	0	0	0	6.3
NE	4.7	1.3	0	0	0	0	6.0
ENE	2.3	0.1	0	**0**	**0**	0	2.4
E	4.8	2.2	0.3	**0**	**0**	0	7.2
ESE	5.1	17.9	10.2	**1.5**	**0.1**	0	34.9
SE	3.9	4.2	3.6	**1.8**	**0.4**	0	13.9
SSE	2.6	0	0	**0**	**0**	0	2.7
S	1.8	0.1	0	**0**	**0**	0	1.9
SSW	1.9	0.6	0	0	0	0	2.6
SW	1.5	0.7	0	0	0	0	2.2
WSW	0.3	0.1	0	0	0	0	0.4
W	0.4	0	0	0	0	0	0.4
WNW	0.8	0	0	0	0	0	0.8
NW	2.1	0	0	0	0	0	2.1
NNW	0.7	0.2	0	0	0	0	0.9
Total	39.5	28.8	14.3	3.3	0.5	0.0	100.0

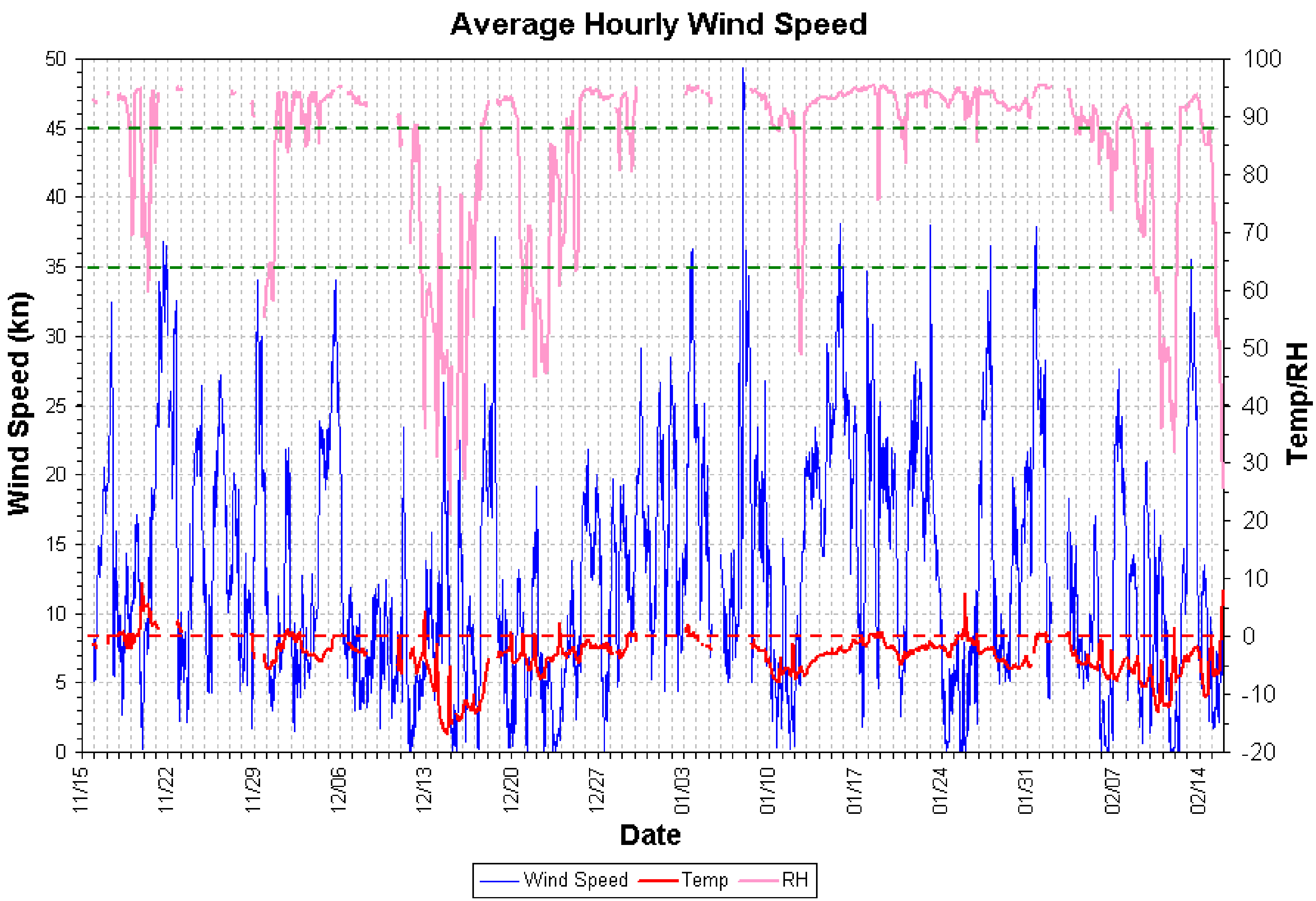

FIGURE 45. AVERAGE HOURLY WIND SPEED, TEMPERATURE, AND RELATIVE HUMIDITY

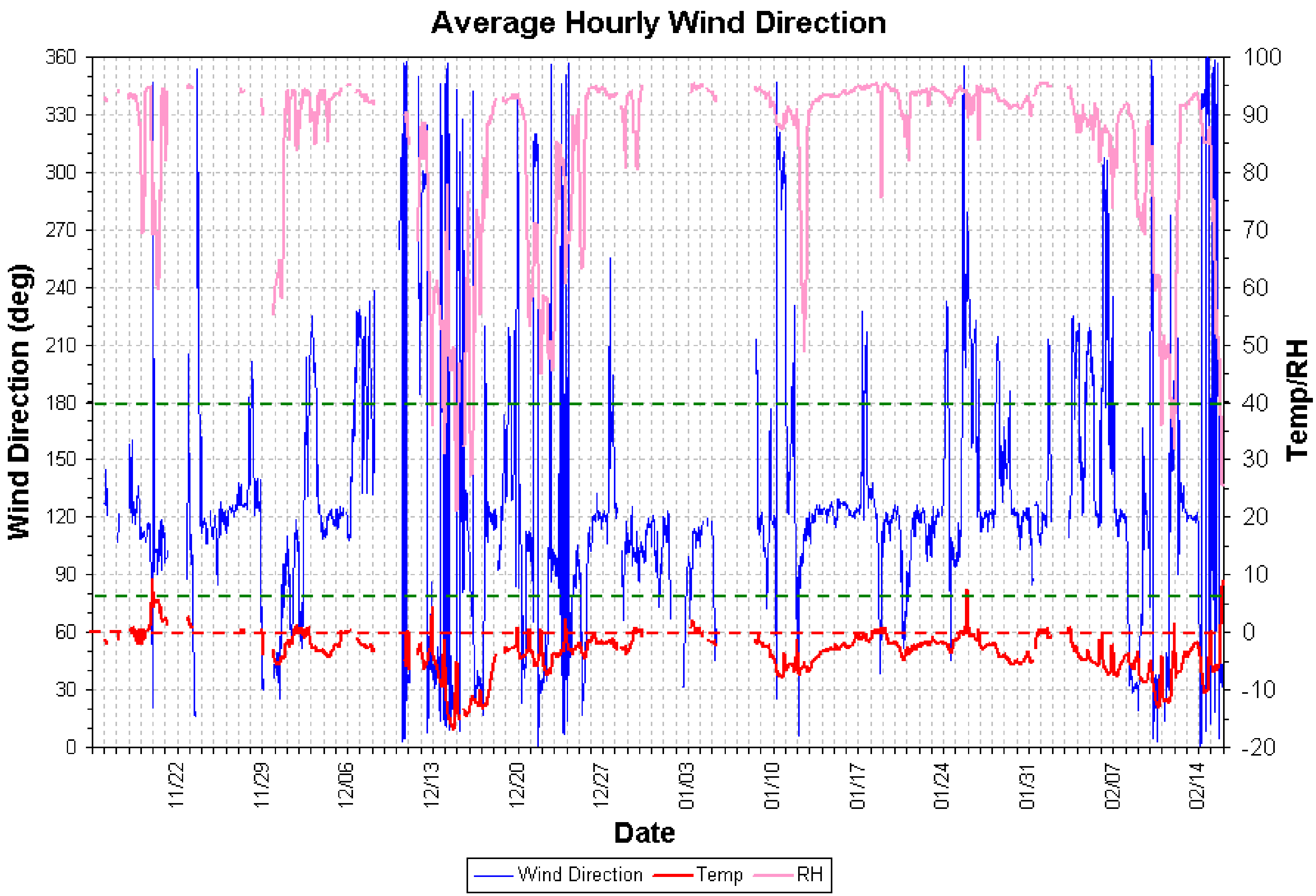

FIGURE 46. AVERAGE HOURLY WIND DIRECTION, TEMPERATURE, AND RELATIVE HUMIDITY

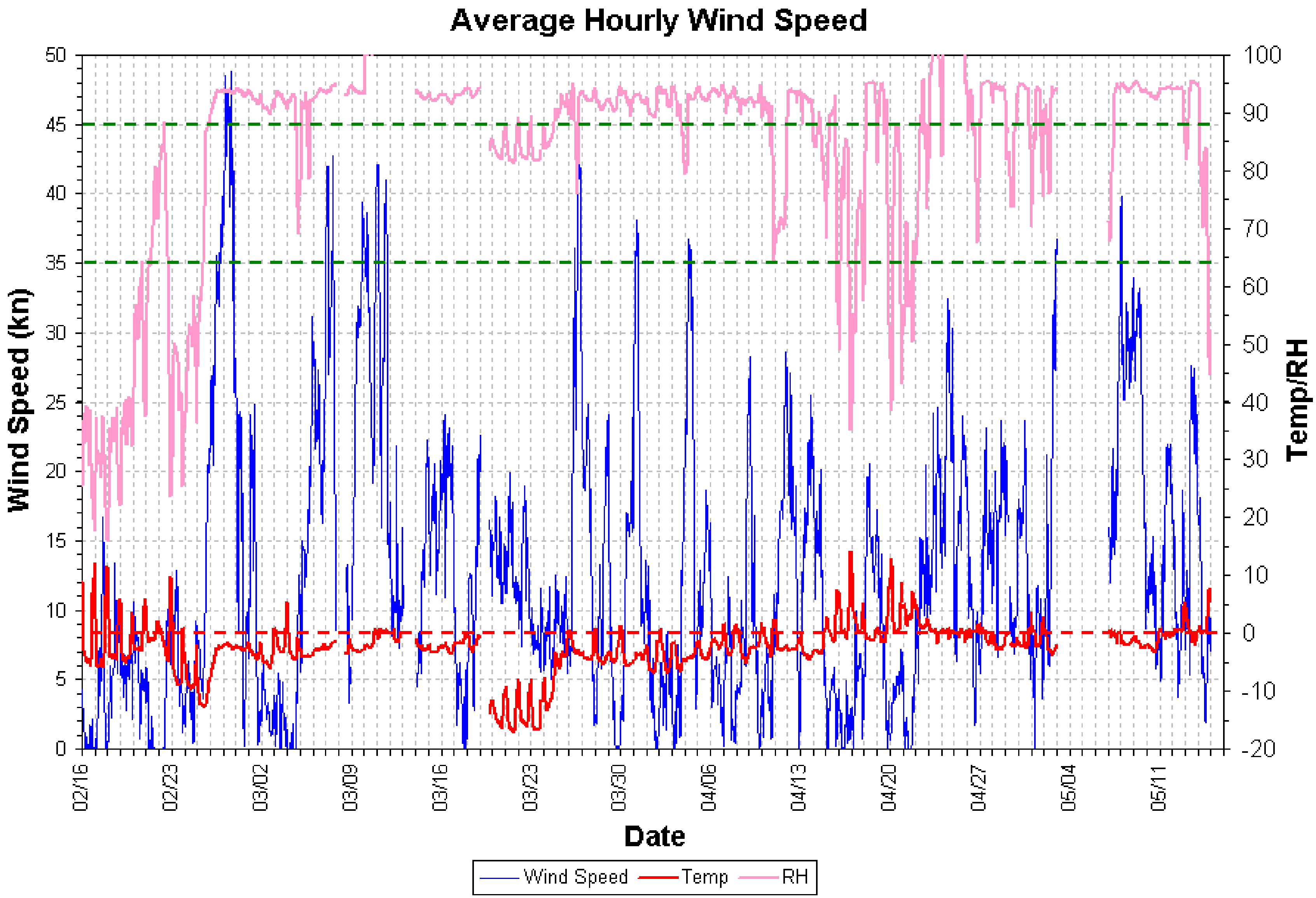

FIGURE 47. AVERAGE HOURLY WIND SPEED, TEMPERATURE, AND RELATIVE HUMIDITY

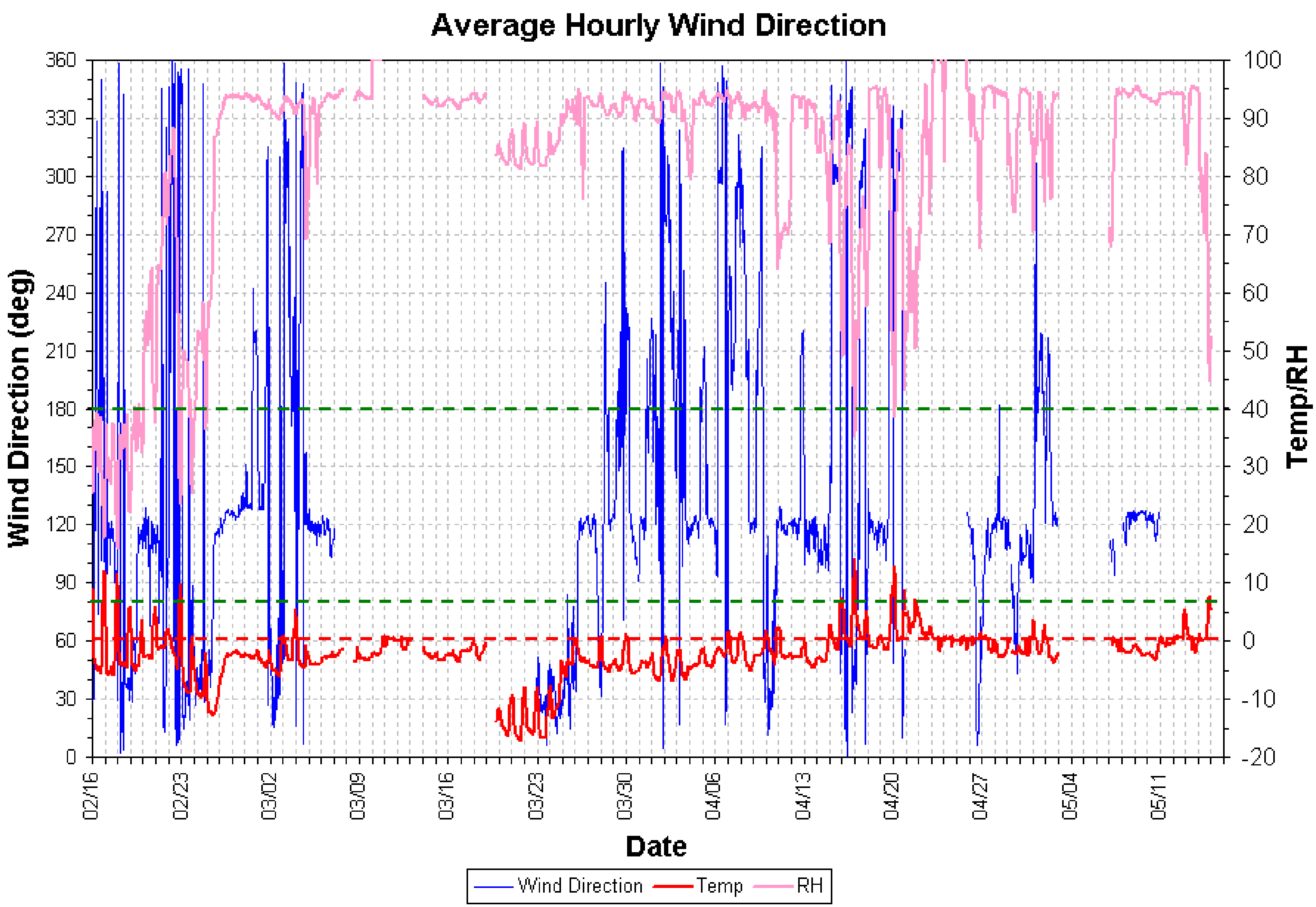

FIGURE 48. AVERAGE HOURLY WIND DIRECTION, TEMPERATURE, AND RELATIVE HUMIDITY

Approximately 3500 hours of test bed data were collected and analyzed over the 184-day period. Video motion clips were constructed and used to visually assess icing. In-depth data analysis was performed for the total ~37 hours of cases where winds exceeded the current limits for Juneau Part 121 air carrier operations (see table 9).

4.3.4.1 Hydro-Tech Wind Sensors.

Performance of the five Hydro-Tech sensors was evaluated by examining the sensor data as compared with the other wind sensors, and by reviewing the corresponding camera images. Due to the planned camera positions throughout the study, no video images of the EC1 sensors were captured.

In general, the Hydro-Tech sensors exhibited minimal icing, and most of the icing was on their respective supporting masts. Figure 49c provides photographs of the Hydro-Tech sensors experiencing icing under southeast flow conditions. Figure 49c and embedded web slide show illustrates one of the few events where icing was observed on the EC2 direction vane, as well as the supporting mast.

Although no video images of the EC1 sensors were collected, inspection of the data revealed that these sensors were affected by icing in more cases than the EC2 sensors. It is suspected that this was due to the location of the sensors on the tower and the greater exposure of these sensors to southeast wind flows than the EC2 sensors. Performance of the EC1 and Test Hydro-Tech rotor anemometers are shown for the 5 southeast flow cases shown in figures 50 through 54. The figures show prolonged periods of low wind speed readings as compared to the other sensors. An interesting aspect of these cases shows that the degradation in performance is gradual, and there are no particular characteristics in the traces that indicate obvious sensor degradation except for the comparison with the other sensors.

Direction vane performance under icing conditions is shown in figures 55 and 56. An unusual event was noted for the direction vane during the period 0830–1745 UTC on January 15, 2002 as shown in the time series in figure 55. The figure shows an unusual wind direction distribution for the mechanical sensor indicating that the azimuthal movement of the direction vane was limited. This effect may indicate the presence of an interfering ice formation on the southeast side of the sensor head stemming up and around from the sensor's mast. This is substantiated by the video images of the NRG sensor for this period, which indicates there was substantial icing and growth of ice on the tower. Finally, degraded performance for the EC1 direction vane is shown in figure 56.

Performance of the sensor was found to be consistent with data from the wind tunnel tests and results from the MWO study. Typical cases showing a comparison of wind speed against the Vaisala anemometer is provided in figures 57 through 60. Due to the inertia of the ruggedized sensor, the observed overspeeding and a low starting threshold was expected. The overspeeding indicated in the figure is particularly pronounced for northerly winds and is possibly exacerbated by the upslope winds at Eagle Crest in this direction. The off-axis overspeed response inherent to the sensor was also noted in the wind tunnel tests.

TABLE 9. PERIODS EXCEEDING OPS SPEC WIND LIMITATIONS

11/21/2000	13:00 - 16:00
	19:00 - 21:00
11/22/2000	17:00 - 18:00
12/05/2000	13:00 - 15:00
12/14/2000	09:00 - 13:00
12/18/2000	14:00 - 16:00
01/03/2001	09:00 - 20:00
01/07/2001	18:00 - 24:00
01/08/2001	01:00 - 02:00
	06:00 - 07:00
01/15/2001	13:00 - 19:00
01/17/2001	22:00 - 23:00
01/18/2001	21:00 - 23:00
01/23/2001	01:00 - 03:00
01/27/2001	18:00 - 19:00
	23:00 - 24:00
01/31/2001	14:00 - 17:00
02/26/2001	09:00 - 11:00
	15:00 - 24:00
02/27/2001	00:00 - 22:00
03/07/2001	00:00 - 04:00
	08:00 - 13:00
03/09/2001	18:00 - 23:00
03/10/2001	03:00 - 05:00
	20:00 - 24:00
03/11/2001	00:00 - 02:00
	13:00 - 18:00
03/26/2001	07:00 - 09:00
	13:00 - 20:00
03/31/2001	01:00 - 08:00
04/04/2001	04:00 - 11:00
04/24/2001	10:00 - 11:00
05/02/2001	20:00 - 24:00
05/03/2001	00:00 - 01:00
	06:00 - 09:00
05/07/2001	19:00 - 20:00
	22:00 - 24:00
05/08/2001	00:00 - 02:00
	20:00 - 22:00

Total Ops Spec hours: 37.2

(a)

(b)

(c)

FIGURE 49. ICING ON HYDRO-TECH EC2 ROTOR MAST (A), TEST SENSOR MAST (B), AND EC2 DIRECTION VANE AND MAST

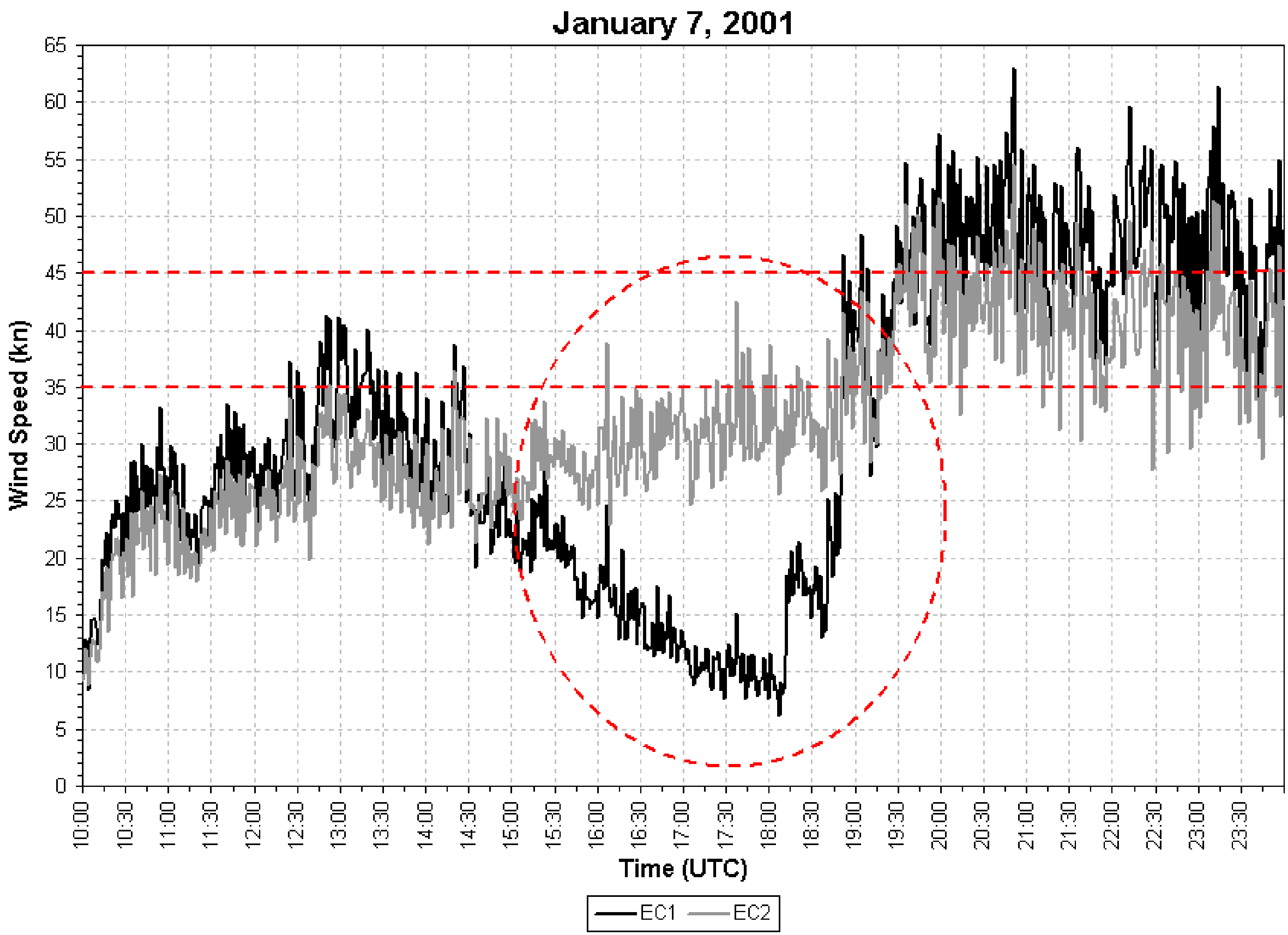

FIGURE 50. COMPARISON OF EC1 AND EC2 WIND SPEEDS

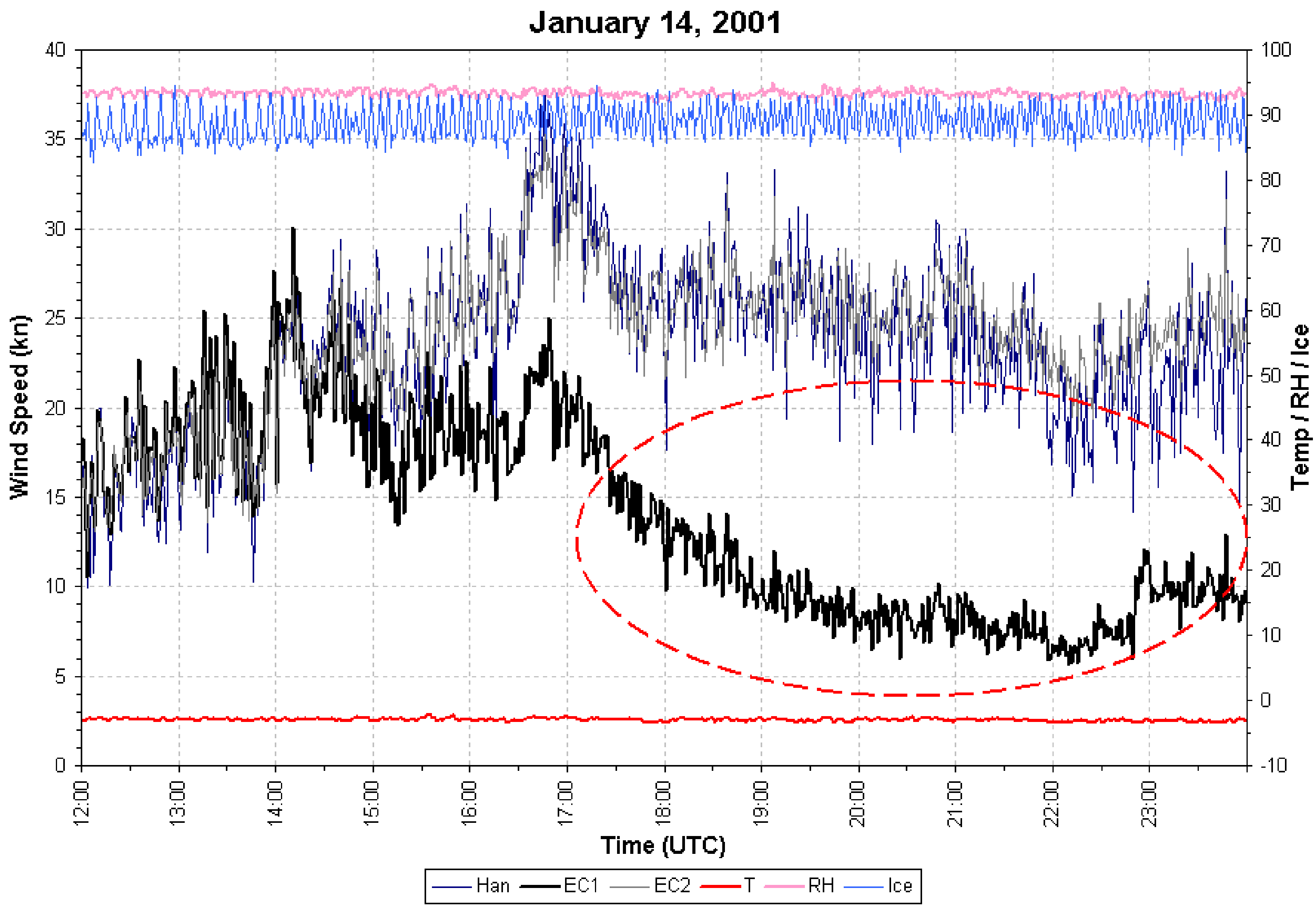

FIGURE 51. COMPARISON OF EC1 WIND SPEED AGAINST EC2 AND VAISALA WIND SPEEDS)

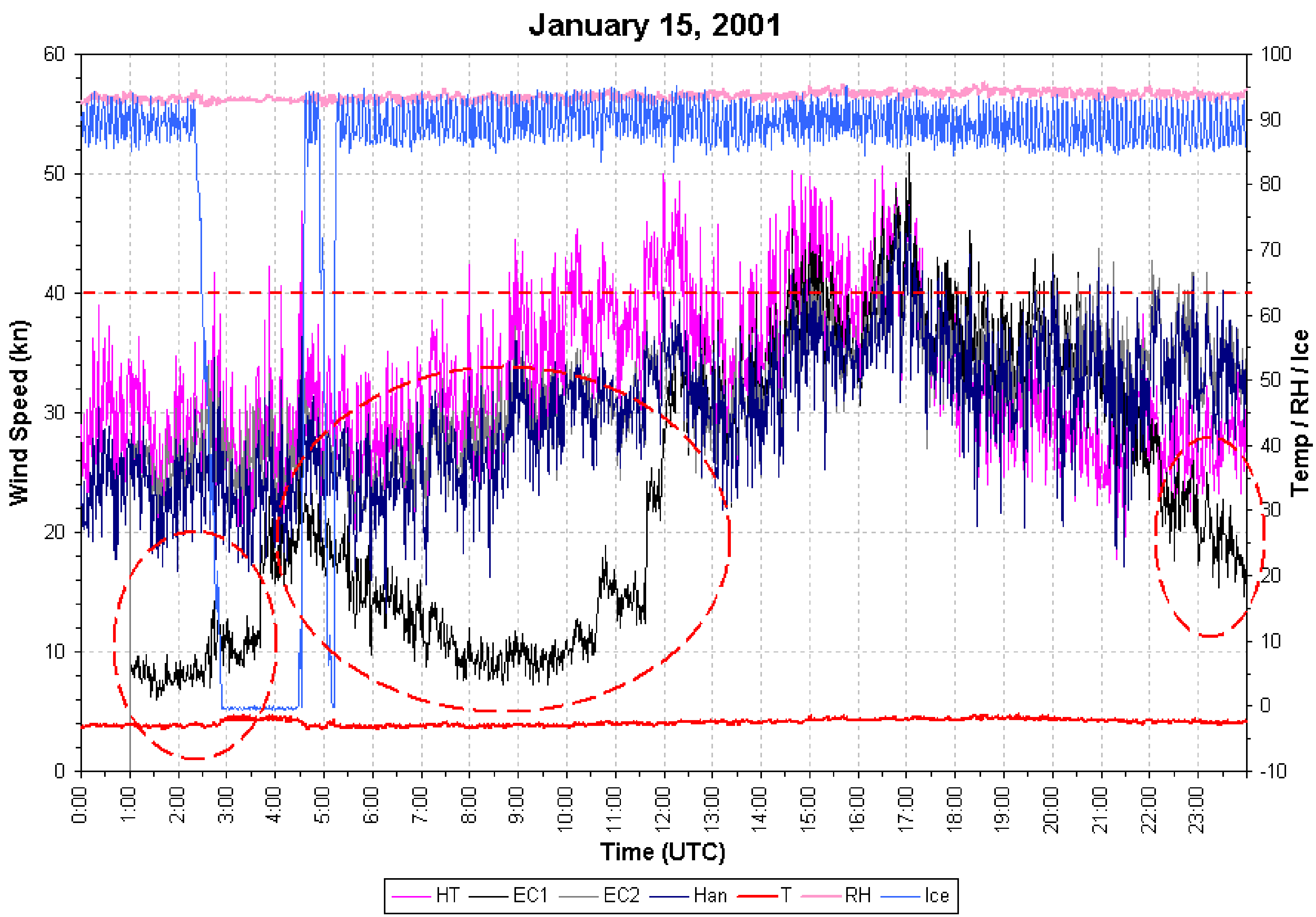

FIGURE 52. COMPARISON OF EC1 WIND SPEEDS DURING AN ICING EVENT

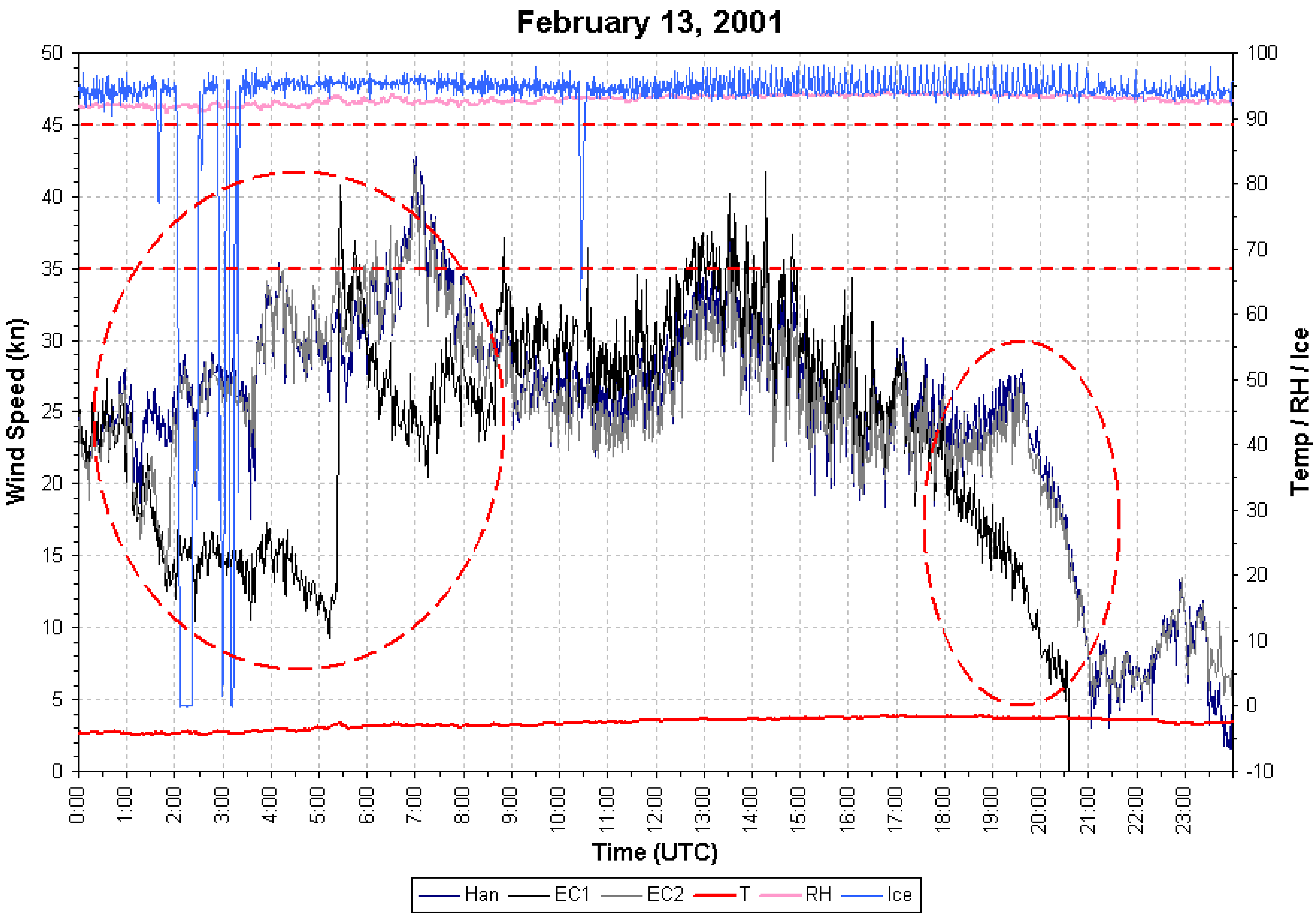

FIGURE 53. DEGRADED EC1 ROTOR PERFORMANCE DURING AN ICING EVENT

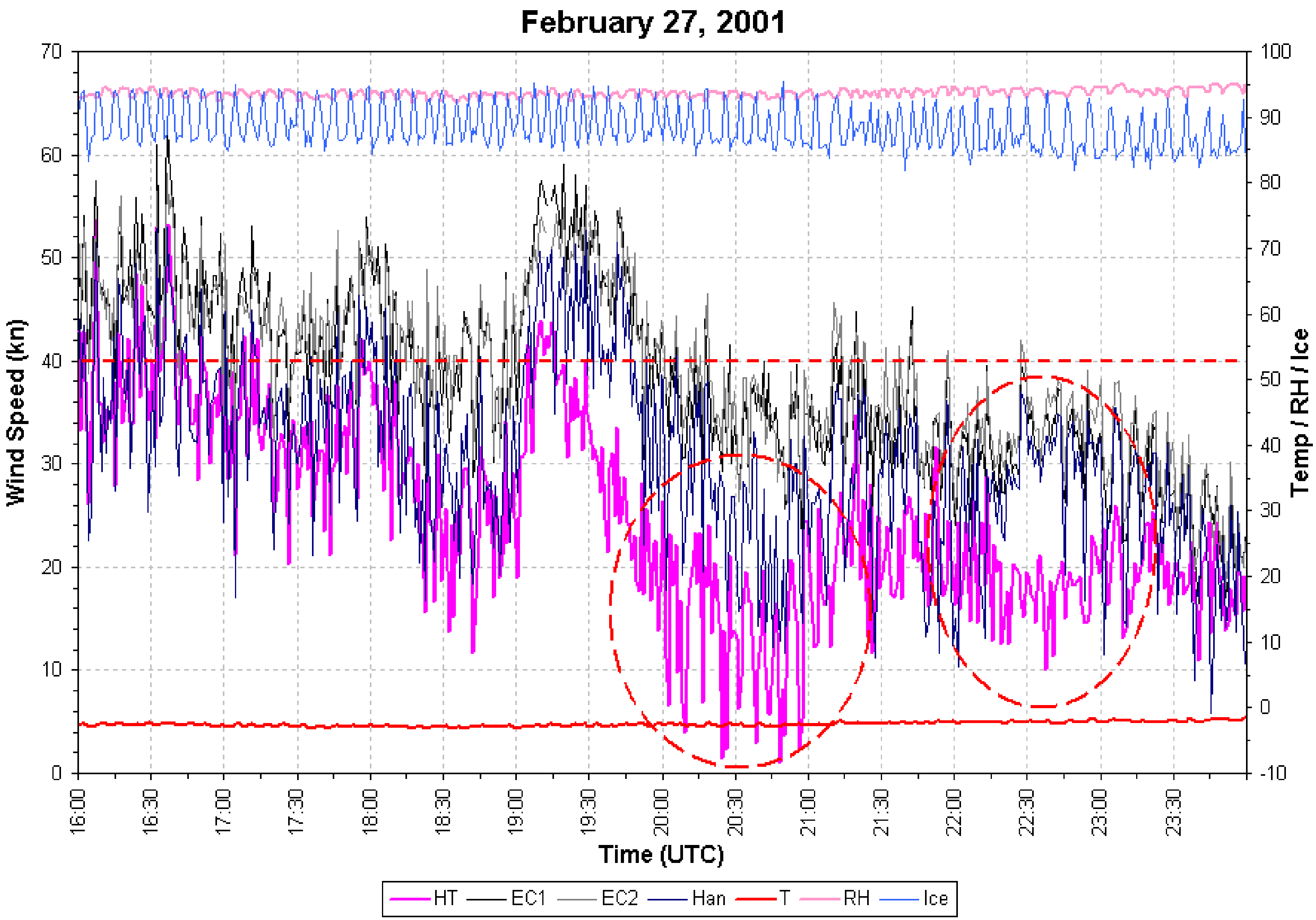

FIGURE 54. TEST HYDRO-TECH ROTOR FAILURE DURING AN ICING EVENT

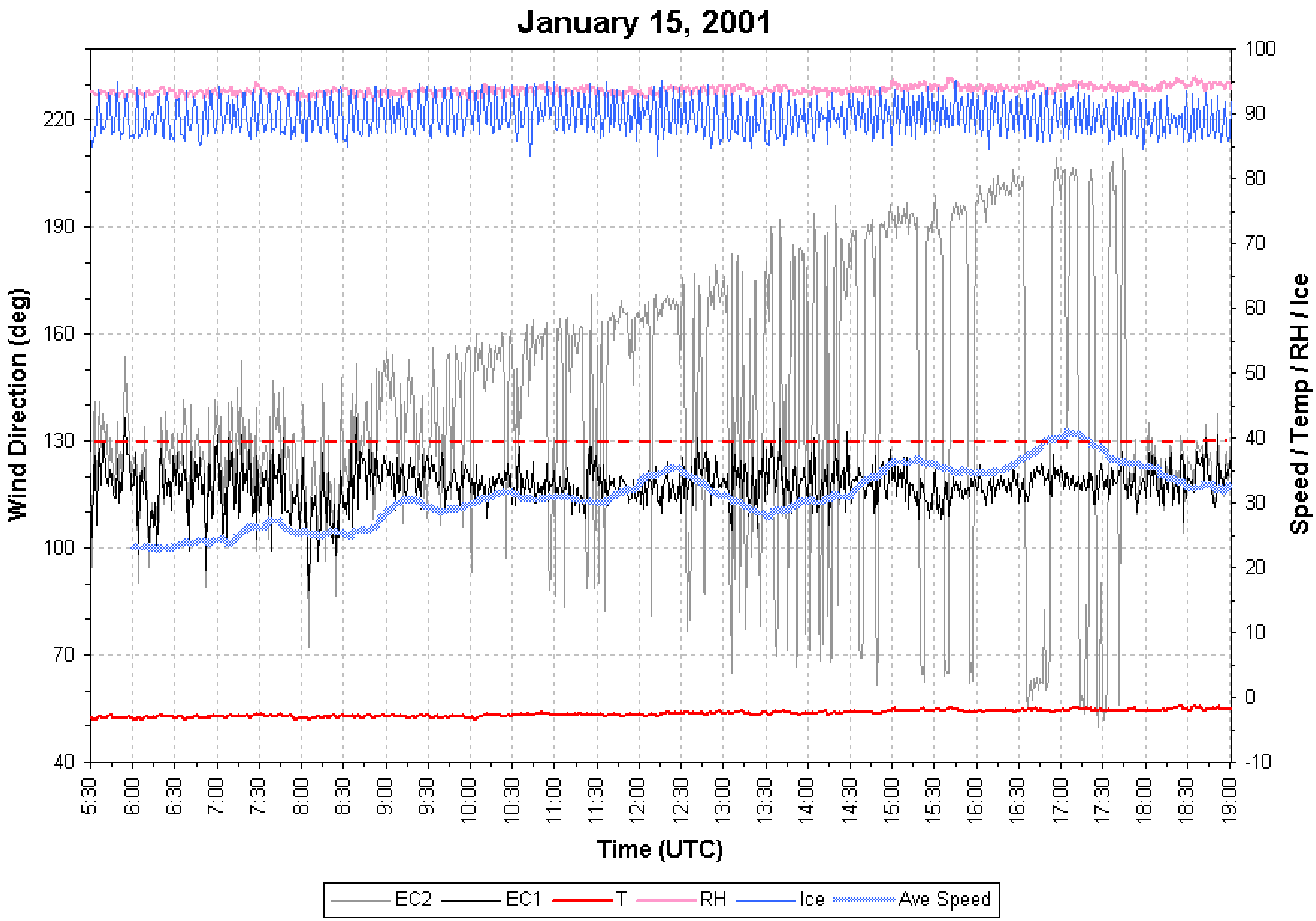

FIGURE 55. EC2 DIRECTION VANE FAILURE DURING AN ICING EVENT

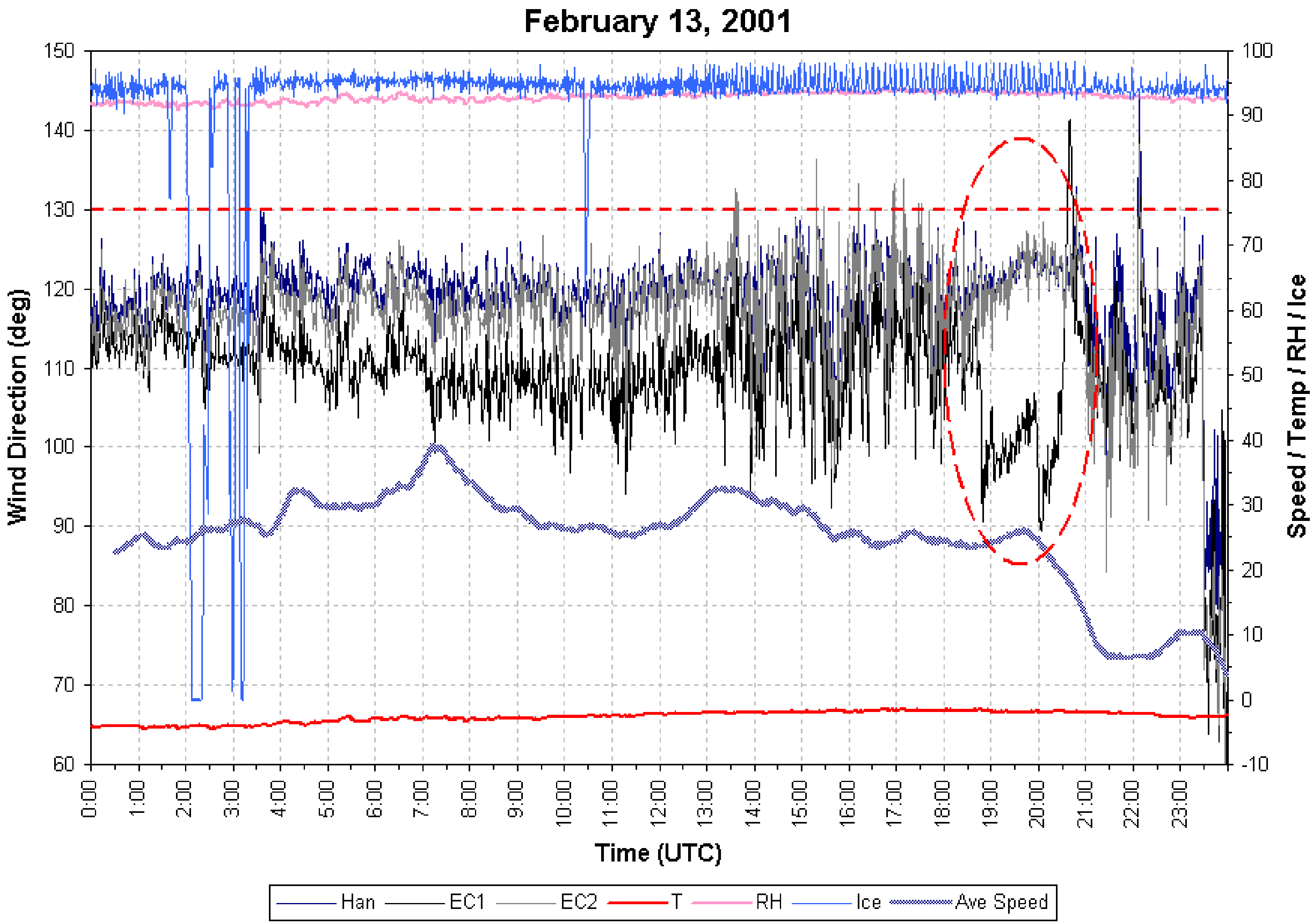

FIGURE 56. EC1 DIRECTION VANE FAILURE DURING AN ICING EVENT

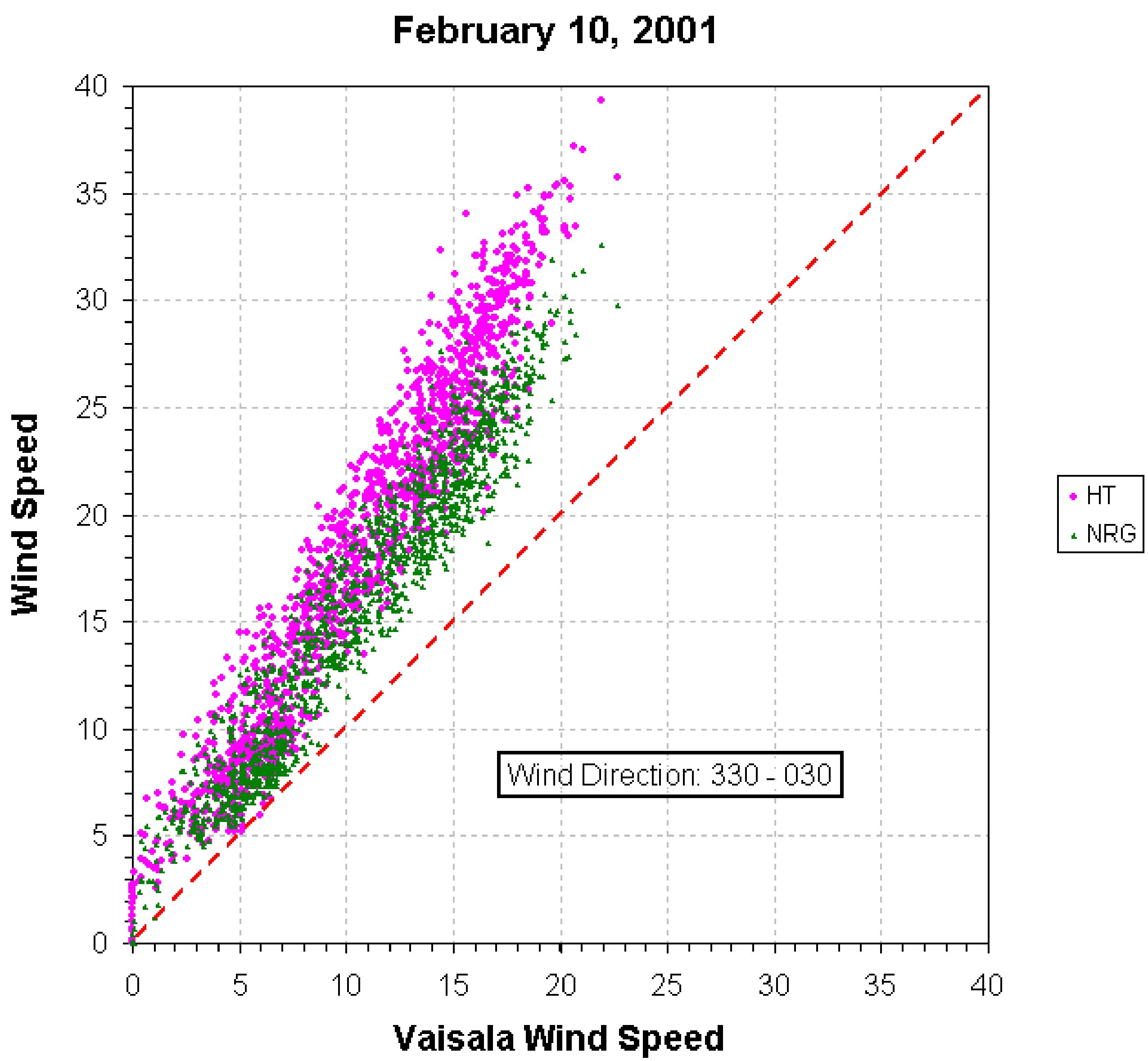

FIGURE 57. WIND SPEED DISTRIBUTION FOR NORTH WIND

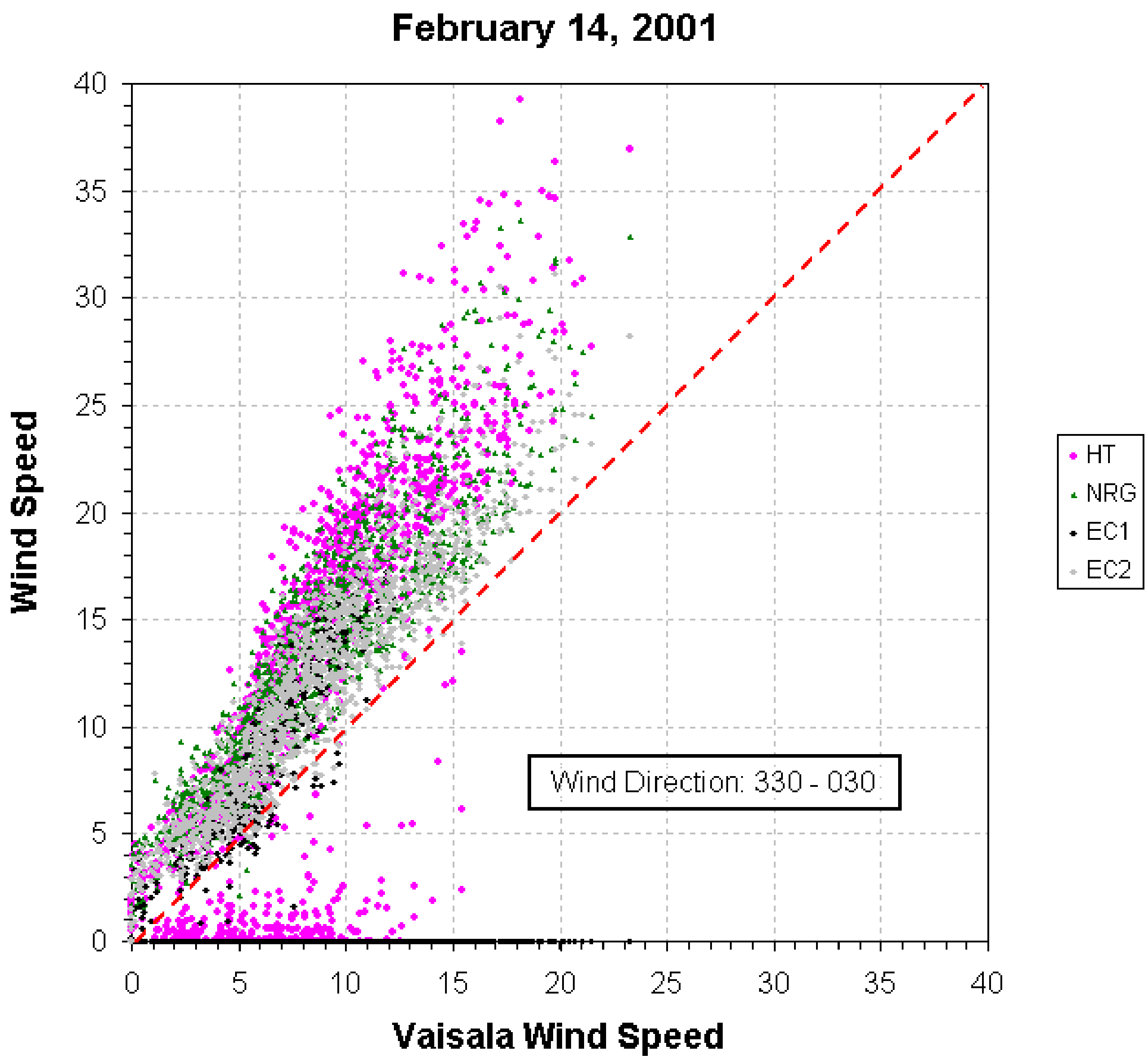

FIGURE 58. WIND SPEED DISTRIBUTION FOR NORTH WIND

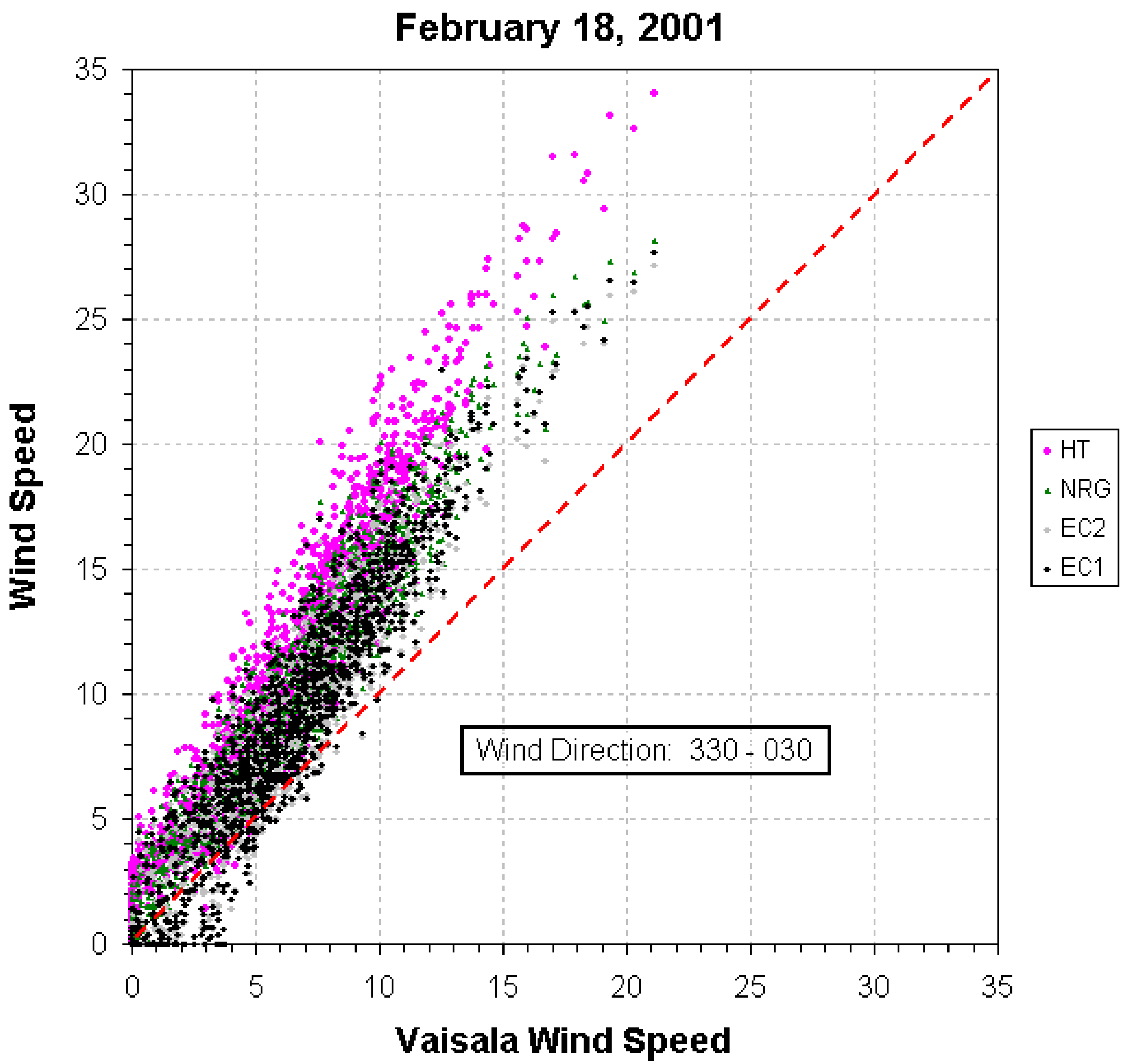

FIGURE 59. WIND SPEED DISTRIBUTION FOR NORTH WIND

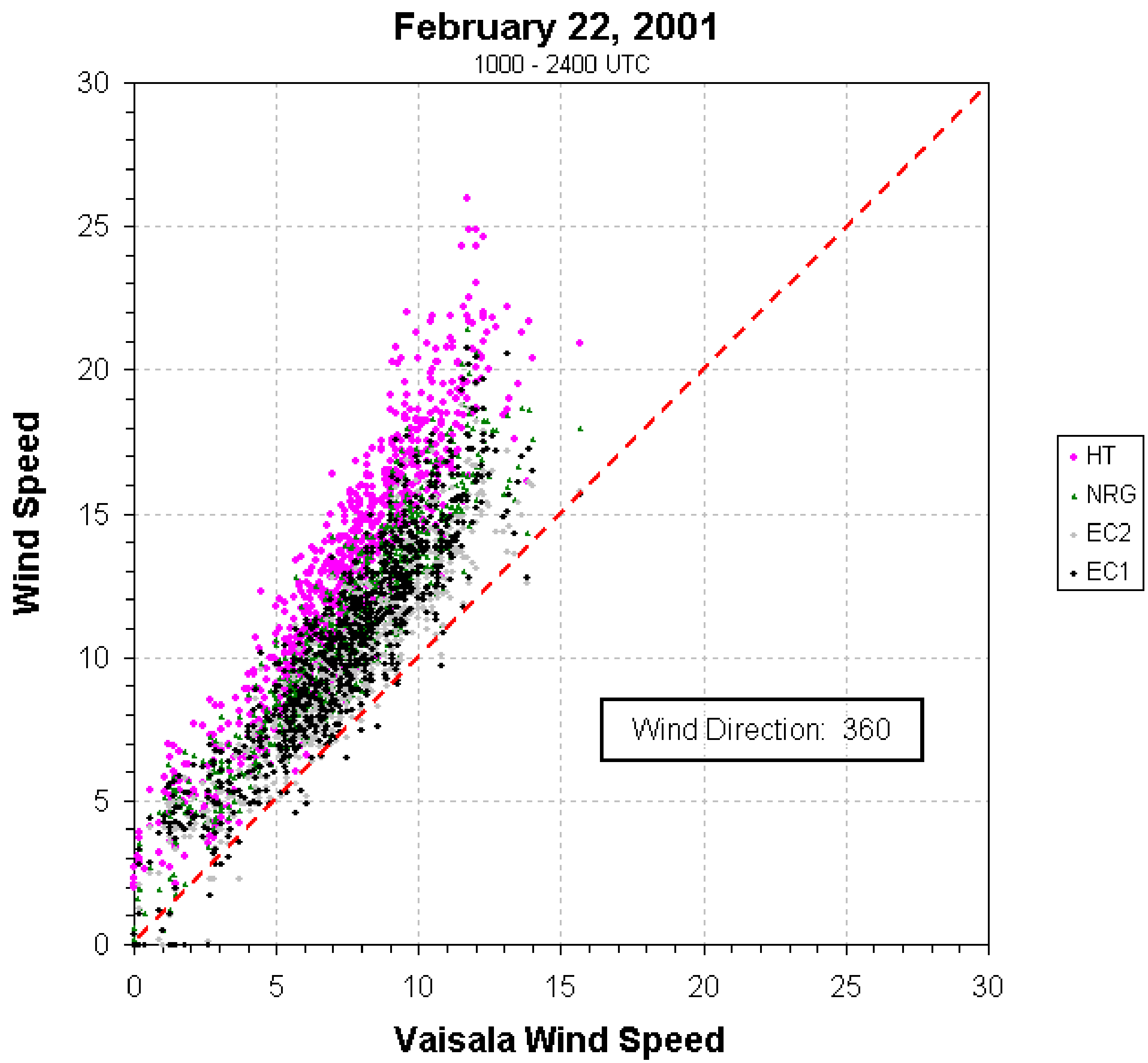

FIGURE 60. WIND SPEED DISTRIBUTION FOR NORTH WIND

4.3.4.2 NRG Wind Sensors.

Significant icing was experienced by the IceFree II anemometers. Time series of wind speed data and corresponding photographs of icing on the rotor sensor are shown in figures 61 through 64. Similar plots for the direction vane are provided in figures 65 through 67. Many of the characteristics shown in the traces are similar to the similar features shown for the mechanical Hydro-Tech sensors during icing conditions.

4.3.4.3 Ultrasonic Wind Sensor.

A total of 3364 hours (~140 days) of sonic anemometer data were recorded and collected. The distribution of failures based on the 1-second raw sensor data is shown in figure 68. The sensor was determined through its internal status, as well as video data, to be degraded by icing 26.4 hours (or 0.8%) of the 6-month period. A failure qualifies as a bad data flag received from the sensor because of unreliable readings. Review of the camera data indicates that the failures appear highly correlated to snow and icing conditions. However, unlike the MWO study where there were instances where the sensor was in complete failure-mode over periods ranging from 2 to 3 continuous hours, the events of sensor failures at JNU were generally intermittent in nature, with frequencies of occurrence proportional to the severity of the weather conditions.

Further analysis of the periods of degraded performance, with respect to the JAWS 1-minute wind reporting requirement, was next performed. The affected 1-minute averages are shown in figure 69. An affected 1-minute average is a 1-minute mean wind value where at least 1 of the 60 constituent 1-second samples is flagged as bad. The composition of the affected 1-minute averages is reflected in the frequency histograms in figure 70. The analysis revealed that in 84% of affected cases, there were at least 75% raw data samples available to derive a valid wind report. During the entire field experiment, only 81 sporadic 1-minute wind reports were derived from 25% or less raw 1-second samples.

Closer inspection was performed to determine the validity of the affected 1-minute average values when ice was apparent on the anemometer. Time series of Vaisala wind speed and direction values during significant icing events are depicted in figures 71 through 77. In these figures, the sample size of valid data, in percent, comprising the 1-minute averages is shown in yellow against the secondary ordinate axis.

4.3.4.4 Rosemount Wind Sensor.

The Rosemount 1774W pressure-type probe exhibited optimistic performance as shown in figure 78. However, the sensor was installed late in the season and the resulting data set was unfortunately limited.

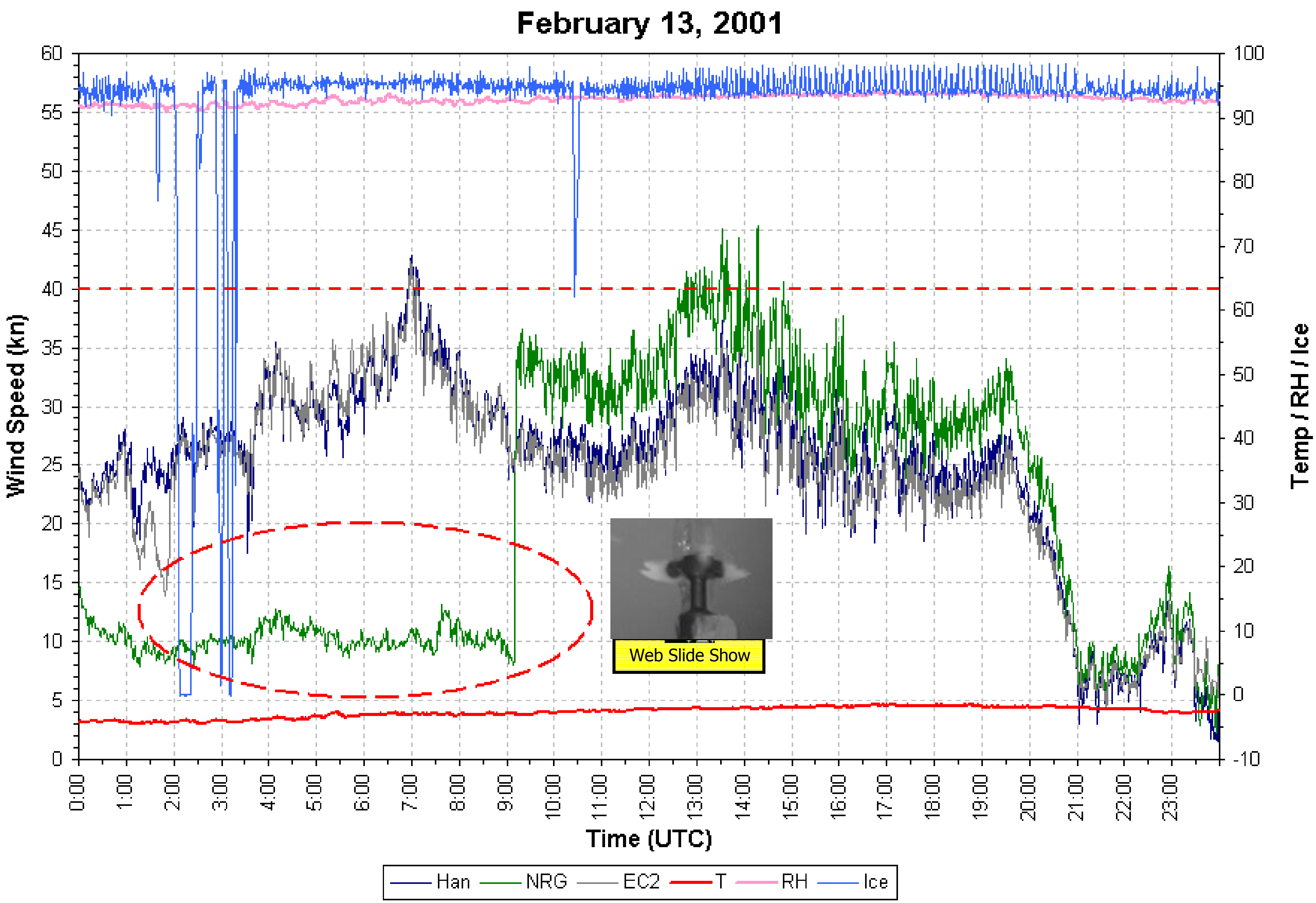

FIGURE 61. NRG ROTOR FAILURE DURING AN ICING EVENT

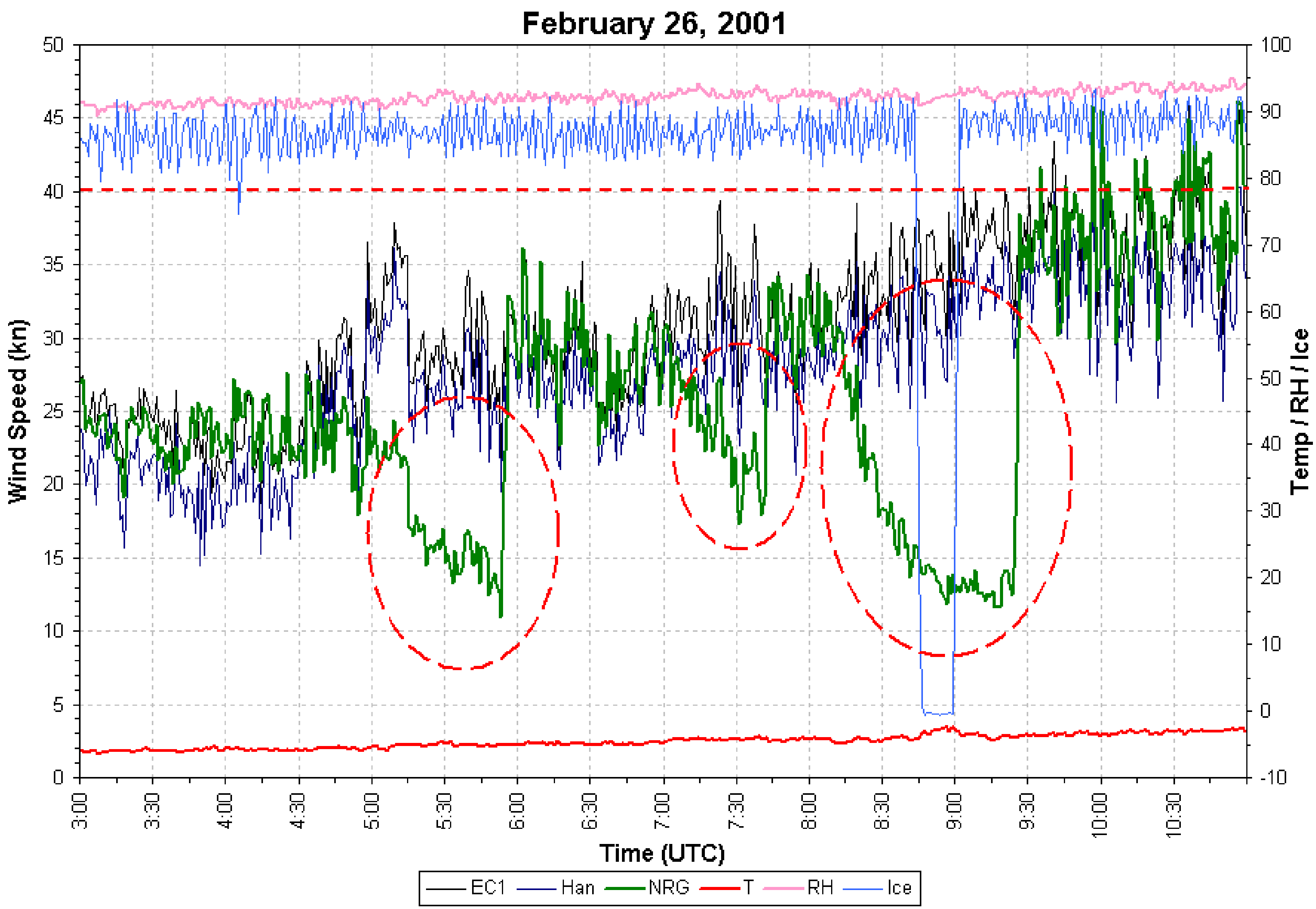

FIGURE 62. NRG ROTOR FAILURES DURING AN ICING EVENT

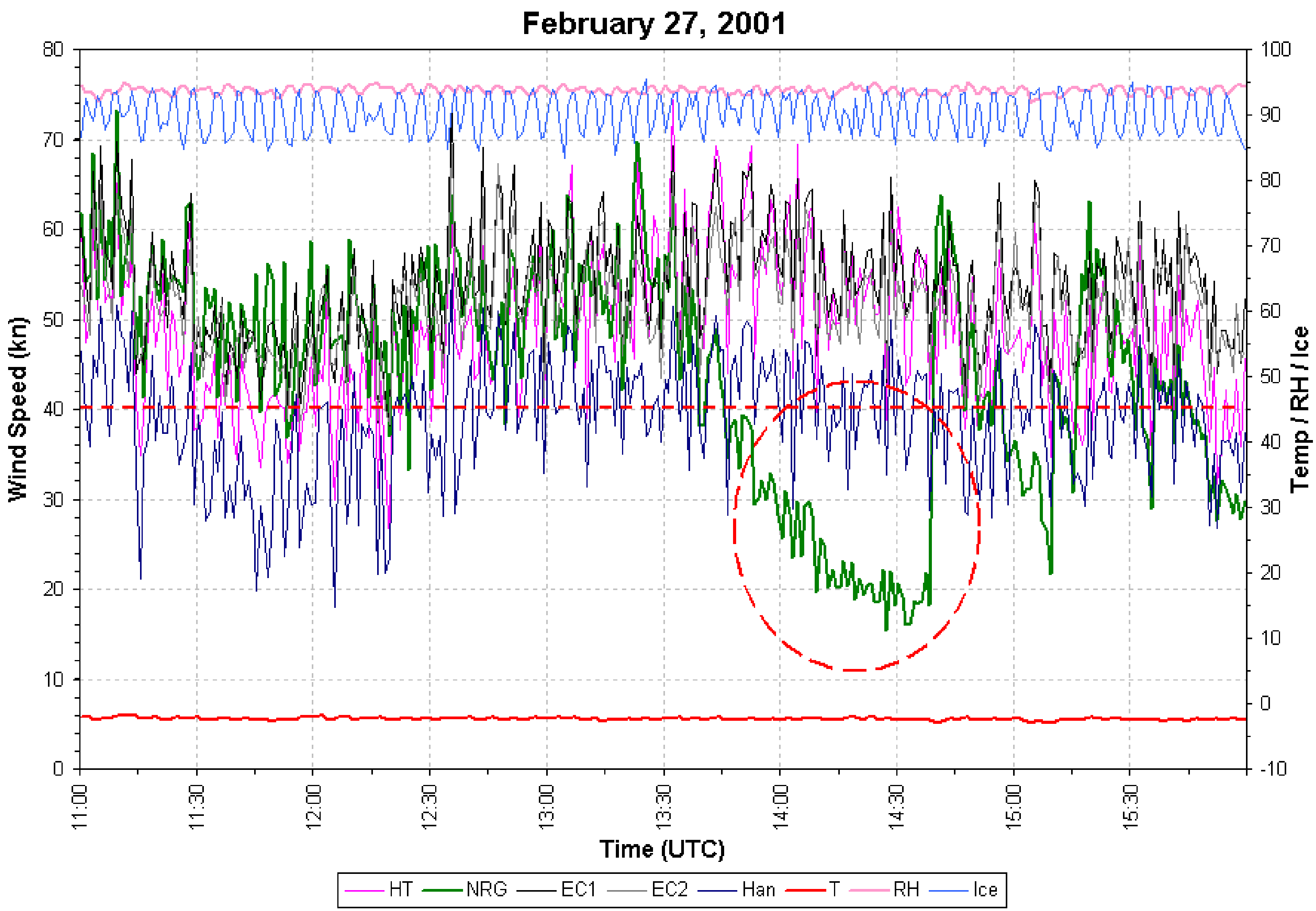

FIGURE 63. NRG ROTOR FAILURE DURING AN ICING EVENT

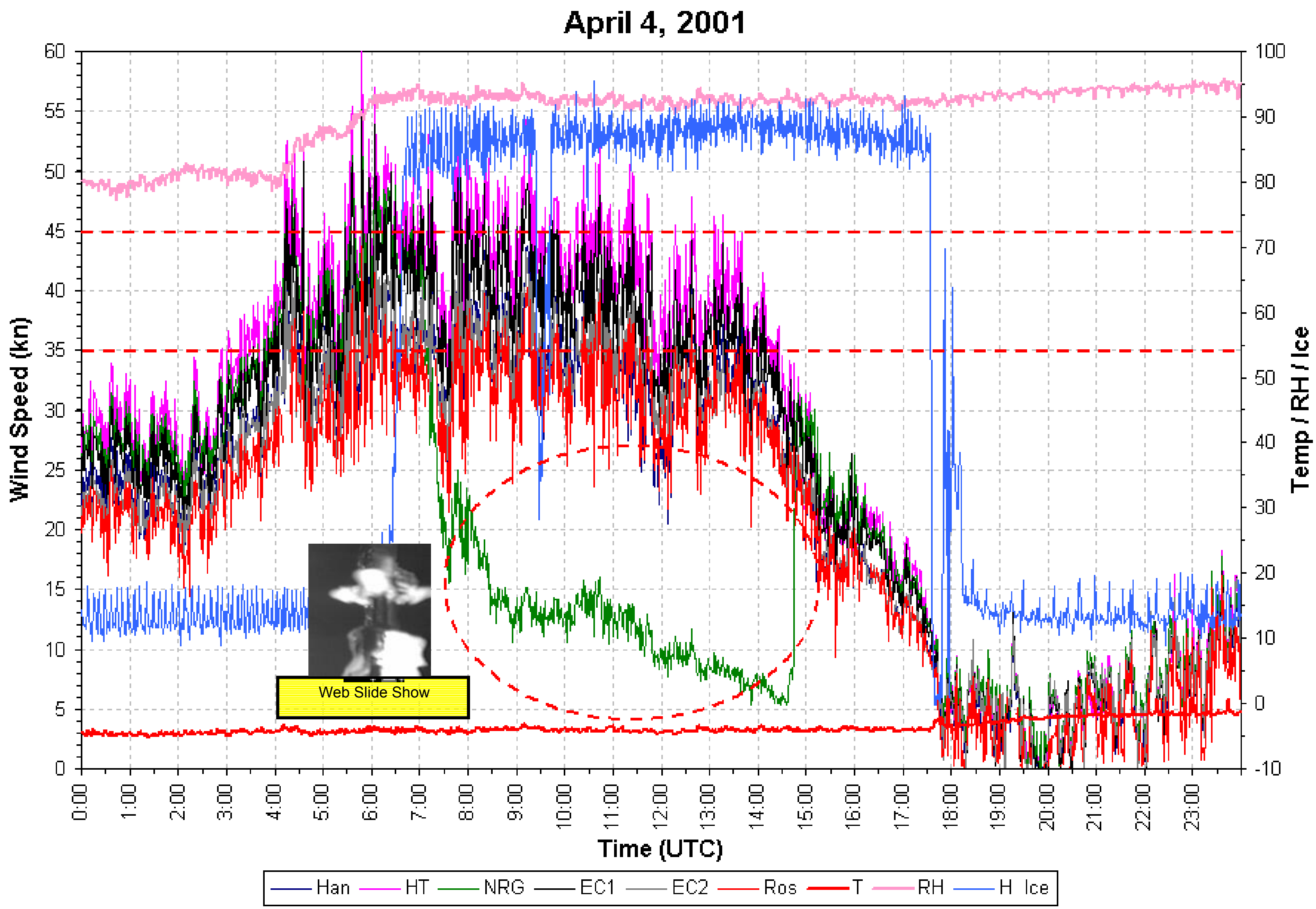

FIGURE 64. NRG ROTOR FAILURE DURING AN ICING EVENT

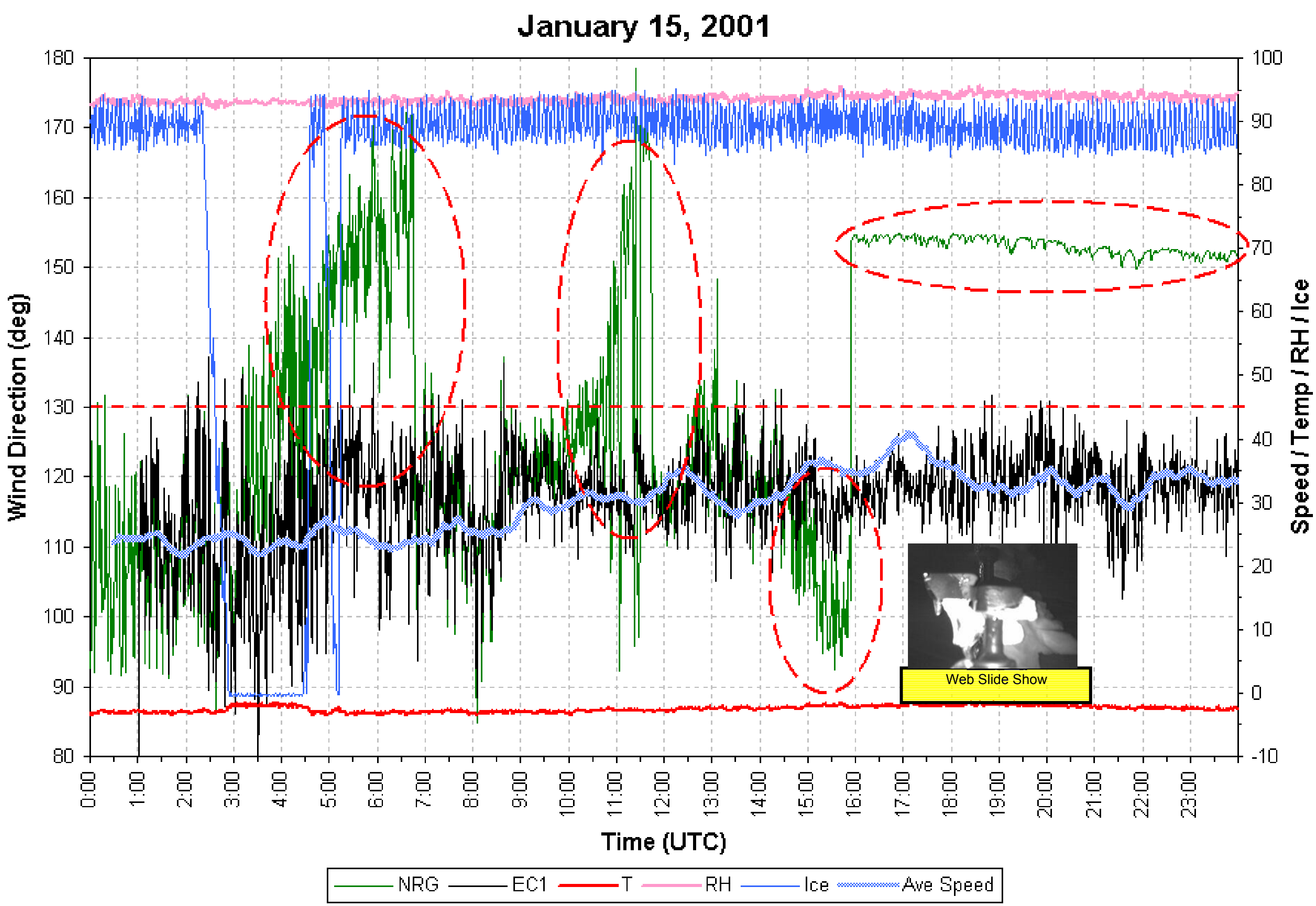

FIGURE 65. NRG DIRECTION VANE FAILURE DURING AN ICING EVENT

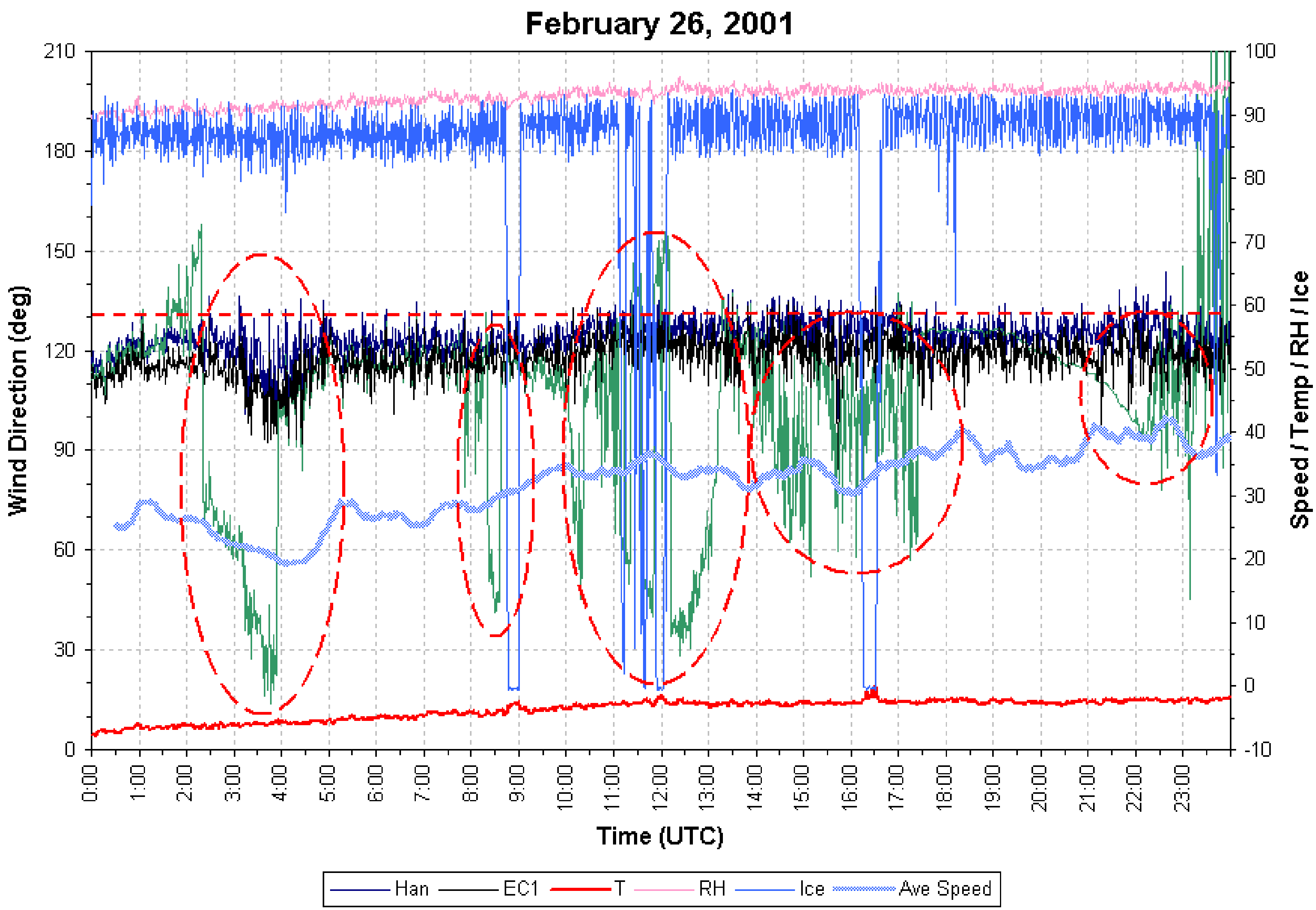

FIGURE 66. NRG DIRECTION VANE FAILURES DURING AN ICING EVENT

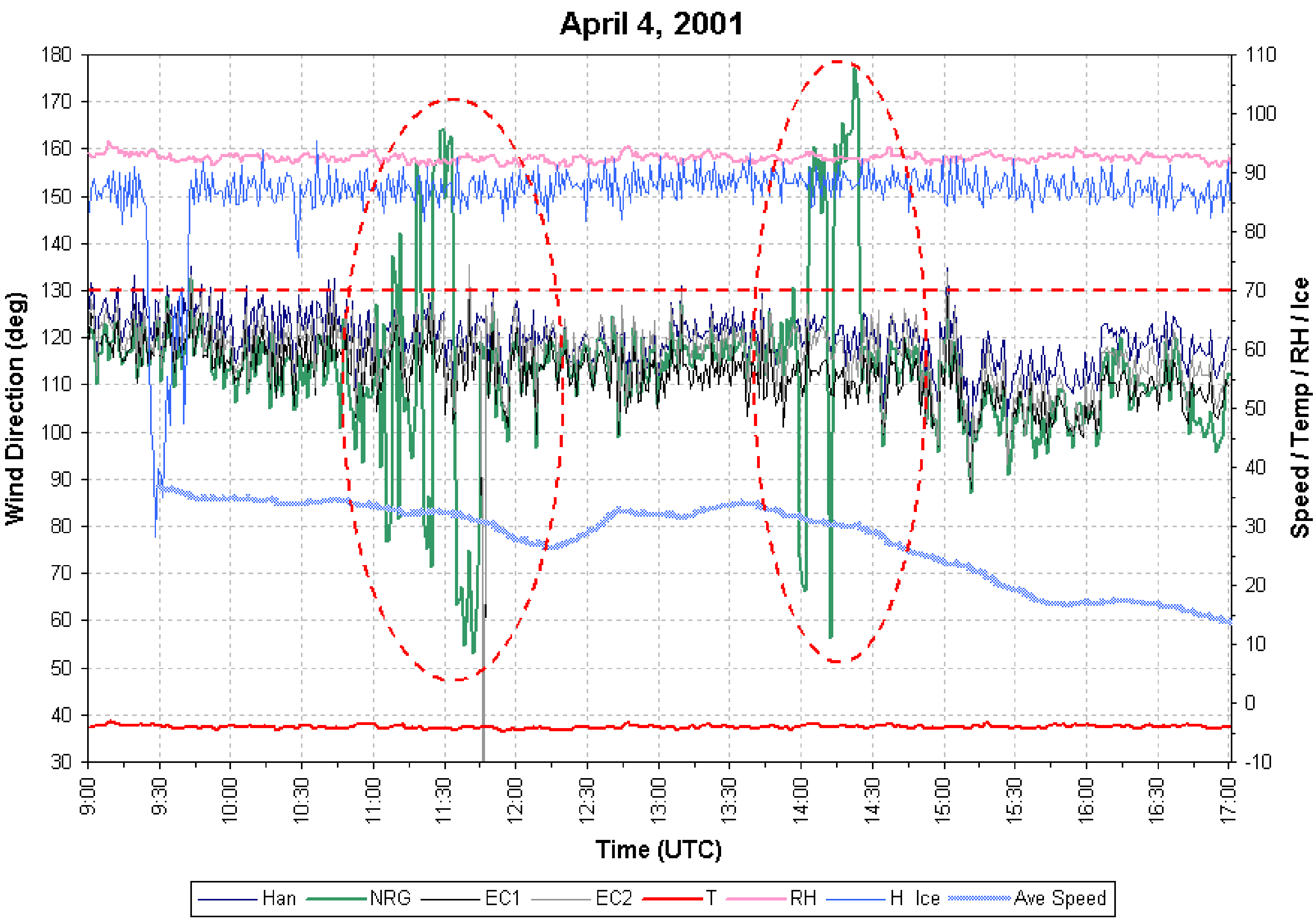

FIGURE 67. NRG DIRECTION VANE FAILURES DURING AN ICING EVENT

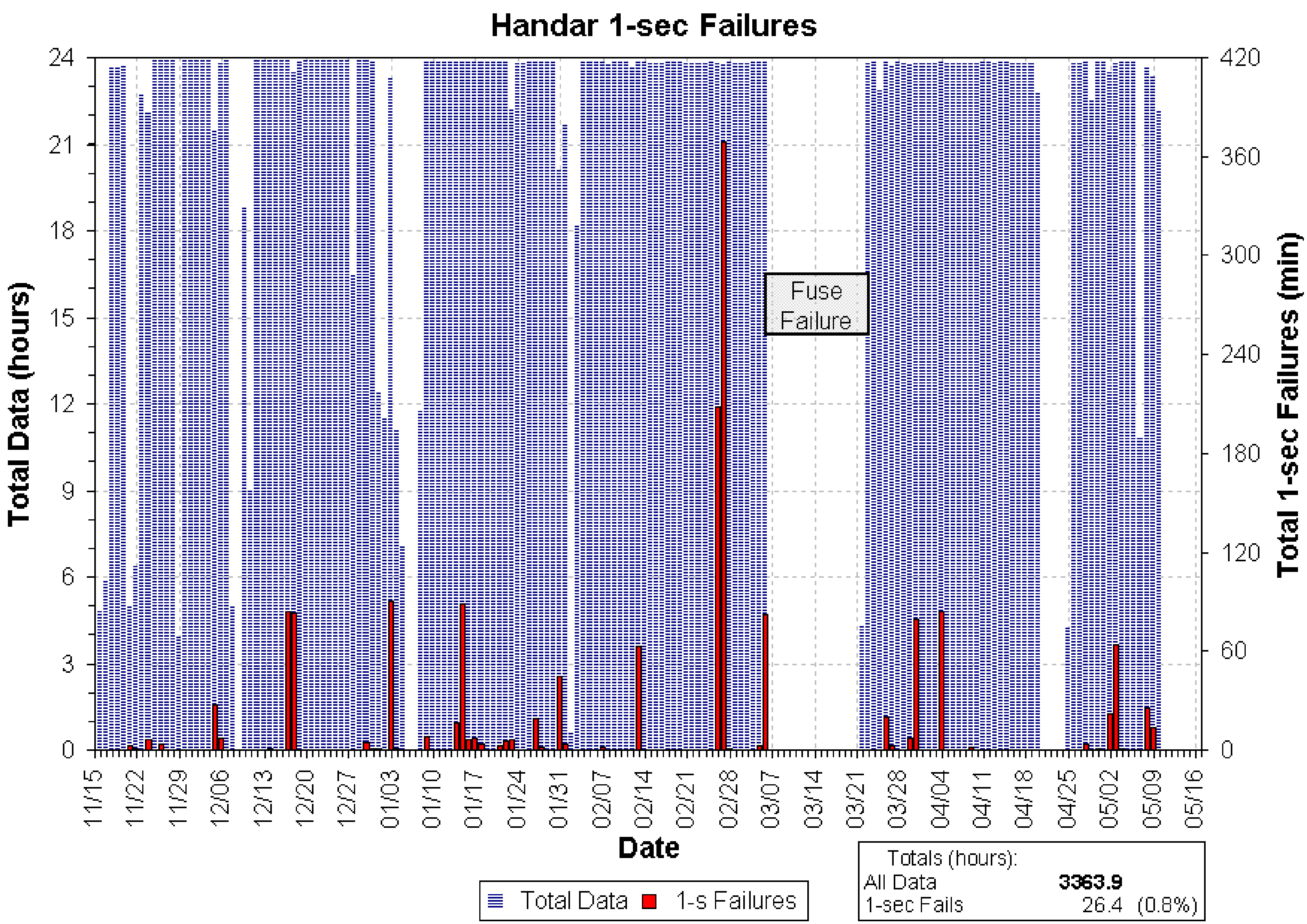

FIGURE 68. DISTRIBUTION OF VAISALA 1-SECOND SENSOR FAILURES

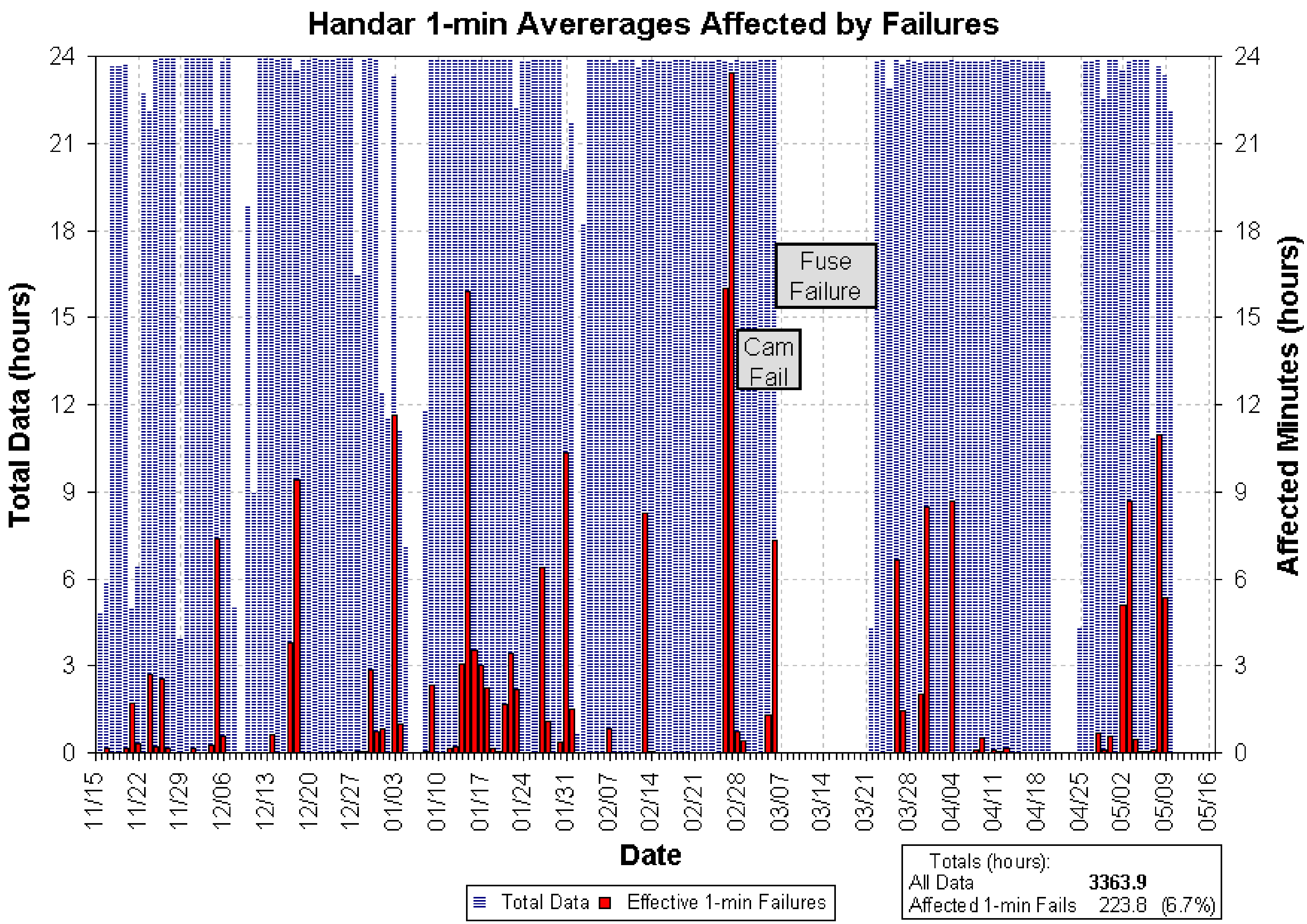

FIGURE 69. DISTRIBUTION OF VAISALA 1-MINUTE AVERAGES AFFECTED BY SENSOR FAILURES

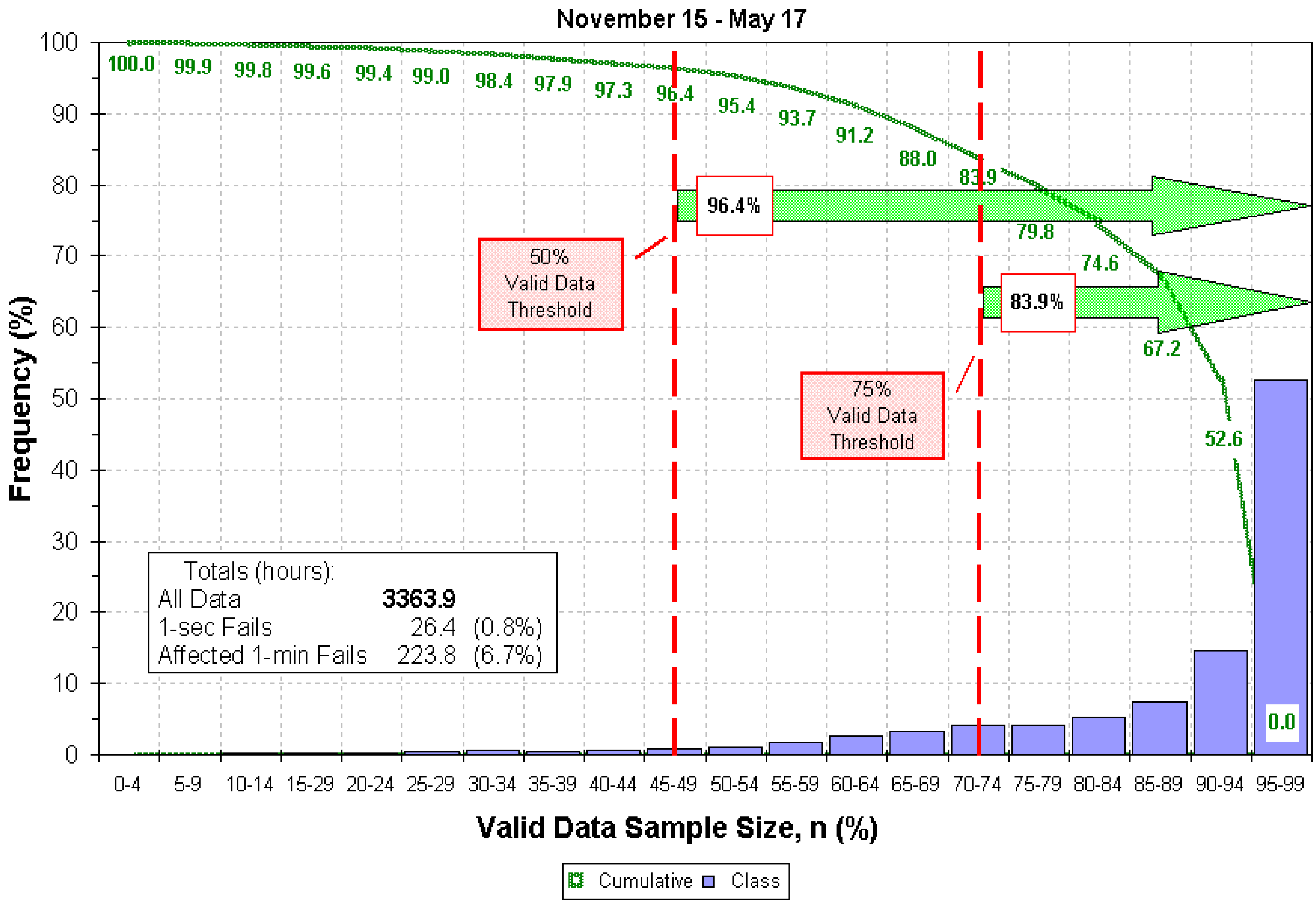

FIGURE 70. FREQUENCY DISTRIBUTION OF SAMPLE SIZES FOR VAISALA 1-MINUTE AVERAGES AFFECTED BY SENSOR FAILURES

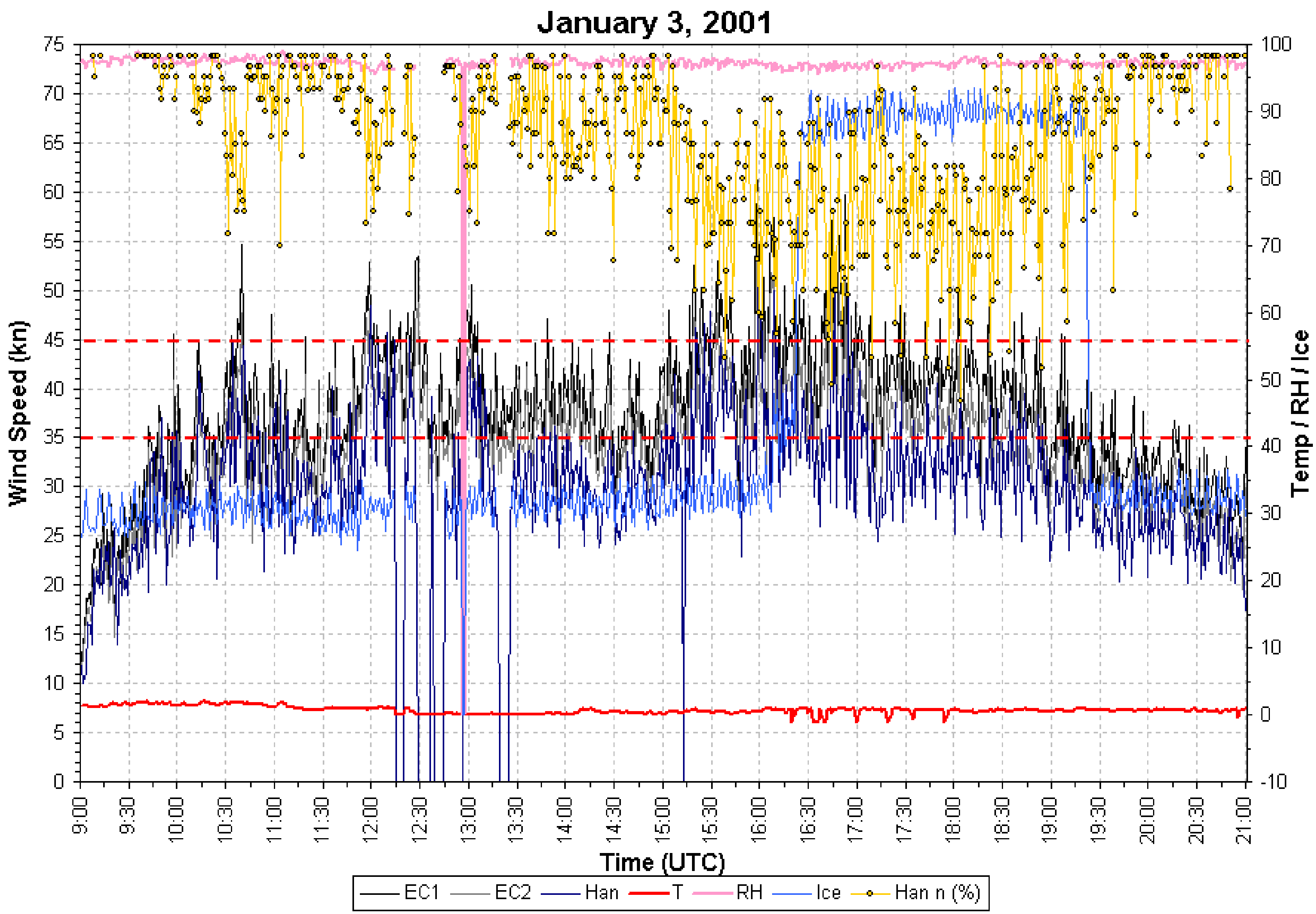

FIGURE 71. VAISALA 1-MINUTE WIND SPEED AVERAGES DURING AN ICING EVENT

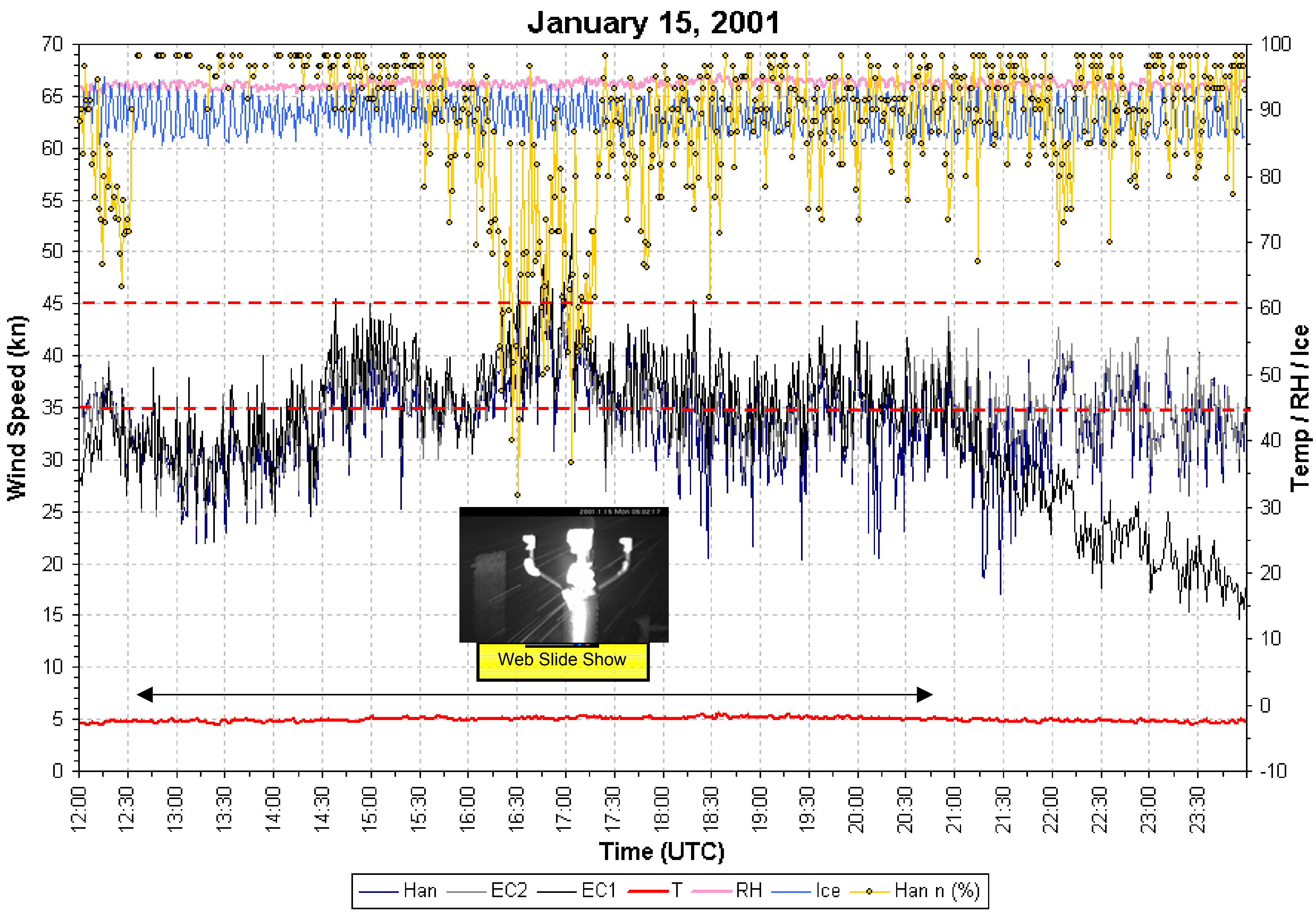

FIGURE 72. VAISALA 1-MINUTE WIND SPEED AVERAGES DURING AN ICING EVENT

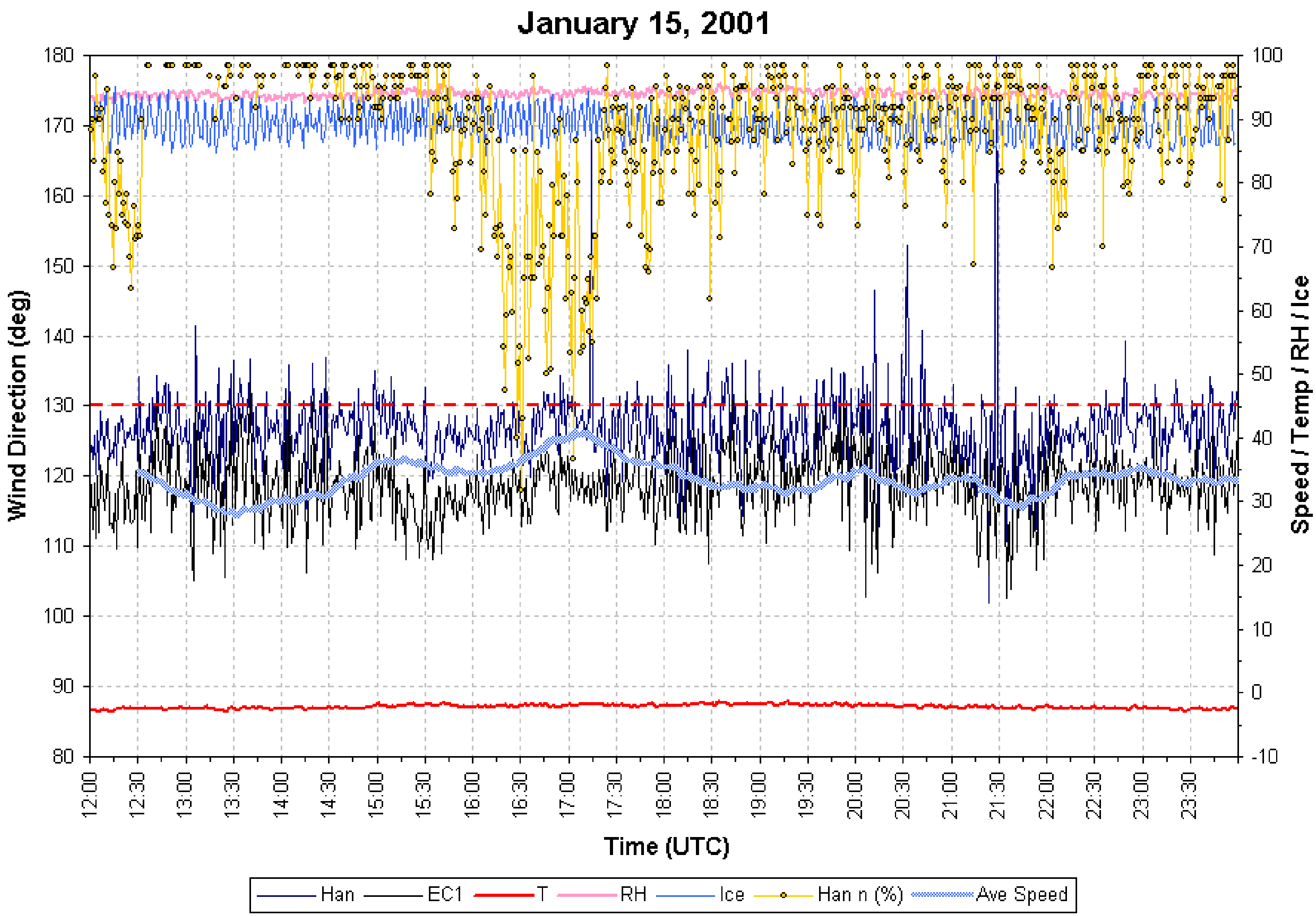

FIGURE 73. VAISALA 1-MINUTE WIND DIRECTIONS DURING AN ICING EVENT

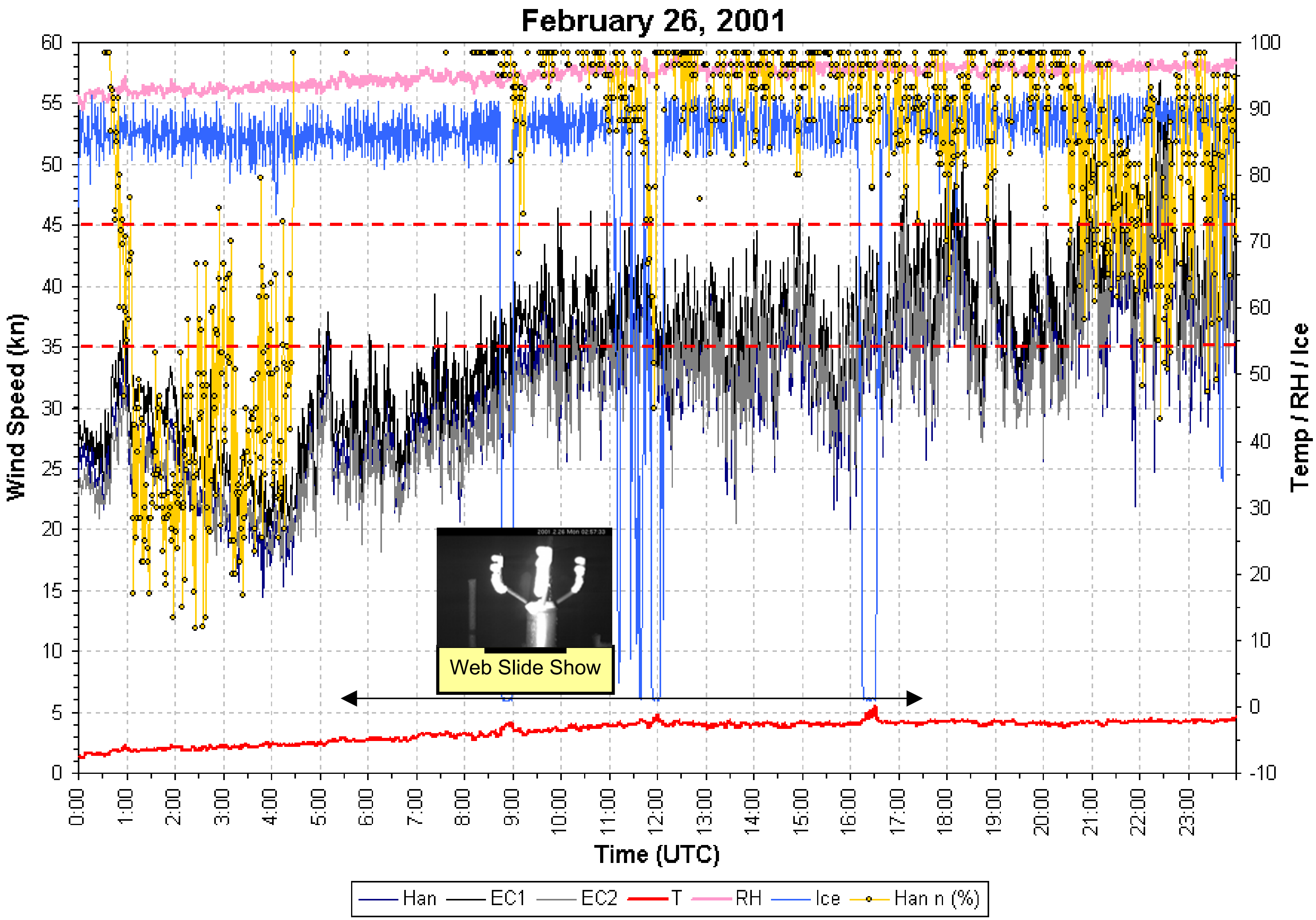

FIGURE 74. VAISALA 1-MINUTE WIND SPEED AVERAGES DURING AN ICING EVENT

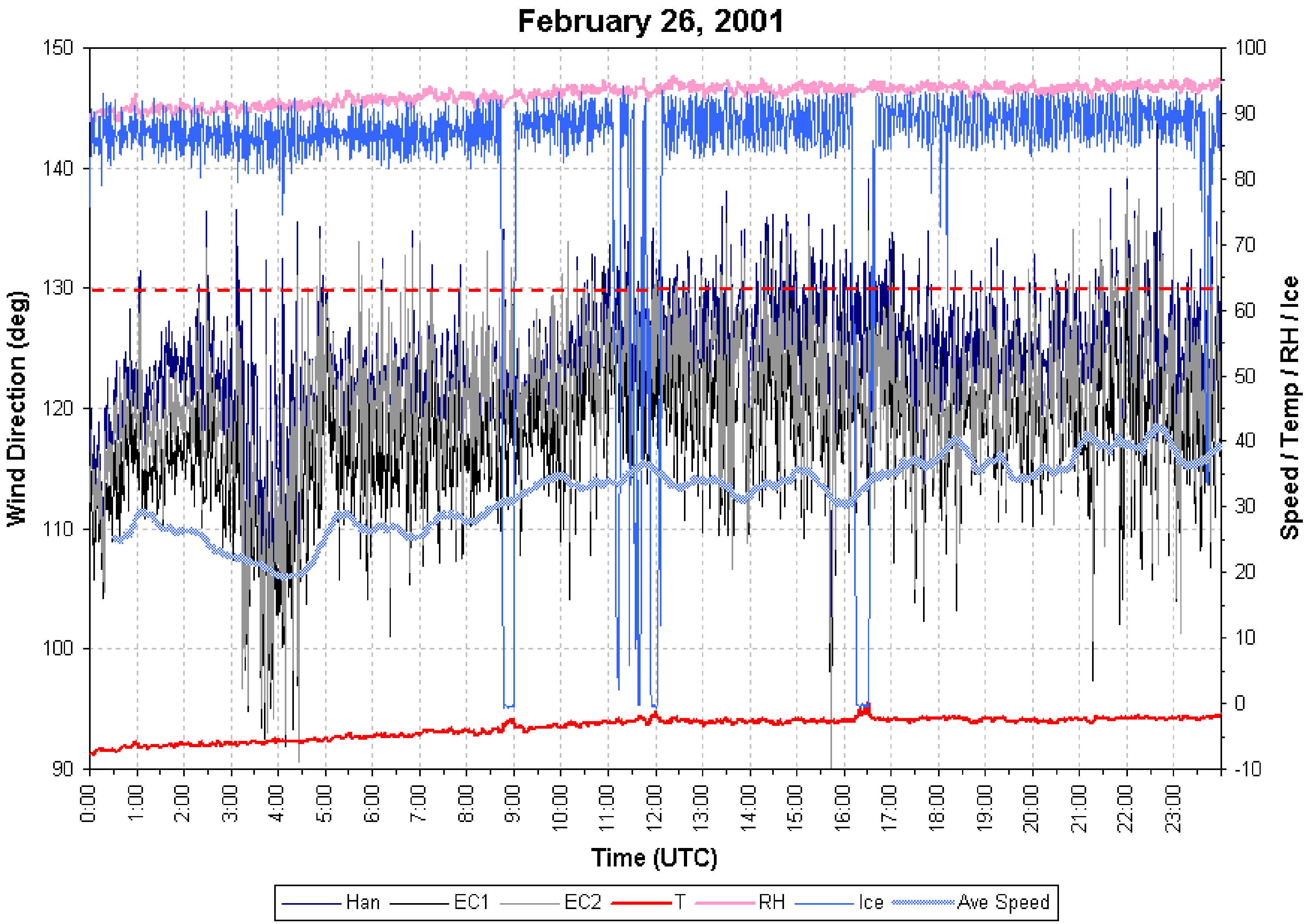

FIGURE 75. VAISALA 1-MINUTE WIND DIRECTION AVERAGES DURING AN ICING EVENT

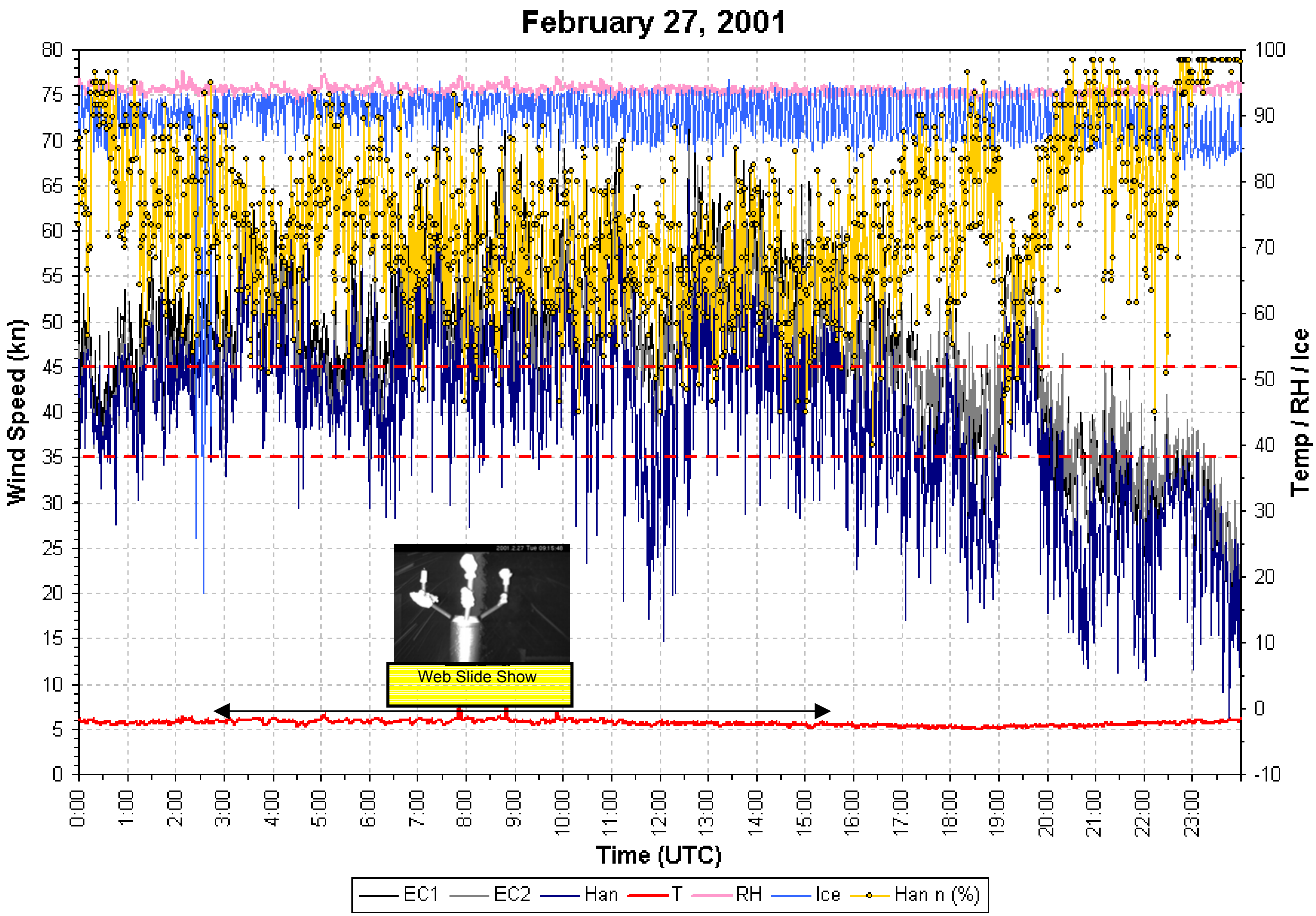

FIGURE 76. VAISALA 1-MINUTE WIND SPEED AVERAGES DURING AN ICING EVENT

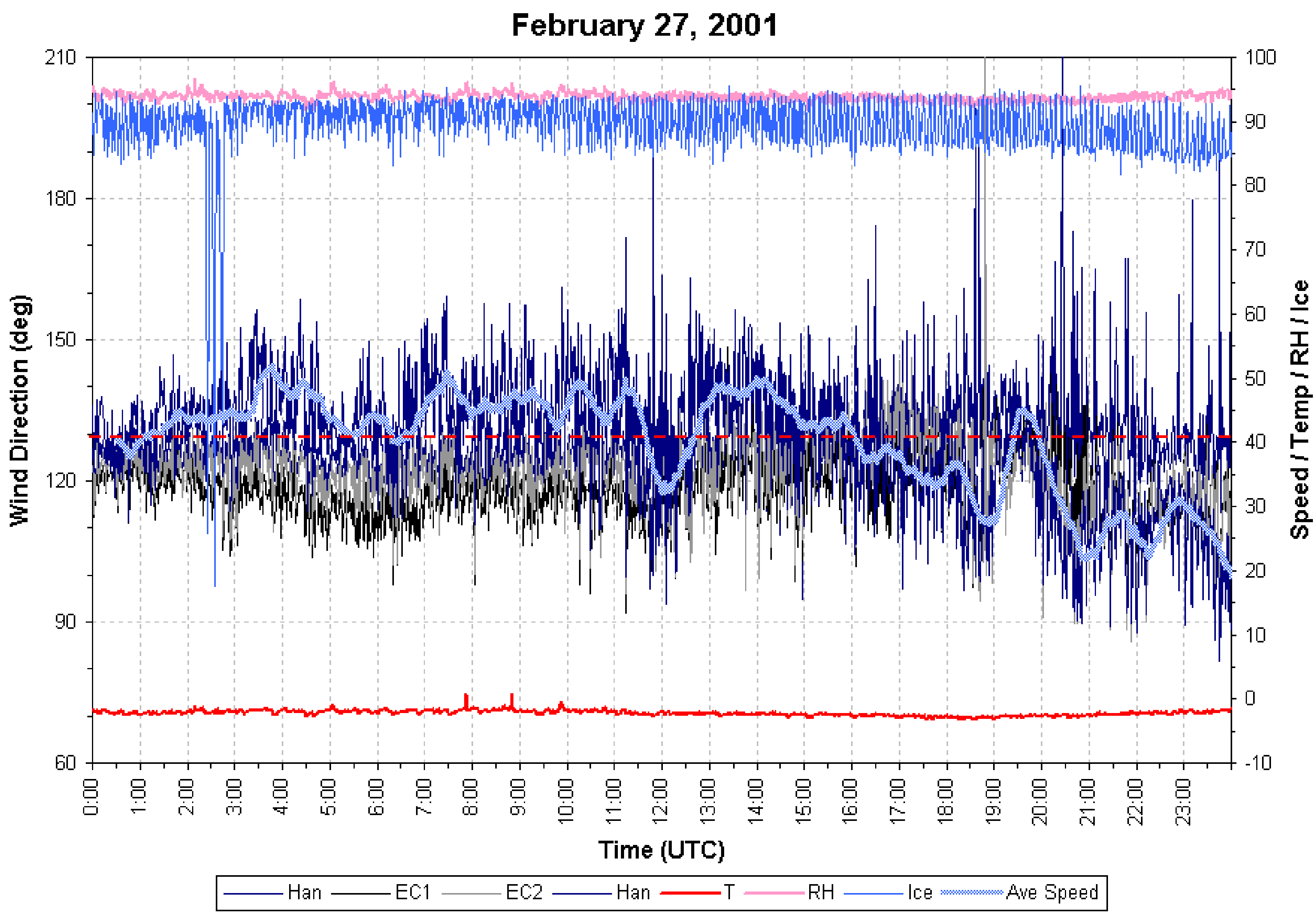

FIGURE 77. VAISALA 1-MINUTE WIND DIRECTION AVERAGES DURING AN ICING EVENT

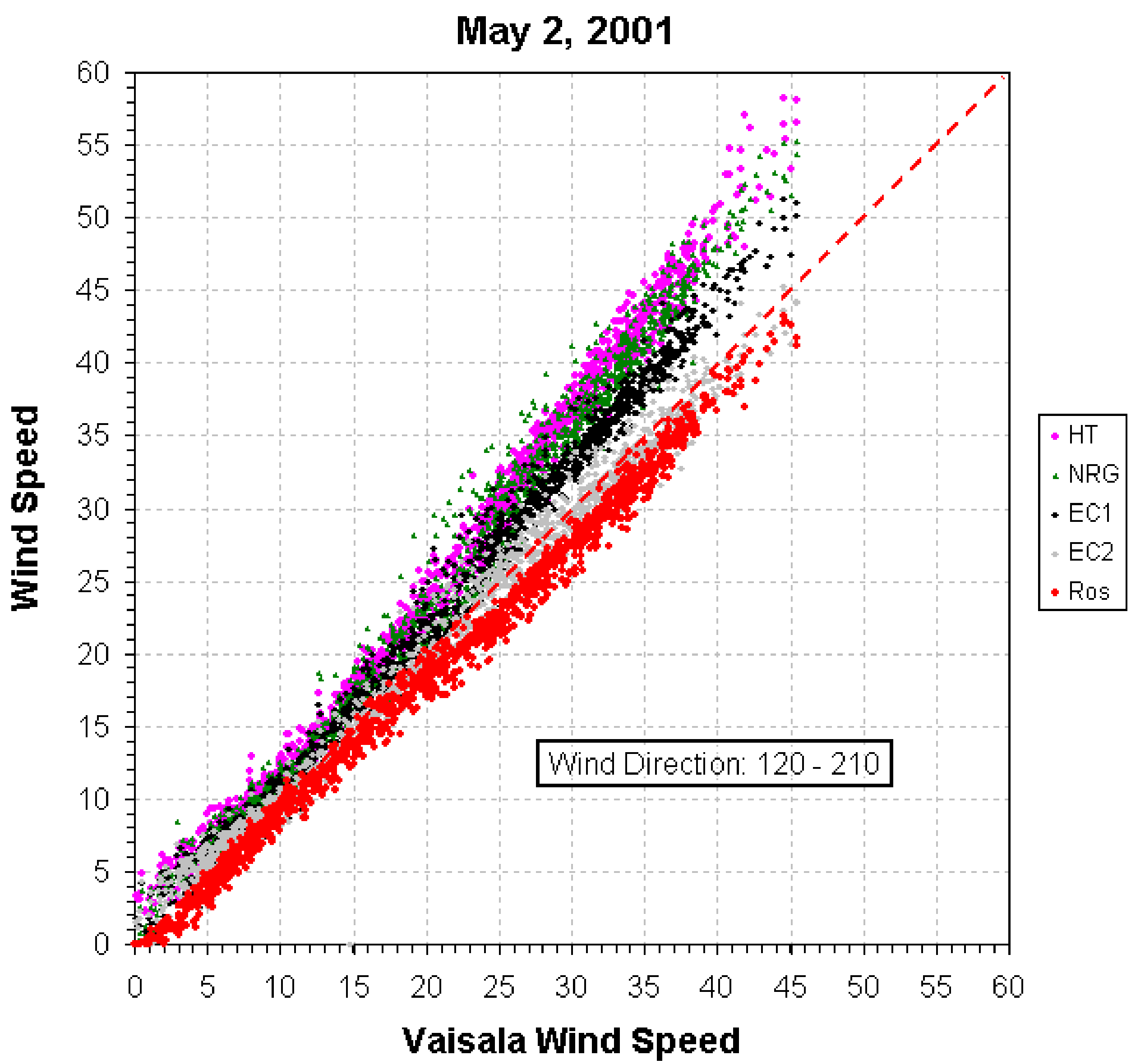

FIGURE 78. WIND SPEED DISTRIBUTION FOR SOUTH WIND

4.3.5 Conclusions.

The following are conclusions on the wind sensors:

a. In general, the Hydro-Tech sensors exhibited minimal icing, and most of the icing was on their supporting masts. Performance of the sensors was found to be consistent with data from wind tunnel tests and results from the MWO study. The Hydro-Tech speed sensors experienced significant overspeeding particularly for off-axis winds, and slower dynamic response due to the mass of the ruggedized sensor.

b. Significant icing was experienced by the IceFree II anemometers, and was found to be operationally unsuitable for the mountain ridge-top locations due to extended ice-related outages.

c. Favorable performance was exhibited by the ultrasonic anemometer. Although this sensor also experienced icing, animated video clips revealed that the modified superheated instrument was highly effective in shedding ice from the transducer arms and sensor body.

d. The sensor was determined through its internal status, as well as video data, to be degraded by icing 0.8% of the 6-month period. Further analysis of the periods of degraded performance (with respect to the JAWS 1-minute wind reporting requirement), revealed that in 84% of affected cases, there were at least 75% raw data samples available to derive a valid wind report. During the entire field experiment, only 81 sporadic 1-minute wind reports were derived from 25% or less raw 1-second samples. Closer inspection of the valid data when ice was apparent on the anemometer, revealed the actual wind values to be sensible.

e. The Rosemount 1774W pressure-type probe exhibited optimistic performance. However, the sensor was installed late in the season and the resulting data set was unfortunately limited.

5. SUMMARY OF CONCLUSIONS.

The following is the summary of conclusions presented in this report:

a. In general the wind tunnel results were as expected. The mechanical sensors overestimate the wind speed at greater wind speeds. The ultrasonic sensor was more accurate over a wide range of wind speed ranges than the mechanical sensors.

b. The mockup of the test bed at the Technical Center laboratory resulted in the efficient and successful installation of the test bed equipment in Juneau.

c. Favorable performance was exhibited by the ultrasonic anemometer. Although this sensor also experienced icing, animated video clips revealed that the modified superheated instrument was highly effective in shedding ice from the transducer arms and sensor body.

d. Favorable performance was exhibited by the ultrasonic anemometer. Although this sensor also experienced icing, animated video clips revealed that the modified superheated instrument was highly effective in shedding ice from the transducer arms and sensor body.

e. The sensor was determined through its internal status, as well as video data, to be degraded by icing 0.8% of the 6-month period. Further analysis of the periods of degraded performance (with respect to the Juneau Airport Wind System (JAWS) 1-minute wind reporting requirement), revealed that in 84% of affected cases, there were at least 75% raw data samples available to derive a valid wind report. During the entire field experiment, only 81 sporadic 1-minute wind reports were derived from 25% or less raw 1-second samples.

f. The Rosemount 1774W pressure-type probe exhibited optimistic performance, however, the sensor was installed late in the season and the resulting data set was unfortunately limited.

6. RECOMMENDATIONS.

Recommendations from this study are as follows:

a. Preliminary results from this study have supported the Juneau Airport Wind System (JAWS) acquisition and implementation decision to use Vaisala ultrasonic sensor in the end-state JAWS system. However, it should be recognized that the JAWS alert algorithm being developed by a National Center for Atmospheric Research (NCAR) is based on data sets from Hydro-Tech anemometers. Compared to the ultrasonic sensor, theses mechanical sensors are characterized as having a significantly slower dynamic response and a sizeable overspeeding factor that depends on the wind speed and the extent of the off-axis wind. Accordingly, efforts should be undertaken to determine and develop software techniques that will account for the transition from the Hydro-Tech to Vaisala wind sensors in the JAWS system.

b. Based on the success of the test bed setup, and encouraging results obtained from the sensor assessment, it is recommended that a follow-on study be implemented for the Juneau winter of 2001–02. The purpose of the effort is to further assess the 425AH capabilities with various heater modifications. In addition, it is recommended that the Metek sensor be implemented to determine the effects of upslope winds, and the Rosemount 1774W be further evaluated.

7. ACRONYMS AND GLOSSARY.

A	ampere
ACS	Alaska Communications Systems
AFSS	Automated Flight Service Station
AMS	Acquisition Management System

AWRP	Aviation Weather Research Program
AWS	Automatic Weather Station
cm	centimeter
COTS	Commercial Off-the-Shelf
DDE	Dynamic Data Exchange
DQA	Data Quality Analysis
DR&A	Data Reduction and Analysis
DSL	Digital Subscriber Line
F	Fahrenheit
FAA	Federal Aviation Administration
ft	foot
FTP	File Transfer Protocol
GB	gigabyte
GHz	gigahertz
IIS	Internet Information Server
in	inches
IP	Internet Protocol
JAWS	Juneau Airport Wind System
JNU	Juneau International Airport
JPEG	Joint Photographic Experts Group
JWHIS	Juneau Wind Hazard Information System
kbps	kilobytes per second
kHz	kilohertz
km	kilometer
kt	knot
LAN	Local Area Network
LLWAS–RS	Low Level Wind Shear Alert System Relocation and Sustainment
m	meter
MB	megabyte
MHz	megahertz
mi	mile
m/s	meter per second
METAR	Aviation Routine Weather Report

mm	millimeter
mph	mile per hour
MWO	Mount Washington Observatory
NCAR	National Center for Atmospheric Research
NEMA	National Electrical Manufacturers Association
NT	Network
NWS	National Weather Service
OT	Operational Test
PC	personal computer
PDT	Product Development Team
PVC	Polyvinyl Chloride
RAM	Random Access Memory
RAP	Research Application Programs
RC	resistor-capacitor
s	second
SAWS	Stand Alone Weather Sensors
SM	statute mile
UPS	Uninterruptible Power Supply
UTC	Coordinated Universal Time
V	volt
Vdc	volts direct current
W	watt
WAN	Wide Area Network

APPENDIX A

Equipment List

Category	Qty	Model and Description	Manufacturer
EC1	1	Hydro-Tech speed head	Taylor Engineering
	1	Hydro-Tech direction head	
	1	Hydro-Tech heater controller	
	1	QLI50 Data Collector	Vaisala
	1	900 MHz modem	Freewave
	1	Power supply	
	1	NEMA box	
EC2	1	Hydro-Tech speed head	Taylor Engineering
	1	Hydro-Tech direction head	
	1	Hydro-Tech heater controller	
	1	Temperature/humidity sensor	Vaisala
	1	QLI50 Data Collector	Vaisala
	1	900 MHz modem	Freewave
	1	Power supply	
	1	NEMA box	
Sheep Mountain Relay	1	900 MHz modem	Freewave
Wind Sensors	1	Hydro-Tech WD-3 Rotor Anemometer with 1500 W heater	Taylor Engineering
	1	Handar 425AH Ultrasonic anemometer	Vaisala
	1	IceFree II cup anemometer	NRG
	1	IceFree II direction vane	
	1	USA1 Ultrasonic anemometer	Metek
Ice Detection	1	871FA Ice Detector and enclosure	Rosemount
Temperature	1	MP100H temperature and humidity probe with 12-plate Gill radiation shield and canister enclosure	Rotronic
Processors	1	E-4400 800 MHz Pentium III PC with 256 MB RAM and 75 GB hard disk for backup and archive	Gateway
	1	E-4200 800 MHz Pentium III PC with 256 MB RAM and an 18 GB hard disk for data host and server	

	1	CR23X Micrologger data collection and processor	Campbell Scientific
Video	2	V60EB6080 Arctic Hawk CCTV black and white video camera	Silent Witness
	2	SPT-M324 black and white video camera	Sony
	2	AP21CH1 pressurized and heated aluminum video camera housing for Sony camera	Videolarm
	1	SNT-V304 Video Server	Sony
	1	HSR-2 Digital Videocassette Recorder	
Deicing	5	Custom thermostatically-controlled heater blankets for video cameras and ice detector enclosure	Benchmark Thermal
Communication	5	SS100 EtherPath RS-232-to-Ethernet LAN adapter	Data Comm for Business
	2	WS-H009NX 8-Port Ethernet Hub	
	2	XE-3 wireless Ethernet bridge	Speedlan
	2	A241NJ Antenna Amplifier	Wave Wireless Networking
	2	PC-2415 2.3 GHz antenna with heater	Yagi
	1	Etherland Model ISB2 LAN DSL router	Nexland
	1	NTEX35 BAAB DSL modem	Nortel Networks
Power/Lighting	2	Model 1000XL Uninterruptible Power Supply (UPS) with a 670 W output capacity	APC
	3	QT250 Quartz flood lamps	RAB
	4	Photodetectors	

APPENDIX B

Cabling Diagrams

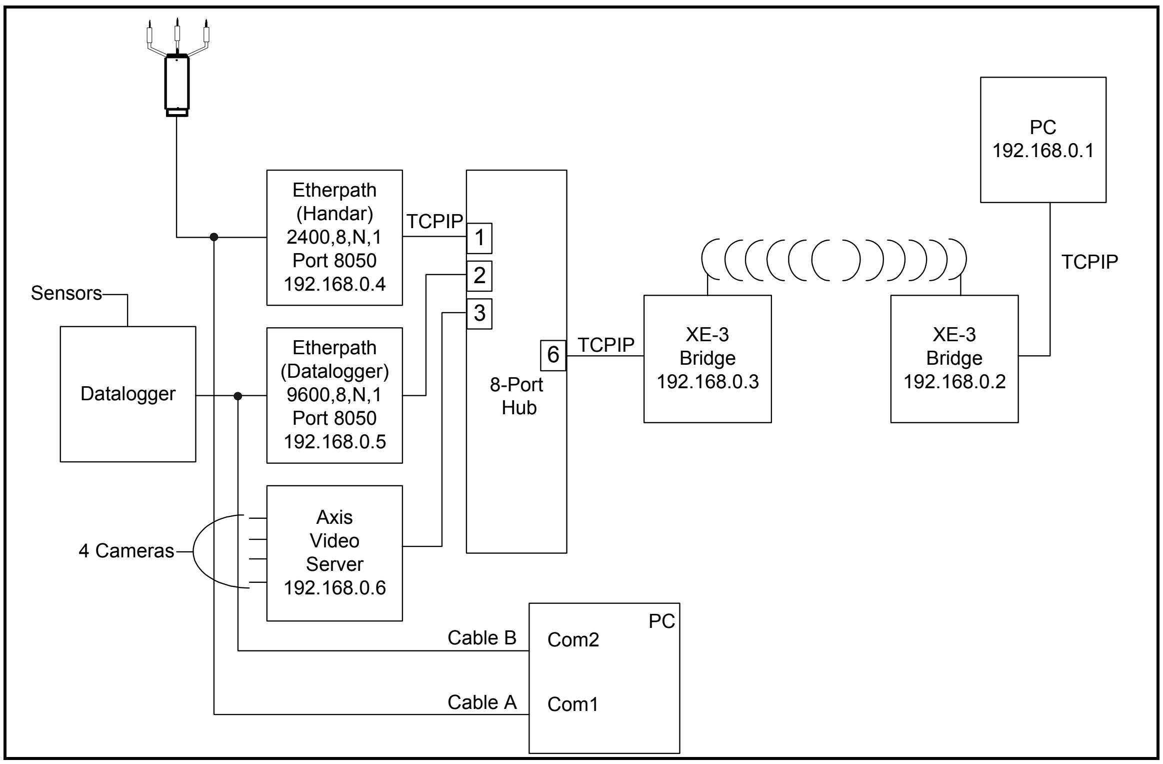

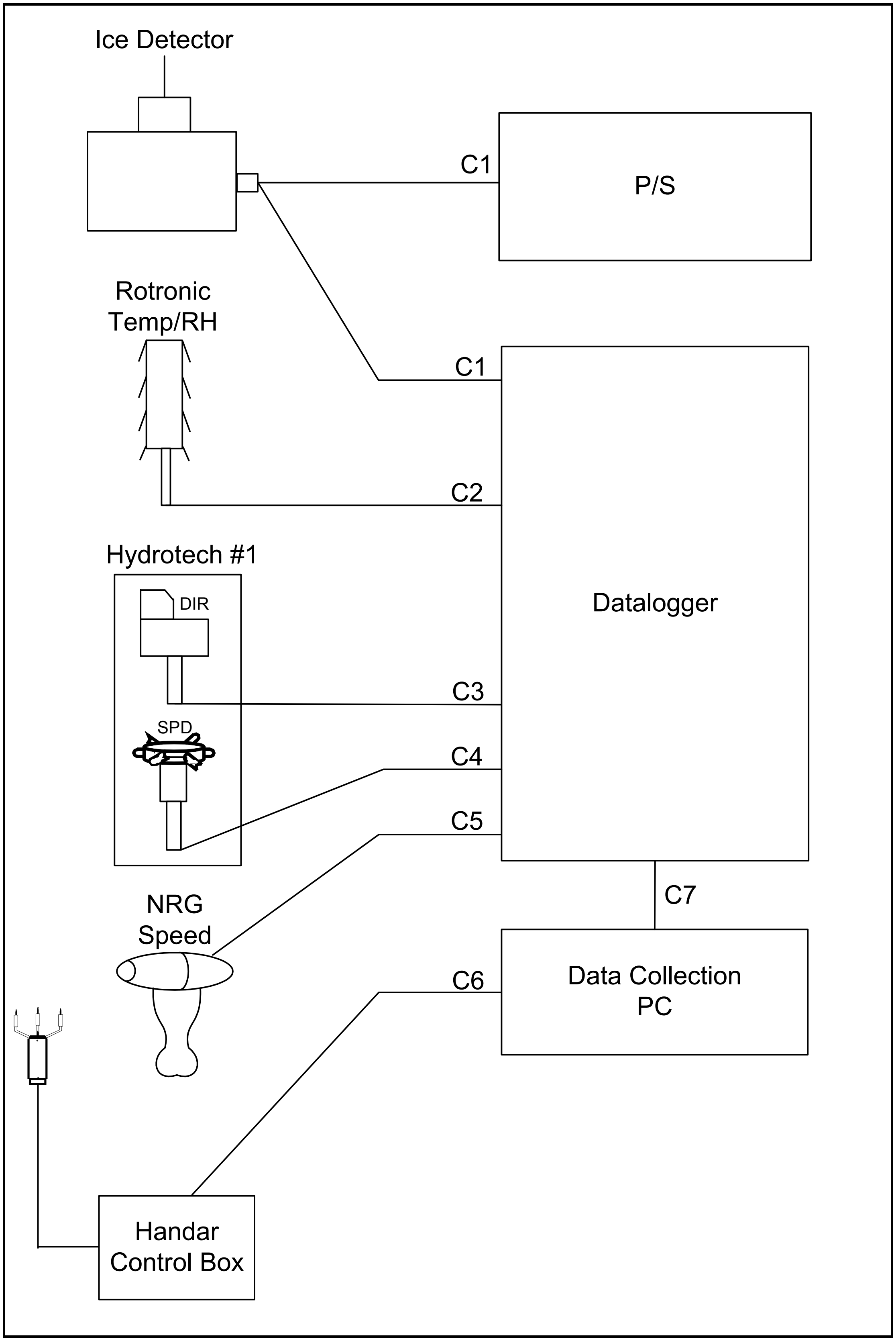
Ice Detector
C1
P/S
Rotronic
Temp/RH
C1
C2
Hydrotech #1
DIR
Datalogger
C3
SPD
C4
C5
NRG
Speed
C7
C6
Data Collection
PC
Handar
Control Box

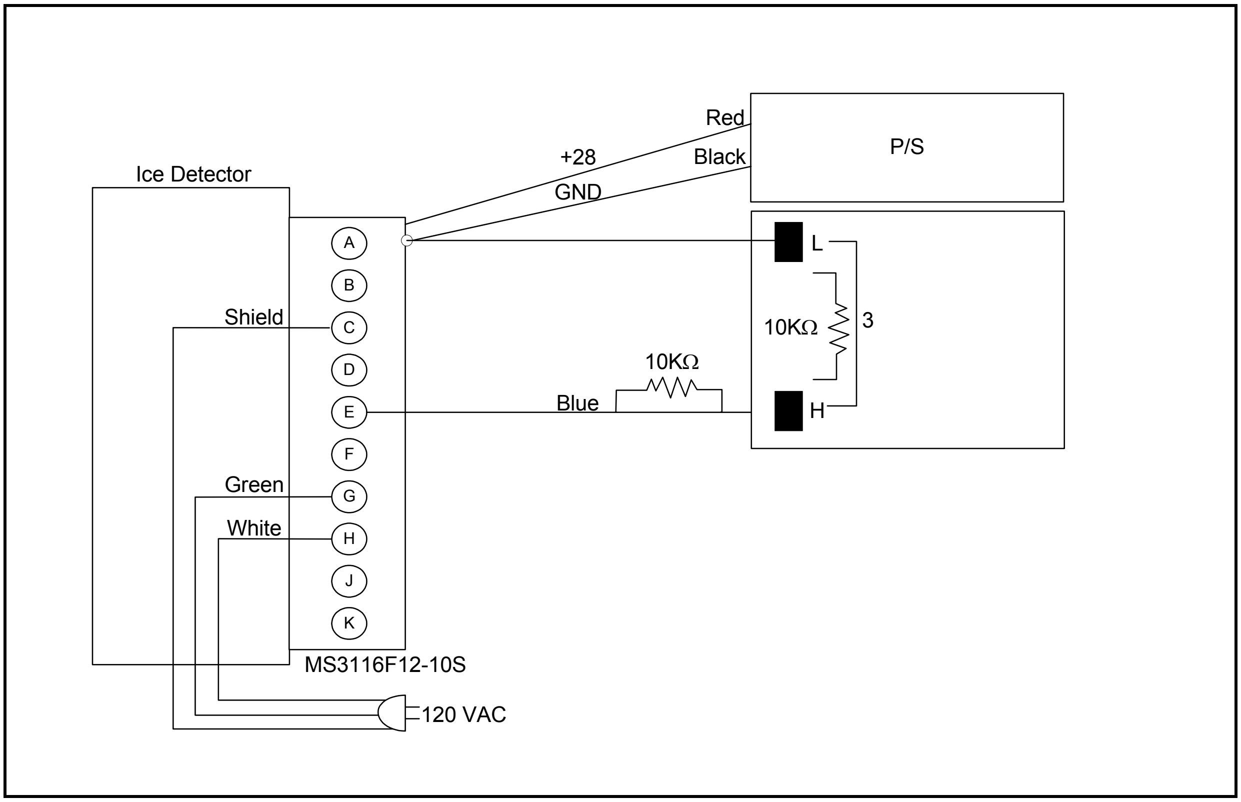
Ice Detector
+28
GND
Red
Black
P/S
A
B
C
D
E
F
G
H
J
K
Shield
Green
White
Blue
10KΩ
10KΩ
L
H
3
MS3116F12-10S
120 VAC

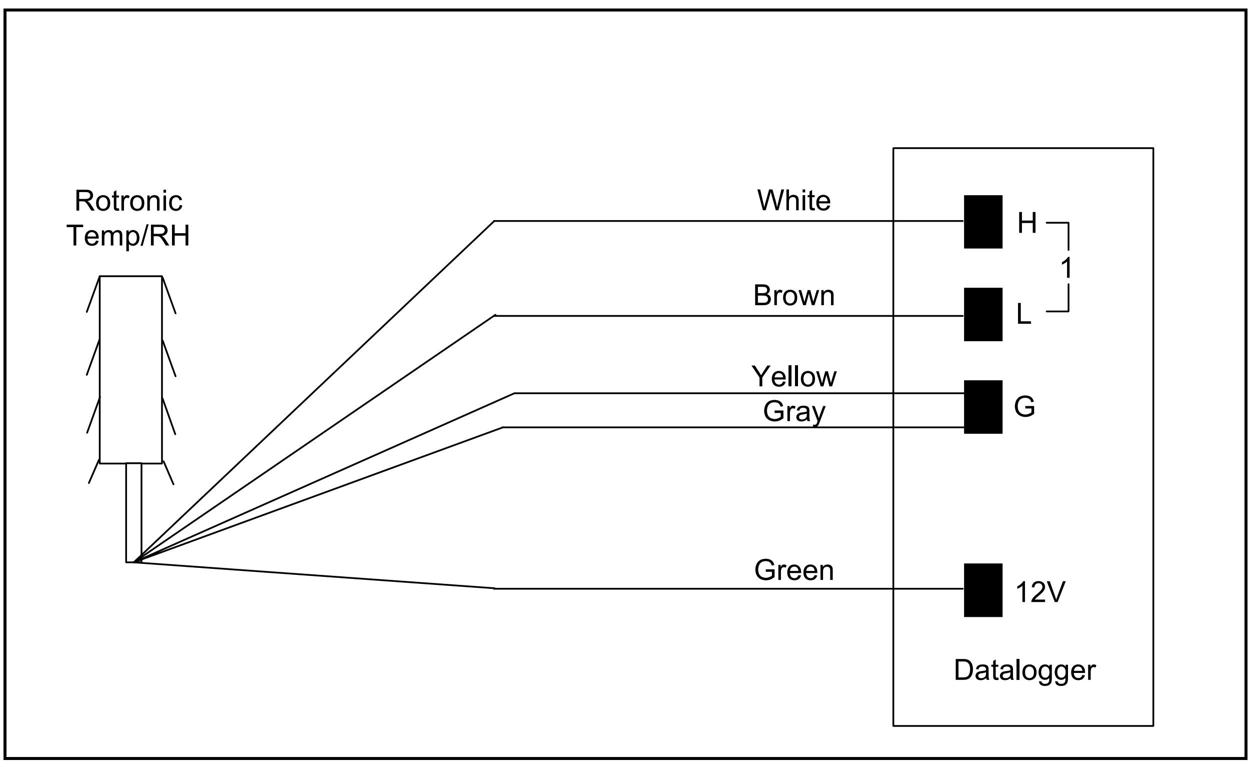
Rotronic
Temp/RH
White
Brown
Yellow
Gray
Green
H
L
1
G
12V
Datalogger

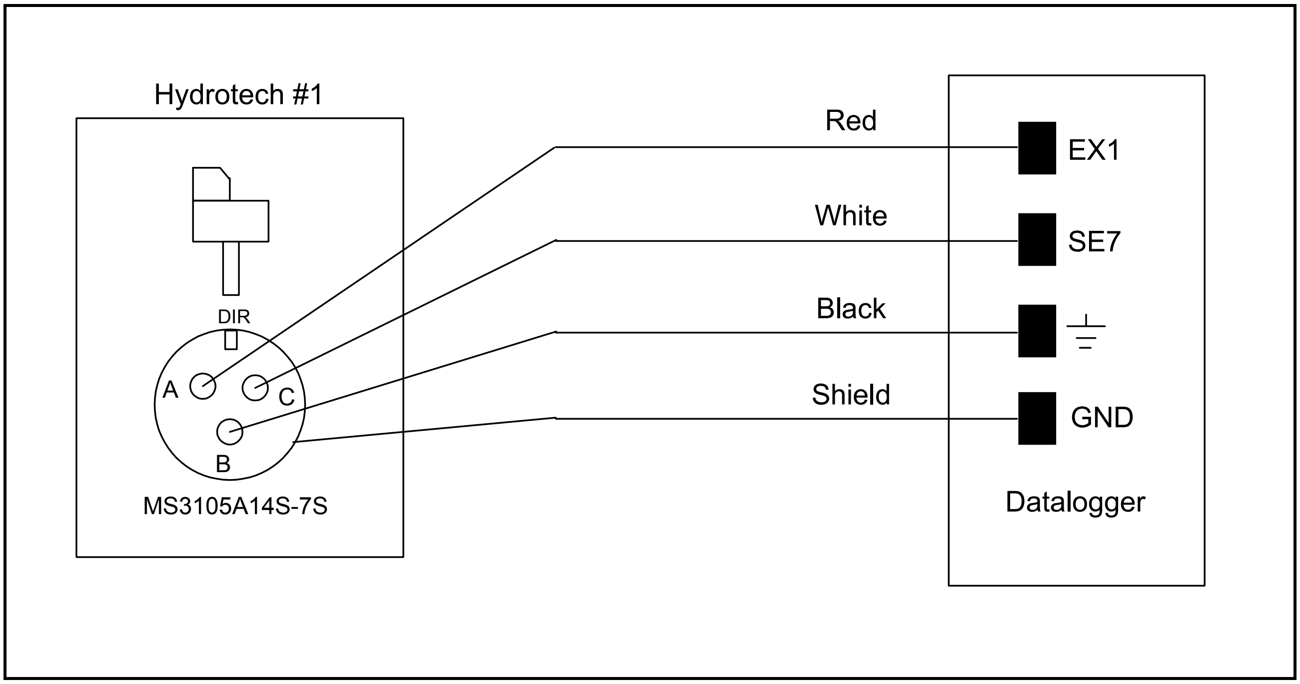
Hydrotech #1
DIR
A
C
B
MS3105A14S-7S
Red
White
Black
Shield
EX1
SE7
GND
Datalogger

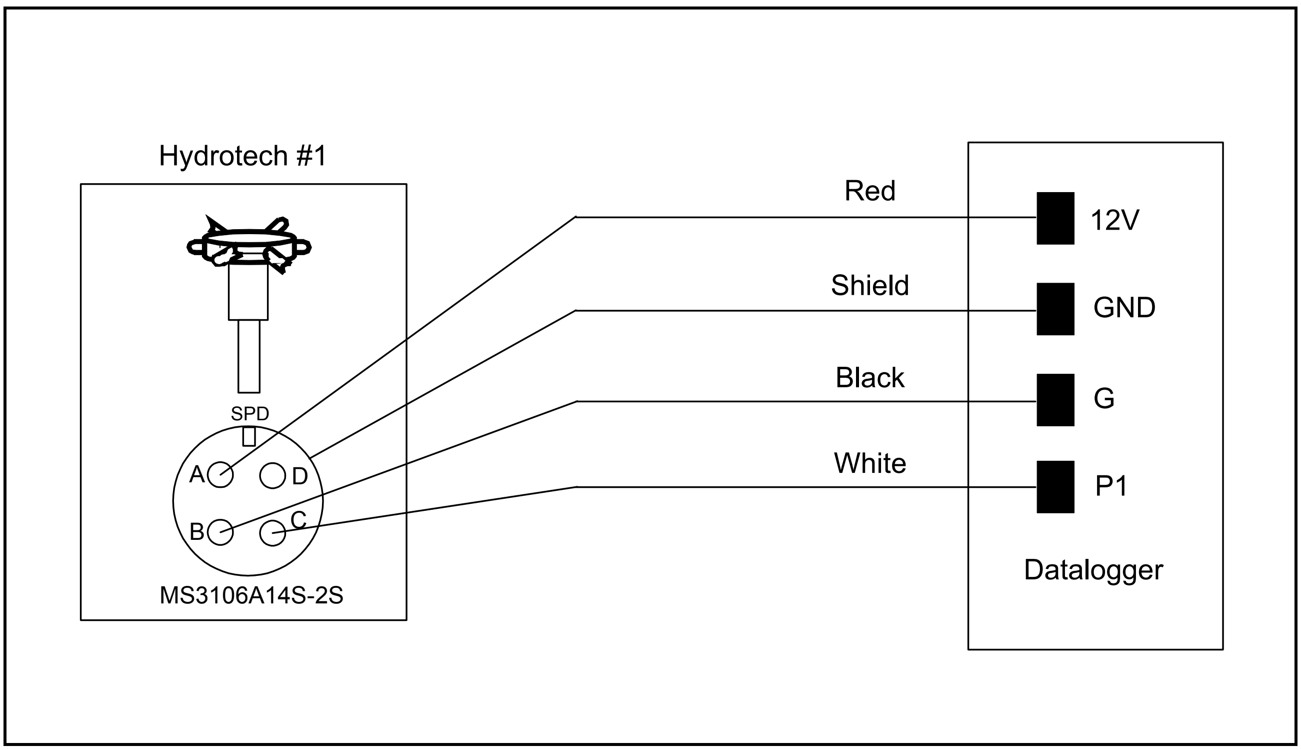
Hydrotech #1
SPD
A
D
B
C
MS3106A14S-2S
Red
Shield
Black
White
12V
GND
G
P1
Datalogger

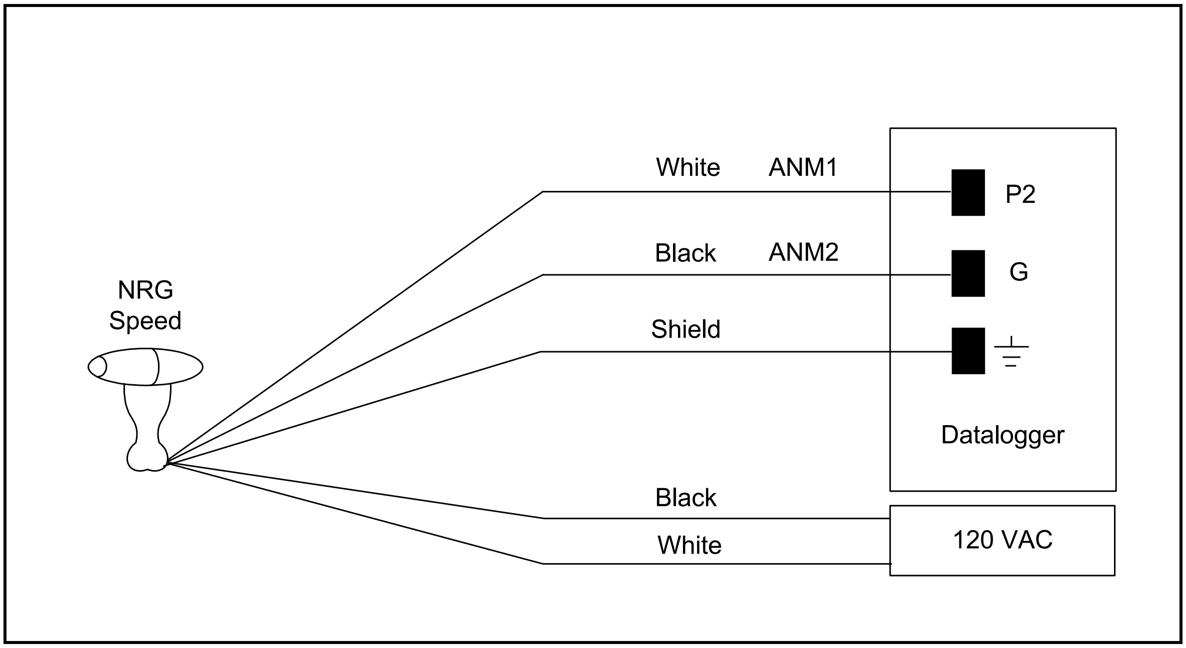
White
ANM1
P2
Black
ANM2
G
NRG
Speed
Shield
Datalogger
Black
White
120 VAC

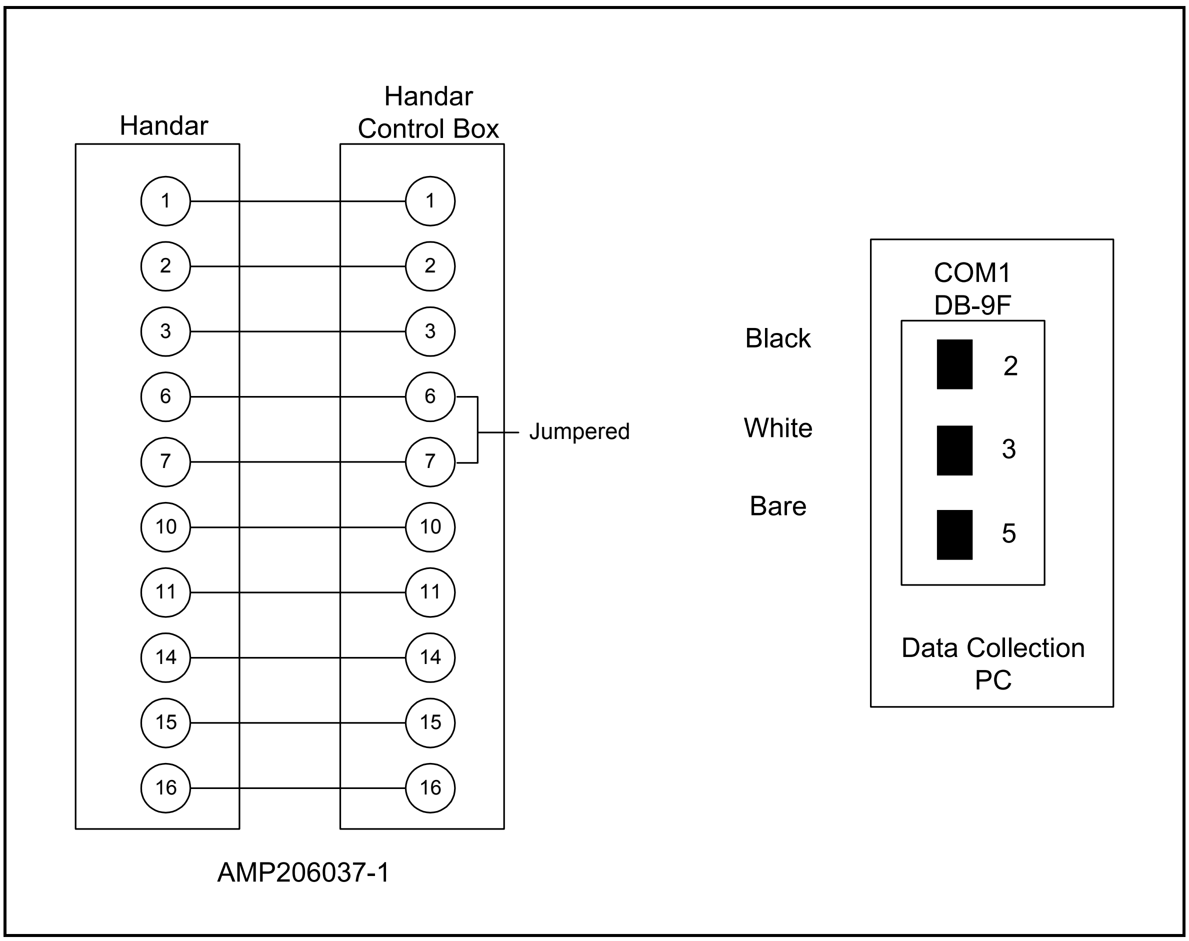
Handar
Handar
Control Box
1
2
3
6
7
10
11
14
15
16
Jumpered
COM1
DB-9F
Black
White
Bare
2
3
5
Data Collection
PC
AMP206037-1

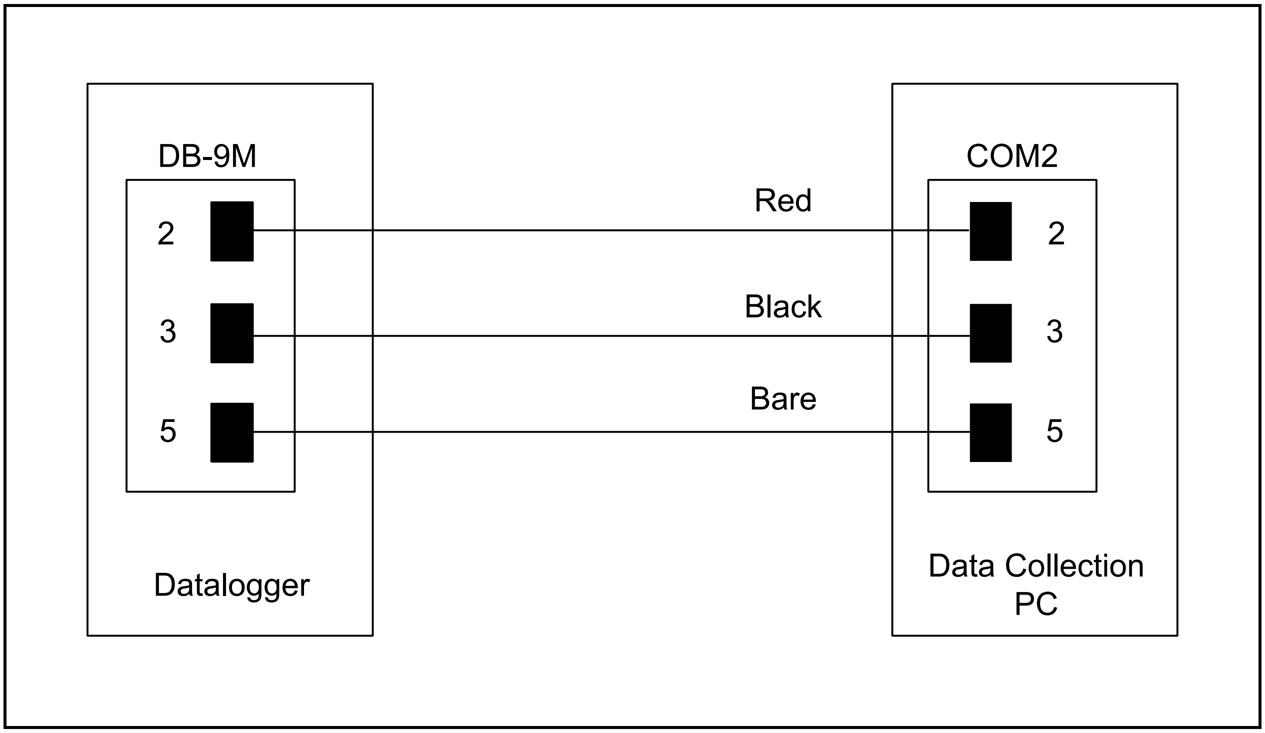
DB-9M
2
3
5
Datalogger
Red
Black
Bare
COM2
2
3
5
Data Collection PC